SSSU 62
ISSN 0140 3818

UNIVERSITY OF SOUTHAMPTON

DEPARTMENT OF SHIP SCIENCE

FACULTY OF ENGINEERING AND APPLIED SCIENCE

INTERFACIAL WAVES PRODUCED BY A SUBMERGED BODY MOVING IN A LAYERED FLUID

W. G. Price
P. C. Westlake

Ship Science Report No. 62

July 1993

Interfacial waves produced by a submerged body moving in a layered fluid
Ship Science Report No. 62

W.G.Price
P.C.Westlake

July 20, 1993

Contents

Nomenclature

$A(\xi)$	Longitudinal sectional area function of the body
C_w	Nondimensional wave resistance coefficient $= \frac{R_w}{\frac{1}{2}\rho_j s U_0^2}$
d	Maximum diameter of the body
$E(x,y)$	Magnitude of the free surface strain vector $= \sqrt{u_x^2 + v_y^2}$
F_n	Froude number $= \frac{U_0}{\sqrt{gL}}$
f	Depth of the axis of revolution of the prolate spheroid from the undisturbed free surface $= -\zeta$
$G_{ij}(\boldsymbol{x},\boldsymbol{\xi})$	Greens function in Oxyz
g	Gravity acceleration
$H(z)$	Heaviside unit step function
h_i	Vertical separation of the i^{th} interface and free surface
h_j	Vertical separation of the origin and free surface
i	Layer number, 1^{st} layer = upper layer
j	Layer number in which the body is located
L	Length of body
l	Summation index $(1 \leq l \leq N_r)$
$N(z)$	Brunt-Väisälä frequency
N_r	Number of roots of nonzero $D(k,\theta) = 0$
$Oxyz$	Moving reference coordinate system located vertically above the body's centroid on the undisturbed free surface or interface
$O(x)$	Landau order symbol
$o(x)$	Landau order symbol
$P.V.$	Cauchy's principal value integral
$Q(\xi)$	Longitudinal source strength distribution representing the body
$q(x,y)$	Magnitude of the free surface velocity vector $= \sqrt{u^2 + v^2}$
R_w	Wave resistance
s	Surface area of body, for a prolate spheroid $s = \frac{1}{2}\pi(d^2 + \frac{Ld}{\epsilon}\arcsin\epsilon)$
t_1	Thickness of upper layer
t_2	Thickness of middle layer
U_{cl}	Lower critical velocity of the fluid system
U_{cu}	Upper critical velocity of the fluid system
U_0	Velocity of body
$\boldsymbol{u}(x,y,z)$	Disturbance velocity vector in $Oxyz = (u,v,w)$
$\boldsymbol{x}$	Position vector of the field point (x,y,z) in $Oxyz$
α_l	l^{th} non zero root of k from $D(k,\theta) = 0$
δ_1	Upper density ratio $= \frac{\rho_1}{\rho_2}$
δ_2	Lower density ratio $= \frac{\rho_2}{\rho_3}$
δ_{ij}	Kronecker delta function
ϵ	$= \sqrt{1 - \left(\frac{d}{L}\right)^2}$
$\zeta_1(x,y)$	Free surface elevation
$\zeta_2(x,y)$	Upper interface elevation
$\zeta_3(x,y)$	Lower interface elevation
$\boldsymbol{\xi}$	Position vector of source point (ξ,η,ζ) in $Oxyz$
ρ_1	Density of fluid in the upper layer
ρ_2	Density of fluid in the middle layer
ρ_3	Density of fluid in the lower layer
$\phi_{ij}(\boldsymbol{x},\boldsymbol{\xi})$	Disturbance velocity potential in $Oxyz$
$\psi_{ij}(\boldsymbol{x},\boldsymbol{\xi})$	Disturbance stream function in $Oxyz$

Abstract

Velocity potential solutions are derived for an arbitrary shaped body moving horizontally in a fluid system consisting of three layers, the lower layer of infinite depth. The body may be located in any one of the three layers. The boundary conditions on the free surface and interface are linearised and a radiation condition imposed. Expressions for the far field free surface and interface elevations are derived. A three dimensional extension of Lagally's theory provides a method which allows the wave resistance of the body to be determined. The application of a slender body approximation permits the derivation of analytical expressions for the elevations and wave resistance. Plots of the far field free surface and interface wave systems are presented when the body is located in each layer. The wave resistance of a prolate spheroid length L to diameter d for a series of L/d ratios is calculated over a Froude number range. The "dead water" effect being apparent in every case. The results of other parametric studies are also included.

1 Introduction

Generally the fluid in which vessels navigate is not homogeneous, a degree of stratification is present. This stratification may be weak, one or two parts in one thousand occur in the ocean; in estuaries and fjords stratification may reach thirty parts in one thousand. The presence of stratification is due to a variation of density, temperature or salinity with depth. Stratifications due to a change in density, temperature or salinity are known as pynoclines, thermoclines and haloclines respectively. The effects of stratification on the forward motion and control of ships has been recorded by many mariners, many compiled by Ekman (1904). The most noticeable effect observed was a decrease in the forward speed of the vessel caused by an increase in resistance due to the additional energy expended creating waves within the fluid. This effect initiated research into the generation of ship waves in a stratified fluid. More recently the application of remote sensing techniques to the oceans surface has revealed 'v' shape images in the wake of ships, the cause of which is suspected to be due to internal wave generation. Experimenters have reproduced these images under controlled conditions (Apel and Gjessing, 1989). Accurate mathematical models of the fluid pertabations caused by the body are required in order that the mechanism which produces these images can be fully explained.

Although stratification in the ocean is continuous with depth, many theoretical studies idealise this continuous medium by a series of discrete layers each of finite depth and of constant fluid density. The overall fluid density profile is not constant and discontinuities occur at the layer interfaces. Stratified fluid models have been considered previously, see for example, Hudimac (1961), Sabuncu (1961), Crapper (1967), Rarity (1967), Keller and Monk (1970) , Miles (1971), Hughes (1986), Price et al (1988), Dysthe and Trulsen (1989), Wang (1989) and Tulin and Miloh (1990) but many of these studies concentrate on the description of the wave patterns generated on the free surface and interface(s) by an isolated source rather than detailed descriptions of the interaction between a defined body shape and the surrounding medium. Because of fluid stratification, internal waves occur naturally in oceans and these can be generated locally by turbulence or externally by a distant storm. A body moving in a stratified fluid produces a pressure field within the fluid creating internal and free surface disturbances. Since waves always radiate energy away from the region where they are being formed, the stratification of the fluid provides an additional outlet for this radiation to occur.

For a ship or submerged body moving horizontally with constant forward speed in a constant density fluid medium which is assumed "idealised", Baar and Price (1988) developed numerical procedures to determine solutions of the steady body motion problem. That is, predictions of wavemaking resistance, wave patterns generated on the free surface, pressure fields within the fluid, etc. These were derived from a linearised three dimensional flow formulation and they describe the disturbance potential of the steady perturbed flow about the moving body. The solutions were obtained by means of a Kelvin wave source distribution method. This is based on an integral identity for the Neumann-Kelvin potential involving an integral distribution of Kelvin wave sources over the body's surface and waterline contour (if the vessel is surface piercing). The unknown source strength is determined by solving the Fredholm integral equation of the second kind which ensures that the kinematic condition at the hull surface is satisfied. This theoretical approach and iterative numerical approximation procedure were applied to six different

hull forms and the calculated results showed good agreement with experimental data in both a qualitative and quantative manner. see for example, Andrew et al (1988).

This approach was extended by Price et al (1988) to solve the similar problem in a stratified fluid. A panel method was developed allowing the modelling of the geometric shape of an arbitrary shaped body. This method was, applied to a prolate spheroid and the predicted results were compared with those derived using a slender body approach. A comparison of the predicted values revealed only minor variations thus justifying the use of the slender body approach for this body shape. This has the advantage of reducing the computational effort significantly without diminishing the description of the physical processes arising in the stratified fluid - structure interaction. For these reasons, the slender body approach is used in the calculations described herein.

2 Model definition

This report describes the first stage of an investigation into the problem of a body moving in a stratified fluid. Here the mathematical model describing a stably stratified fluid is discretised into three layers. In each layer the density of the fluid is constant and the lower layer is of infinite depth. A prolate spheroid, which is completely contained in any one of the three layers, moves with constant horizontal velocity along a straight track extending from its axis of revolution. The disturbance created within the fluid is described by velocity potential functions.

2.1 Fluid Model

The fluid in each layer is assumed inviscid, incompressible and the fluids are immiscible at the interfaces. The disturbance produced in each layer by the moving body may therefore be represented by a velocity potential flow theory.

The density profile can be expressed as:

$$\rho(z) = \rho_1 H(-z) + (\rho_2 - \rho_1)H[-(z+t_1)] + (\rho_3 - \rho_2)H[-(z+t_1+t_2)] \quad \rho_1 < \rho_2 < \rho_3 \tag{1}$$

where the plane $z = 0$ denotes the undisturbed free surface. The coordinate z is defined negative pointing into the fluid and $H(z)$ denotes the Heaviside unit step function.

The Brunt-Väisälä frequency, $N(z)$ is defined as

$$N^2(z) = -\frac{g}{\rho(z)}\frac{d\rho(z)}{dz} \tag{2}$$

which for this model is discontinuous across the interfaces and zero within each layer.

2.2 Body Model

In general, a submarine, idealised here by a prolate spheroid, has a streamline form with a maximum diameter, d, substantially smaller than its length, L. A slender body approximation may therefore be employed to simplify the hydrodynamic analysis. The disturbance velocity potential is represented by a source distribution along the longitudinal axis of the body, the strength $Q(\xi)$ of a source at position ξ , $-\frac{L}{2} \leq \xi \leq \frac{L}{2}$ is given by:

$$Q(\xi) = -\frac{U_0}{4\pi}\frac{dA(\xi)}{d\xi} \tag{3}$$

For a prolate spheroid this becomes:

$$Q(\xi) = \frac{U_0}{2}\left(\frac{d}{L}\right)^2 \xi \tag{4}$$

The achievement of exact body shape cannot be fully realised using this method due to the proximity of the free surface and interface wave systems which modify the streamline $\psi_{jj}(\boldsymbol{x}, \boldsymbol{\xi}) = 0$. An accurate

description of the shape of the body can only be achieved using an additional boundary condition ensuring no fluid particles penetrate the wetted surface of the body. The problem can then be regarded as a Neumann-Kelvin problem, a solution of which can be obtained using panel methods and numerical computation. However, it has been shown that for slender bodies the discrepancy between the two methods does not merit the increase in computational effort required for the Neumann-Kelvin theory, see Price et al (1988).

2.3 Coordinate System

Figure 1 illustrates the location and orientation of the orthogonal, right handed, coordinate axis system chosen to simplify the mathematics of the three layer system. For example, for a body in the upper layer the undisturbed free surface is the plane $z = 0$, the x-axis lies along the direction of motion of the body and the positive y-axis is chosen to satisfy the orthogonality condition. The origin of the coordinate system lies vertically above the body's centroid. For a body in one of the lower layers the undisturbed interface above the body becomes the plane $z = 0$.

3 Statement and solution of the boundary value problem

3.1 Boundary Conditions

Using a body fixed coordinate system the linearised boundary conditions imposed to describe the velocity potential disturbance $\phi_{ij}(\boldsymbol{x}, \boldsymbol{\xi})$ in the i^{th} layer created by the steady motion of the body moving in the j^{th} layer of a three layer fluid system are given by (Wang, 1989, pages 51-62) :

(1) The continuity equation

$$\nabla^2 \phi_{ij} = 0 \quad \text{for } i = 1, 2, 3 \tag{5}$$

(2) The free surface condition

$$\phi_{1j_{xx}} + k_0 \phi_{1j_x} = 0 \quad \text{on } z = h_j \tag{6}$$

(3) The interface condition

$$\phi_{(i-1)j_z} = \phi_{ij_z} \quad \text{on } z = h_j - h_i \quad \text{for } i = 2, 3 \tag{7}$$

$$\rho_{(i-1)}[\phi_{(i-1)j_{xx}} + k_0 \phi_{(i-1)j_z}] = \rho_i[\phi_{ij_{xx}} + k_0 \phi_{ij_z}] \quad \text{on } z = h_j - h_i \quad \text{for } i = 2, 3 \tag{8}$$

(4) The radiation condition

$$\phi_{ij} = \begin{cases} O(\frac{1}{|\boldsymbol{x}|}) & \text{for } x > 0 \\ o(1) & \text{for } x < 0 \end{cases} \quad \text{as } |\boldsymbol{x}| \to \infty \quad \text{for } i = 1, 2, 3 \tag{9}$$

(5) The bottom condition

$$\nabla \phi_{3j} \to 0 \quad \text{as } z \to -\infty \tag{10}$$

where $k_0 = \frac{g}{U_0^2}$, $O(x)$ and $o(x)$ denote the Landau order symbols as defined by Erdelyi (1956). Here h_i is the vertical separation of the free surface and i^{th} interface, h_j is the vertical separation of the origin and the free surface.

Equation 5 ensures the fluid disturbance can be described by potential flow theory. Equation 6 describes a combination of the kinematic and dynamic conditions applied on the free surface. The kinematic condition ensures that the fluid particles cannot pass through the disturbed free surface, the dynamic condition constrains the pressure in the fluid at the disturbed free surface to be atmospheric. The application of this boundary condition allows the presence of wave systems on the free surface. Equation 7 ensures the vertical velocity is continuous across the interfaces. Equation 8 describes a similar condition to equation 6 but applied at the interfaces. Equation 9 requires that the waves only exist behind the body and there are no waves upstream. Equation 10 imposes the condition that the disturbance velocity potential decays with increasing depth.

3.2 Derivation of Green's Functions

The disturbance velocity potential solution can be obtained from the summation of a Green's function solution, $G_{ij}(\boldsymbol{x}\ ,\boldsymbol{\xi})$. That is, the Green's function solution is an expression modelling a single source of unit strength in the fluid system.

$$\phi_{ij}(\boldsymbol{x}\ ,\boldsymbol{\xi}) = \int_{-\frac{L}{2}}^{\frac{L}{2}} Q(\xi) G_{ij}(\boldsymbol{x};\xi,0,\zeta=-f)d\xi \tag{11}$$

This implies that $\phi_{ij}(\boldsymbol{x}\ ,\boldsymbol{\xi})$ in the boundary conditions 5 - 10 can be replaced by $G_{ij}(\boldsymbol{x}\ ,\boldsymbol{\xi})$

To ensure that equation 5 is satisfied, it is assumed that the Green's functions are of the form

$$G_{ij}(\boldsymbol{x}\ ,\boldsymbol{\xi}\ ) = -\frac{\delta_{ij}}{2\pi}\int_{-\pi}^{\pi}\int_{0}^{\infty} e^{k[iw\pm(z-\zeta)]}dkd\theta \qquad \begin{matrix} + & z-\zeta<0 \\ - & z-\zeta>0 \end{matrix}$$

$$+\int_{-\pi}^{\pi}\int_{0}^{\infty}\left[A_{ij}(k,\theta)e^{kz}+B_{ij}(k,\theta)e^{-kz}\right]e^{ikw}dkd\theta \tag{12}$$

for j=1,2,3 and i=1,2,3. Here δ_{ij} denotes the Kronecker delta function,

$$w = (x-\xi)\cos\theta + (y-\eta)\sin\theta \tag{13}$$

and $B_{3j}(k,\theta)=0$ to comply with the condition stated in equation 10.

The method of solution involves the substitution of the Green's functions into the free surface and interface conditions, thus forming a system of equations from which the unknown coefficients $A_{ij}(k,\theta)$ and $B_{ij}(k,\theta)$ can be determined.

3.3 Derivation of Greens Functions for the body in the upper layer

Substituting equation 12 into the boundary conditions 5-8 when $j = 1$ produces the system of equations

$$\begin{bmatrix} 1 & a & 0 & 0 & 0 \\ \delta_1 e^{-kt_1} & a\delta_1 e^{kt_1} & -e^{-kt_1} & -ae^{kt_1} & 0 \\ e^{-kt_1} & -e^{kt_1} & -e^{-kt_1} & e^{kt_1} & 0 \\ 0 & 0 & \delta_2 e^{-k(t_1+t_2)} & a\delta_2 e^{k(t_1+t_2)} & -e^{-k(t_1+t_2)} \\ 0 & 0 & e^{-k(t_1+t_2)} & -e^{k(t_1+t_2)} & -e^{-k(t_1+t_2)} \end{bmatrix} \begin{Bmatrix} A_{11} \\ B_{11} \\ A_{21} \\ B_{21} \\ A_{31} \end{Bmatrix} = \frac{1}{2\pi} \begin{Bmatrix} ae^{k\zeta} \\ \delta_1 e^{-k(t_1+\zeta)} \\ e^{-k(t_1+\zeta)} \\ 0 \\ 0 \end{Bmatrix} \tag{14}$$

where $\delta_1 = \frac{\rho_1}{\rho_2}$, $\delta_2 = \frac{\rho_2}{\rho_3}$, $k_f = \frac{k_0}{\cos^2\theta}$ and $a = \frac{k+k_f}{k-k_f}$.
Solving for $A_{i1}(k,\theta)$ and $B_{i1}(k,\theta)$ then substituting into equation 12, we obtain the results:

$$G_{11}(\boldsymbol{x}\ ,\boldsymbol{\xi}) = -\frac{1}{2\pi}\int_{-\pi}^{\pi}\int_{0}^{\infty} e^{k[iw\pm(z-\zeta)]}dkd\theta$$

$$+\frac{1}{2\pi}\int_{-\pi}^{\pi}\int_{0}^{\infty} \frac{ae^{k(iw+z)}\left\{(1+a\delta_2)e^{kt_2}\left[(1+a\delta_1)e^{k(t_1+\zeta)}+(1-\delta_1)e^{-k(t_1+\zeta)}\right]+(1-\delta_2)e^{-kt_2}\left[a(1-\delta_1)e^{k(t_1+\zeta)}+(a+\delta_1)e^{-k(t_1+\zeta)}\right]\right\}}{(1+a\delta_2)e^{kt_2}\left[(1+a\delta_1)e^{kt_1}+a(1-\delta_1)e^{-kt_1}\right]+a(1-\delta_2)e^{-kt_2}\left[(1-\delta_1)e^{kt_1}+(a+\delta_1)e^{-kt_1}\right]}dkd\theta$$

$$+\frac{1}{2\pi}\int_{-\pi}^{\pi}\int_{0}^{\infty} \frac{e^{k(iw-z)}(ae^{k(\zeta-t_1)}-e^{-k(\zeta+t_1)})\left[(1-\delta_1)(1+a\delta_2)e^{kt_2}+(a+\delta_1)(1-\delta_2)e^{-kt_2}\right]}{(1+a\delta_2)e^{kt_2}\left[(1+a\delta_1)e^{kt_1}+a(1-\delta_1)e^{-kt_1}\right]+a(1-\delta_2)e^{-kt_2}\left[(1-\delta_1)e^{kt_1}+(a+\delta_1)e^{-kt_1}\right]}dkd\theta \quad 0 \geq z \geq -t_1 \tag{15}$$

$$G_{21}(\boldsymbol{x}\ ,\boldsymbol{\xi}) = -\frac{1}{2\pi}\int_{-\pi}^{\pi}\int_{0}^{\infty} \frac{\delta_1(1+a)(e^{-k\zeta}-ae^{k\zeta})\left[(1+a\delta_2)e^{k(z+t_1+t_2)}+(1-\delta_2)e^{-k(z+t_1+t_2)}\right]e^{ikw}}{(1+a\delta_2)e^{kt_2}\left[(1+a\delta_1)e^{kt_1}+a(1-\delta_1)e^{-kt_1}\right]+a(1-\delta_2)e^{-kt_2}\left[(1-\delta_1)e^{kt_1}+(a+\delta_1)e^{-kt_1}\right]}dkd\theta \quad -t_1 \geq z \geq -(t_1+t_2) \tag{16}$$

$$G_{31}(\boldsymbol{x}\ ,\boldsymbol{\xi}) = -\frac{1}{2\pi}\int_{-\pi}^{\pi}\int_{0}^{\infty} \frac{\delta_1\delta_2(1+a)^2(e^{-k\zeta}-ae^{k\zeta})e^{k(iw+z+t_1+t_2)}}{(1+a\delta_2)e^{kt_2}\left[(1+a\delta_1)e^{kt_1}+a(1-\delta_1)e^{-kt_1}\right]+a(1-\delta_2)e^{-kt_2}\left[(1-\delta_1)e^{kt_1}+(a+\delta_1)e^{-kt_1}\right]}dkd\theta \quad -(t_1+t_2) \geq z > -\infty \tag{17}$$

3.4 Derivation of Greens Functions for the body in the middle layer

Substituting equation 12 into the boundary conditions 5-8 when $j = 2$ produces the system of equations

$$\begin{bmatrix} e^{kt_1} & ae^{-kt_1} & 0 & 0 & 0 \\ 1 & -1 & -1 & 1 & 0 \\ -\delta_1 & -a\delta_1 & 1 & a & 0 \\ 0 & 0 & e^{-kt_2} & -e^{kt_2} & -e^{-kt_2} \\ 0 & 0 & \delta_2 e^{-kt_2} & a\delta_2 e^{kt_2} & -e^{-kt_2} \end{bmatrix} \begin{Bmatrix} A_{12} \\ B_{12} \\ A_{22} \\ B_{22} \\ A_{32} \end{Bmatrix} = \frac{1}{2\pi} \begin{Bmatrix} 0 \\ e^{k\zeta} \\ ae^{k\zeta} \\ e^{-k(t_2+\zeta)} \\ \delta_2 e^{-k(t_2+\zeta)} \end{Bmatrix} \tag{18}$$

Solving for $A_{i2}(k,\theta)$ and $B_{i2}(k,\theta)$ then substituting into equation 12, we obtain the results:

$$G_{12}(\boldsymbol{x},\boldsymbol{\xi}) = \frac{1}{2\pi}\int_{-\pi}^{\pi}\int_{0}^{\infty} \frac{(1+a)e^{ikw}\left[(1+a\delta_2)e^{k(t_2+\zeta)} + (1-\delta_2)e^{-k(t_2+\zeta)}\right]\left(ae^{k(z-t_1)} - e^{-k(z-t_1)}\right)}{(1+a\delta_2)e^{kt_2}\left[(1+a\delta_1)e^{kt_1} + a(1-\delta_1)e^{-kt_1}\right] + a(1-\delta_2)e^{-kt_2}\left[(1-\delta_1)e^{kt_1} + (a+\delta_1)e^{-kt_1}\right]} dkd\theta \quad t_1 \geq z \geq 0 \tag{19}$$

$$G_{22}(\boldsymbol{x},\boldsymbol{\xi}) = -\frac{1}{2\pi}\int_{-\pi}^{\pi}\int_{0}^{\infty} e^{k[iw\pm(z-\zeta)]}dkd\theta$$

$$+\frac{1}{2\pi}\int_{-\pi}^{\pi}\int_{0}^{\infty} \frac{ae^{k(iw+z)}\left\{(1-\delta_1)e^{kt_1}\left[(1+a\delta_2)e^{k(t_2+\zeta)} + (1-\delta_2)e^{-k(t_2+\zeta)}\right] + (a+\delta_1)e^{-kt_1}\left[(1+a\delta_2)e^{k(t_2+\zeta)} + (1-\delta_2)e^{-k(t_2+\zeta)}\right]\right\}}{(1+a\delta_2)e^{kt_2}\left[(1+a\delta_1)e^{kt_1} + a(1-\delta_1)e^{-kt_1}\right] + a(1-\delta_2)e^{-kt_2}\left[(1-\delta_1)e^{kt_1} + (a+\delta_1)e^{-kt_1}\right]} dkd\theta$$

$$-\frac{1}{2\pi}\int_{-\pi}^{\pi}\int_{0}^{\infty} \frac{(1-\delta_2)e^{k(iw-z-t_2)}\left\{e^{kt_1}\left[(1+a\delta_1)e^{-k\zeta} - a(1-\delta_1)e^{k\zeta}\right] + ae^{-kt_1}\left[(1-\delta_1)e^{-k\zeta} - (a+\delta_1)e^{k\zeta}\right]\right\}}{(1+a\delta_2)e^{kt_2}\left[(1+a\delta_1)e^{kt_1} + a(1-\delta_1)e^{-kt_1}\right] + a(1-\delta_2)e^{-kt_2}\left[(1-\delta_1)e^{kt_1} + (a+\delta_1)e^{-kt_1}\right]} dkd\theta \quad 0 \geq z \geq -t_2 \tag{20}$$

$$G_{32}(\boldsymbol{x},\boldsymbol{\xi}) = \frac{1}{2\pi}\int_{-\pi}^{\pi}\int_{0}^{\infty} \frac{\delta_2(1+a)e^{k(iw+z+t_2)}\left\{e^{kt_1}\left[a(1-\delta_1)e^{k\zeta} - (1+a\delta_1)e^{-k\zeta}\right] + ae^{-kt_1}\left[(a+\delta_1)e^{k\zeta} - (1-\delta_1)e^{-k\zeta}\right]\right\}}{(1+a\delta_2)e^{kt_2}\left[(1+a\delta_1)e^{kt_1} + a(1-\delta_1)e^{-kt_1}\right] + a(1-\delta_2)e^{-kt_2}\left[(1-\delta_1)e^{kt_1} + (a+\delta_1)e^{-kt_1}\right]} dkd\theta \quad -t_2 \geq z > -\infty \tag{21}$$

3.5 Derivation of Greens Functions for the body in the lower layer

Substituting equation 12 into the boundary conditions 5-8 when $j = 3$ with the body in the lower layer produces the system of equations

$$\begin{bmatrix} e^{k(t_1+t_2)} & ae^{-k(t_1+t_2)} & 0 & 0 & 0 \\ \delta_1 e^{kt_2} & a\delta_1 e^{-kt_2} & -e^{-kt_2} & -ae^{-kt_2} & 0 \\ e^{kt_2} & -e^{-kt_2} & -e^{-kt_2} & e^{-kt_2} & 0 \\ 0 & 0 & -\delta_2 & -a\delta_2 & 1 \\ 0 & 0 & 1 & -1 & -1 \end{bmatrix} \begin{Bmatrix} A_{13} \\ B_{13} \\ A_{23} \\ B_{23} \\ A_{33} \end{Bmatrix} = \frac{e^{k\zeta}}{2\pi} \begin{Bmatrix} 0 \\ 0 \\ 0 \\ a \\ 1 \end{Bmatrix} \tag{22}$$

Solving for $A_{i3}(k,\theta)$ and $B_{i3}(k,\theta)$ then substituting into equation 12, we obtain the results:

$$G_{13}(\boldsymbol{x},\boldsymbol{\xi}) = \frac{1}{2\pi}\int_{-\pi}^{\pi}\int_{0}^{\infty} \frac{(1+a)^2 e^{k(iw+\zeta)}(ae^{k(z-t_1-t_2)} - e^{-k(z-t_1-t_2)})}{(1+a\delta_2)e^{kt_2}\left[(1+a\delta_1)e^{kt_1} + a(1-\delta_1)e^{-kt_1}\right] + a(1-\delta_2)e^{-kt_2}\left[(1-\delta_1)e^{kt_1} + (a+\delta_1)e^{-kt_1}\right]} dk d\theta \quad t_1+t_2 \geq z \geq t_2 \tag{23}$$

$$G_{23}(\boldsymbol{x},\boldsymbol{\xi}) = \frac{1}{2\pi}\int_{-\pi}^{\pi}\int_{0}^{\infty} \frac{(1+a)e^{k(iw+\zeta)}\left\{ae^{k(z-t_2)}\left[(1-\delta_1)e^{kt_1} + (a+\delta_1)e^{-kt_1}\right] - e^{-k(z-t_2)}\left[(1+a\delta_1)e^{kt_1} + a(1-\delta_1)e^{-kt_1}\right]\right\}}{(1+a\delta_2)e^{kt_2}\left[(1+a\delta_1)e^{kt_1} + a(1-\delta_1)e^{-kt_1}\right] + a(1-\delta_2)e^{-kt_2}\left[(1-\delta_1)e^{kt_1} + (a+\delta_1)e^{-kt_1}\right]} dk d\theta \quad t_2 \geq z \geq 0 \tag{24}$$

$$G_{33}(\boldsymbol{x},\boldsymbol{\xi}) = -\frac{1}{2\pi}\int_{-\pi}^{\pi}\int_{0}^{\infty} e^{k[iw\pm(z-\zeta)]} dk d\theta$$

$$+\frac{1}{2\pi}\int_{-\pi}^{\pi}\int_{0}^{\infty} \frac{ae^{k(iw+z+\zeta)}\left\{e^{kt_1}\left[(1+a\delta_1)(1-\delta_2)e^{kt_2} + (1-\delta_1)(a+\delta_2)e^{-kt_2}\right] + e^{-kt_1}\left[a(1-\delta_1)(1-\delta_2)e^{kt_2} + (a+\delta_1)(a+\delta_2)e^{-kt_2}\right]\right\}}{(1+a\delta_2)e^{kt_2}\left[(1+a\delta_1)e^{kt_1} + a(1-\delta_1)e^{-kt_1}\right] + a(1-\delta_2)e^{-kt_2}\left[(1-\delta_1)e^{kt_1} + (a+\delta_1)e^{-kt_1}\right]} dk d\theta \quad 0 \geq z > -\infty \tag{25}$$

3.6 Application of the radiation condition

The Green's functions 15 - 17, 19 - 21 and 23 - 25 now satisfy the boundary conditions 5-8 and 10, the radiation condition however has yet to be addressed. The wavenumber integration, involving the circumvention of the singularities present in the Green's functions, provides an opportunity to examine the functions as $x \rightarrow \infty$. The upstream expressions are then subtracted from the Green's functions to provide equations satisfying all boundary conditions. An example of this process for a body located in the upper layer of a two layer fluid is given by Wang (1989), pages 70-78.

3.7 Complete velocity potentials

The following Green's functions comply with all the boundary conditions described in 3.1

$$G_{ij}(\boldsymbol{x}\ ,\boldsymbol{\xi}) = -\delta_{ij}\left(\frac{1}{r_1}+\frac{1}{r_2}\right)+\frac{1}{\pi}\int_0^{\frac{\pi}{2}} P.V.\int_0^{\infty}\frac{F_{ij}(k,\theta)C(k,\theta)}{(k-k_f)D(k,\theta)}dkd\theta+\int_0^{\frac{\pi}{2}}\frac{F_{0_j}(\theta)S(k_f,\theta)}{D_0(\theta)}d\theta$$

$$+\sum_{l=1}^{N_r}\int_{\theta_0}^{\frac{\pi}{2}}\frac{F_{ij}(\alpha_l,\theta)S(\alpha_l,\theta)}{(\alpha_l-k_f)D_k(\alpha_l,\theta)}d\theta \tag{26}$$

here *P.V.* denotes Cauchy's principal value integral, α_l is the l^{th} root of k determined from the equation $D(k,\theta)=0$ and N_r is the number of non zero roots of $D(k,\theta)=0$,

$$C(k,\theta) = \cos[k(x-\xi)\cos\theta]\cos[k(y-\eta)\sin\theta] \tag{27}$$

$$D(k,\theta) = \delta_1 k(1-\delta_2)(k+k_f)e^{-kt_2}\sinh(kt_1)$$

$$-[\cosh(kt_1)+\delta_1\sinh(kt_1)][\cosh(kt_2)+\delta_2\sinh(kt_2)][k-\frac{k(1-\delta_1)\tanh(kt_1)}{1+\delta_1\tanh(kt_1)}][k-\frac{k(1-\delta_2)\tanh(kt_2)}{1+\delta_2\tanh(kt_2)}] \tag{28}$$

$$D_0(k,\theta) = -[\delta_1\delta_2+(1-\delta_1)\delta_2 e^{-2k_f t_1}+(1-\delta_2)e^{-2k(t_1+t_2)}] \tag{29}$$

$$D_k(k,\theta) = \frac{\partial\{D(k,\theta)\}}{\partial k}e^{-k(t_1+t_2)} \tag{30}$$

$$F_{0_1}(\theta) = -4\delta_1\delta_2 k_f e^{k_f(z+\zeta)} \tag{31}$$

$$F_{0_2}(\theta) = -4\delta_2 k_f e^{k_f(z+\zeta-2t_1)} \tag{32}$$

$$F_{0_3}(\theta) = -4k_f e^{k_f(z+\zeta-2t_1-2t_2)} \tag{33}$$

$$r_1 = \sqrt{(x-\xi)^2+(y-\eta)^2+(z-\zeta)^2} \tag{34}$$

$$r_2 = \sqrt{(x-\xi)^2+(y-\eta)^2+(z+\zeta)^2} \tag{35}$$

$$S(k,\theta) = \sin[k(x-\xi)\cos\theta]\cos[k(y-\eta)\sin\theta] \tag{36}$$

and the 'F' functions are defined as

$$F_{11}(k,\theta) = -\frac{1}{2}(k+k_f)e^{kz}\left[(k-k_f)+\delta_2(k+k_f)\right]\left\{\left[(k-k_f)+\delta_1(k+k_f)\right]e^{k\zeta}+(k-k_f)(1-\delta_1)e^{-k(2t_1+\zeta)}\right\}$$

$$-\frac{1}{2}(k+k_f)(k-k_f)(1-\delta_2)e^{k(z-2t_2)}\left\{(k+k_f)(1-\delta_1)e^{k\zeta}+\left[(k+k_f)+\delta_1(k-k_f)\right]e^{-k(2t_1+\zeta)}\right\}$$

$$-\frac{1}{2}(k-k_f)e^{-k(2t_1+z)}\left[(k+k_f)e^{k\zeta}-(k-k_f)e^{-k\zeta}\right]\left\{(1-\delta_1)\left[(k-k_f)+\delta_2(k+k_f)\right]+(1-\delta_2)\left[(k+k_f)+\delta_1(k-k_f)\right]e^{-2kt_2}\right\} \tag{37}$$

$$F_{12}(k,\theta) = -k\left\{\left[(k-k_f)+\delta_2(k+k_f)\right]e^{k\zeta}+(1-\delta_2)(k-k_f)e^{-k(2t_2+\zeta)}\right\}\left[(k+k_f)e^{k(z-2t_1)}-(k-k_f)e^{-kz}\right] \tag{38}$$

$$F_{13}(k,\theta) = -2k^2e^{k\zeta}\left[(k+k_f)e^{(z-2t_1-2t_2)}-(k-k_f)e^{-kz}\right] \tag{39}$$

$$F_{21}(k,\theta) = -\delta_1 k\left[(k+k_f)e^{k\zeta}-(k-k_f)e^{-k\zeta}\right]\left\{\left[(k-k_f)+\delta_2(k+k_f)\right]e^{kz}+(1-\delta_2)(k-k_f)e^{-k(z+2t_1+2t_2)}\right\} \tag{40}$$

$$F_{22}(k,\theta) = -\frac{1}{2}(k+k_f)e^{kz}\left\{\left[(k-k_f)+\delta_2(k+k_f)\right]e^{k\zeta}+(1-\delta_2)(k-k_f)e^{-k(2t_2+\zeta)}\right\}\left[(1-\delta_1)(k+k_f)+\left[(k+k_f)+\delta_1(k-k_f)\right]e^{-2kt_1}\right]$$

$$-\frac{1}{2}(1-\delta_2)(k-k_f)e^{-k(z+2t_2)}\left\{(k-k_f)\left[(1-\delta_1)(k+k_f)e^{k\zeta}-\left[(k-k_f)+\delta_1(k+k_f)\right]e^{-k\zeta}\right]+(k+k_f)e^{-2kt_1}\left[\left[(k+k_f)+\delta_1(k-k_f)\right]e^{k\zeta}-(1-\delta_1)(k+k_f)e^{-k\zeta}\right]\right\} \tag{41}$$

$$F_{23}(k,\theta) = -ke^{k\zeta}\left\{(k+k_f)e^{k(z-2t_2)}\left[(1-\delta_1)(k-k_f)+\left[(k+k_f)+\delta_1(k-k_f)\right]e^{-2kt_1}\right]-(k-k_f)e^{-kz}\left[(k-k_f)+\delta_1(k+k_f)+(1-\delta_1)(k+k_f)e^{-2kt_1}\right]\right\} \tag{42}$$

$$F_{31}(k,\theta) = -2\delta_1\delta_2k^2\left[(k+k_f)e^{k\zeta}-(k-k_f)e^{-k\zeta}\right]e^{kz} \tag{43}$$

$$F_{32}(k,\theta) = -\delta_2 ke^{kz}\left\{(k-k_f)\left[(1-\delta_1)(k+k_f)e^{k\zeta}-\left[(k-k_f)+\delta_1(k+k_f)\right]e^{-k\zeta}\right]+(k+k_f)e-2kt_1\left[\left[(k+k_f)+\delta_1(k-k_f)\right]e^{k\zeta}-(1-\delta_1)(k-k_f)e^{-k\zeta}\right]\right\} \tag{44}$$

$$F_{33}(k,\theta) = -\frac{1}{2}(k+k_f)(k-k_f)e^{k(z+\zeta)}\left\{(1-\delta_2)\left[(k-k_f)+\delta_1(k+k_f)\right]+(1-\delta_1)\left[(k+k_f)+\delta_2(k-k_f)\right]e^{-2kt_2}\right\}$$

$$-\frac{1}{2}(k+k_f)e^{k(z+\zeta-2kt_1)}\left\{(1-\delta_1)(1-\delta_2)(k-k_f)(k+k_f)+\left[(k+k_f)+\delta_1(k-k_f)\right]\left[(k+k_f)+\delta_2(k-k_f)\right]e^{-2kt_2}\right\} \tag{45}$$

In these expressions the lower limit of the theta integral, θ_0, is given by

$$\theta_0 = \begin{cases} 0 & N_r = 2 & & U_0 \le U_{cl} \\ 0 & N_r = \begin{cases} 1 & 0 \le \theta < \theta_1 \\ 2 & \theta_1 \le \theta \le \frac{\pi}{2} \end{cases} & & U_{cl} < U_0 \le U_{cu} \\ \theta_2 & N_r = \begin{cases} 1 & \theta_2 \le \theta < \theta_1 \\ 2 & \theta_1 \le \theta \le \frac{\pi}{2} \end{cases} & & U_0 > U_{cu} \end{cases} \tag{46}$$

where

$$\theta_1 = \cos^{-1}\left(\frac{U_{cl}}{U_0}\right) \tag{47}$$

$$\theta_2 = \cos^{-1}\left(\frac{U_{cu}}{U_0}\right) \tag{48}$$

$$U_{cl} = \left(\frac{g}{s_+}\right)^{\frac{1}{2}} \tag{49}$$

$$U_{cu} = \left(\frac{g}{s_-}\right)^{\frac{1}{2}} \tag{50}$$

$$s_\pm = \frac{b \pm (b^2 - 4a)^{\frac{1}{2}}}{2a} \tag{51}$$

$$a = (1 - \delta_1)(1 - \delta_2)t_1 t_2 \tag{52}$$

$$b = (1 - \delta_1)t_1 + (1 - \delta_2)t_2 + \delta_1(1 - \delta_2)t_1 \tag{53}$$

Substituting the Green's functions into equation 11 and completing the ξ integration produces the velocity potential for the i^{th} layer we find that when the body is moving in the j^{th} layer

$$\phi_{ij}(\boldsymbol{x}, \boldsymbol{\xi}) = -\frac{\xi^2 \delta_{ij}}{2}\left(\frac{1}{r_1} + \frac{1}{r_2}\right) + \frac{1}{\pi}\int_0^{\frac{\pi}{2}} P.V. \int_0^\infty \frac{F_{ij}(k,\theta)P_1(k,\theta)}{(k - k_f)D(k,\theta)} dk d\theta + \int_0^{\frac{\pi}{2}} \frac{F_{0_j}(\theta)P_2(k_f,\theta)}{D_0(\theta)} d\theta$$

$$\sum_{l=1}^{N_r} \int_{\theta_0}^{\frac{\pi}{2}} \frac{F_{ij}(\alpha_l,\theta)P_2(\alpha_l,\theta)}{(\alpha_l - k_f)D_k(\alpha_l,\theta)} d\theta \tag{54}$$

where

$$P_1(k,\theta) = \sin(kx\cos\theta)\cos\left[k(y-\eta)\sin\theta\right] P_3(k,\theta) \tag{55}$$

$$P_2(k,\theta) = -\cos(kx\cos\theta)\cos\left[k(y-\eta)\sin\theta\right] P_3(k,\theta) \tag{56}$$

$$P_3(k,\theta) = U_0\left(\frac{d}{kL\cos\theta}\right)^2\left[\sin\left(\frac{kL\cos\theta}{2}\right) - \frac{kL}{2}\cos\theta\cos\left(\frac{kL\cos\theta}{2}\right)\right] \tag{57}$$

and the far field expressions for the velocity potentials are

$$\phi_{ij}(\boldsymbol{x}, \boldsymbol{\xi}) = \int_0^{\frac{\pi}{2}} \frac{F_{0_j}(\theta)P_2(k_f,\theta)}{D_0(\theta)} d\theta$$

$$+ \sum_{l=1}^{N_r} \int_{\theta_0}^{\frac{\pi}{2}} \frac{F_{ij}(\alpha_l,\theta)P_2(\alpha_l,\theta)}{(\alpha_l - k_f)D_k(\alpha_l,\theta)} d\theta \tag{58}$$

The velocity potentials defined in equation 54 reduce to the velocity potentials describing a body moving in a two layer fluid when either of the density ratios δ_1 or δ_2 is equated to unity. The reduction also occurs when either of the layer thicknesses is zero. Finally the velocity potential for a body moving in a homogeneous fluid can be obtained when an appropriate combination of two of the four options above are applied to equation 54.

4 Far field free surface and interface disturbances

The linearised disturbance on the free surface, ζ_1, is given by

$$\zeta_1(x,y) = \frac{U_0}{g}\phi_{1j_x} \tag{59}$$

and on the i^{th} interface

$$\zeta_i(x,y) = \frac{1}{\rho_i - \rho_{i-1}}\frac{U_0}{g}[\rho_i\phi_{ij_x} - \rho_{i-1}\phi_{(i-1)j_x}] \quad \text{for } i = 2,3 \tag{60}$$

Substituting equation 58 into equation 59 yields the far field surface elevation caused by the moving prolate spheroid and this may be written in the form

$$\zeta_1(x,y) = \frac{2U_0}{g}\int_0^{\frac{\pi}{2}} \frac{F_{0_j}(\theta)P_4(k_f,\theta)}{D_0(\theta)}d\theta$$

$$+ \frac{2U_0}{g}\sum_{l=1}^{N_r}\int_{\theta_0}^{\frac{\pi}{2}} \frac{F_{1j}(\alpha_l,\theta)P_4(\alpha_l,\theta)}{(\alpha_l - k_f)D_k(\alpha_l,\theta)}d\theta \tag{61}$$

and the far field interface elevation on the i^{th} interface is given by

$$\zeta_i(x,y) = \frac{2U_0}{g}\int_0^{\frac{\pi}{2}} \frac{F_{0_j}(\theta)P_4(k_f,\theta)}{D_0(\theta)}d\theta$$

$$+ \frac{2U_0}{g}\sum_{l=1}^{N_r}\int_{\theta_0}^{\frac{\pi}{2}} \frac{F_{ij}(\alpha_l,\theta)P_4(\alpha_l,\theta)}{(\alpha_l - k_f)D_k(\alpha_l,\theta)}d\theta \quad \text{for } i = 2,3 \tag{62}$$

where

$$P_4(k,\theta) = \frac{\partial\{P_2(k,\theta)\}}{\partial x} \tag{63}$$

5 Wave resistance

An expression for the wave resistance of the body can be derived using a three dimensional extension of Lagally's method (Sabuncu, 1961; Wang, 1989). In an ideal fluid a singularity $\boldsymbol{x} = (\xi', \eta', \zeta')$ experiences a resultant force due to the free stream and other singularities. The summation of these forces is equal to the wave resistance. Mathematically for a slender body this can be written in the form

$$R_w = -4\pi\rho_j \int_{-\frac{L}{2}}^{\frac{L}{2}} Q(\xi')\phi_{jj_x}(\boldsymbol{x},\boldsymbol{\xi})\Big|_{\boldsymbol{x}=(\xi',\eta,\zeta)} d\xi' \tag{64}$$

The substitution of equations 4, 11 and 26 into equation 64 gives

$$R_w = -4\pi\rho_j \left[2\pi U_0\left(\frac{d}{L}\right)^2\right]^2 \int_{-\frac{L}{2}}^{\frac{L}{2}}\int_{-\frac{L}{2}}^{\frac{L}{2}} \xi'\xi G_{jj_x}(\boldsymbol{x},\boldsymbol{\xi})\Big|_{\boldsymbol{x}=(\xi',\eta,\zeta)} d\xi d\xi' \tag{65}$$

and with the substitution of $G_{jj}(\boldsymbol{x},\boldsymbol{\xi})$ together with the results

$$\int_{-\frac{L}{2}}^{\frac{L}{2}}\int_{-\frac{L}{2}}^{\frac{L}{2}} \xi^{'}\xi \sin[k(\xi^{'}-\xi)\cos\theta]d\xi d\xi^{'} = 0 \tag{66}$$

$$\int_{-\frac{L}{2}}^{\frac{L}{2}}\int_{-\frac{L}{2}}^{\frac{L}{2}} \xi^{'}\xi(\xi^{'}-\xi)\left(\frac{1}{r_1}+\frac{1}{r_2}\right)_x \Big|_{\boldsymbol{x}=(\xi^{'},\eta,\zeta)} d\xi d\xi^{'} = 0 \tag{67}$$

we find that

$$R_w = -\rho_j\left[2\pi U_0\left(\frac{d}{L}\right)^2\right]^2 \int_0^{\frac{\pi}{2}} \frac{k_f\cos\theta F_{0_j}(\theta)T(k_f,\theta)}{D_0(\theta)}d\theta$$

$$+\sum_{l=1}^{N_r}\int_{\theta_0}^{\frac{\pi}{2}} \frac{\alpha_l\cos\theta F_{jj}(\alpha_l,\theta)T(\alpha_l,\theta)}{(\alpha_l-k_f)D_k(\alpha_l,\theta)}d\theta \tag{68}$$

where

$$T(k,\theta) = \left\{\frac{L}{k\cos\theta}\left(\frac{1}{\frac{kL}{2}\cos\theta}\sin(\frac{kL}{2}\cos\theta)-\cos(\frac{kL}{2}\cos\theta)\right)\right\}^2 \tag{69}$$

The wave resistance of a body moving in a two layer or homogeneous fluid may be obtained through reducing the number of fluid layers as detailed in section 3.7.

6 Discussion of results

Figures 2, 3 and 4 are the free surface and interface elevations generated by a prolate spheroid moving in the upper, middle and lower layers respectively. Only the port half of the disturbance is plotted as the wave system is symmetrical about the body centreplane (ie the plane $y = 0$). The area shown commences one body length behind the stern and extends nine body lengths longitudinally and six body lengths transversely from the centreline. The direction of motion of the body is towards the lower right hand side of the page. In all three cases the density of the upper layer, $\rho_1 = 1025\ Kg/m^3$, the density of the middle layer, $\rho_2 = 1026.5\ Kg/m^3$ and the density of the lower layer, $\rho_3 = 1028\ Kg/m^3$. The speed of the body is 2 m/s which lies in the supercritical region ($U_0 > U_{cu}$) for this fluid system. Therefore only the divergent part of the wave system is present. Additional information relevent to the each figure can be found in the captions.

The free surface shears corresponding to figures 2, 3 and 4 are the figures 5, 6 and 7 respectively. As previously, only the port half of the disturbance is plotted and the area shown is the $9L$ x $6L$ rectangle described in the paragraph above. The direction of motion of the body is towards the bottom of the page.

Figure 8 demonstrates the effect of the ratio L/d on the wave resistance experienced by the body. Here $L/d = 15$, 10 and 5 whilst a constant displacement is maintained. The effect of the diameter can readily be seen in equation 68, for the diameter dimension appears only outside the integral as a fourth power, the effect of length cannot be so easily determined as L also appears in the function $T(k,\theta)$. The non dimensional wave resistance coefficient is defined as $R_w/\frac{1}{2}\rho_j sU_0^2$. When the body is in the upper layer the effect of the free surface on C_w can clearly be observed. The presence of the stratification in the form of fluid layers produces a large spike at low Froude numbers when the body is moving in any layer. It is this spike which causes the "dead water" effect.

Figure 9 reveals how the maximum values of free surface and interface elevations are related to the speed of the body when the body is located in each layer. The maximum values of free surface and interface elevations are the maximum values present in the area behind the body (ie $9L$ x $6L$) as

previously described. The interfaces closest to the body display two maxima and a minimum, other interface disturbances have single peaks then decay monotonically with increasing speed.

Figures 10, 11, 12 and 13 display the change in the appearance of the free surface and interface wave patterns when the speed of the body is increased. At $U_0 = 0.25\ m/s$ the speed of the body is below the lower critical speed. The wave system consists of transverse waves and no divergent waves are present. As U_0 increases to $0.50\ m/s$, a speed which is between the lower and upper critical speeds a transition appears, a divergent contribution to the wave system is also apparent. Above the upper critical speed the tranverse portion of the wave system disappears and the disturbance consists of only the divergent waves. Any further increase in U_0 causes the disturbance to be contained within a decreasingly small angle given by $\frac{\pi}{2} - \theta_0$. These transitions are continuous, the divergent part of the wave system gradually becomes more prominent whilst the transverse part slowly decays. This implies that as the speed of the body increases the energy in the wave system shifts from a conc entration at low frequency to a concentration at high frequency.

The free surface shears corresponding to the wave systems generated at $U_0 = 0.25, 0.50, 1.50$ and $3.00\ m/s$, ie the figures 10, 11, 12 and 13 are the figures 14, 15, 16 and 17 respectively.

Figures 18 and 19 display the effect of the variation of the middle layer density when all other variables remain constant. The maximum values of elevations, currents and strains are the maximum values present in the area behind the body (ie $9L$ x $6L$) as previously described. When $\rho_2 = \rho_1$ or $\rho_2 = \rho_3$ the three layer fluid system reduces to a two layer fluid system. The points marked by triangles are the maximum values of the disturbance obtained from two layer theory. The trend clearly is towards the two layer results. The free surface disturbance increases when ρ_2 tends to ρ_1 whilst the first interface disturbance displays a maximum when ρ_2 is the average of the densities of the fluid from above and below the middle layer. The second interface disturbance has a maximum and minimum value over the density range.

7 Conclusion

The three layer model qualitively and quantitatively predicts the fluid disturbances and body forces produced by a body moving in a three layer fluid. The velocity potential, free surface elevation and wave resistance expressions reduce firstly to two layer expressions then to expressions describing a body in a homogeneous fluid. The "dead water" effect popularised by Ekman has been demonstrated to exist, its magnitude now calculable from a velocity potential solution. The results of the three layer fluid system will provide a useful comparison when the second stage of this investigation, a continuously stratified fluid, requires validation.

From a **submarine operational viewpoint**, if we assume a correlation between wavemaking resistance and wave pattern characteristics, there is evidence presented herein (e.g figure 8) to suggest that there is a small window of Froude numbers where the wavemaking resistance is a minimum and hence the wave pattern generated within the stratified fluid is less detectable. However before this operational benefit can be substantiated, more theoretical and experimental studies are needed.

References

Andrew, R. N., Baar, J. J. M., and Price, W. G. (1988). Prediction of ship wavemaking resistance and other steady flow parameters using neumann-kelvin theory. *Trans R.I.N.A.*, 130:119–133.

Apel, J. R. and Gjessing, D. T. (1989). Internal wave measurements in a Norwegian fjord using multi-frequency radars. *John Hopkins APL technical digest*, 10(4):295–306.

Baar, J. J. M. and Price, W. G. (1988). Developments in the calculation of the wavemaking resistance of ships. *Proc. R. Soc., London*, A416:115–147.

Crapper, G. D. (1967). Ship waves in a stratified ocean. *J. Fluid Mech*, 29(4):667–672.

Dysthe, K. B. and Trulsen, J. (1989). Internal waves from moving point sources. *John Hopkins APL technical digest*, 10(4):307–317.

Ekman, V. W. (1904). On dead water. *Scientific results of the Norwegian North Polar expedition 1893 - 1896*, 5(15):1–152. Publisher Kristiania, Editor Fridtjof Nansen.

Erdelyi, A. (1956). *Asymptotic expansions.* Dover.

Hudimac, A. A. (1961). Ship waves in a stratified ocean. *J. Fluid Mech*, 11:229–243.

Hughes, B. A. (1986). Surface wave wakes and internal wave wakes produced by surface ships. In *Proc. 16th Symp. on Naval Hydrodynamics*, pages 1–17, University of California, Berkeley. National Academy Press.

Keller, J. B. and Monk, W. H. (1970). Internal wave wakes of a body moving in a stratified fluid. *Phys. Fluids*, 13(6):1425–1431.

Miles, J. W. (1971). Internal waves generated by a horizontally moving point source. *Geophys. Fluid Dyn*, 2:63–87.

Price, W. G., Wang, Y., and Baar, J. J. M. (1988). Influence of fluid density on steady ship wave characteristics. In *Proc. 17th Symp. on Naval Hydrodynamics*, pages 63–78, The Hague. National Academy Press.

Rarity, B. S. H. (1967). The two dimensional wave pattern produced by a disturbance moving in an arbitrary direction in a density stratified liqiud. *J. Fluid Mech*, 30(2):329–336.

Sabuncu, T. (1961). The thoeretical wave resistance of a ship travelling under interfacial wave conditions. Norwegian ship model experiment tank publication 63, The Technical University of Norway.

Tulin, M. and Miloh, T. (1990). Ship internal waves in a shallow thermocline : the supersonic case. In *Proc. 18th Symp. on Naval Hydrodynamics*, pages 567–581, The University of Michigan, Ann Arbor. National Academy Press. I.S.B.N. 0-309-04575-4.

Wang, Y. (1989). *The influence of fluid stratification on wave making resistance and other steady flow parameters.* PhD thesis, Brunel University.

List of Figures

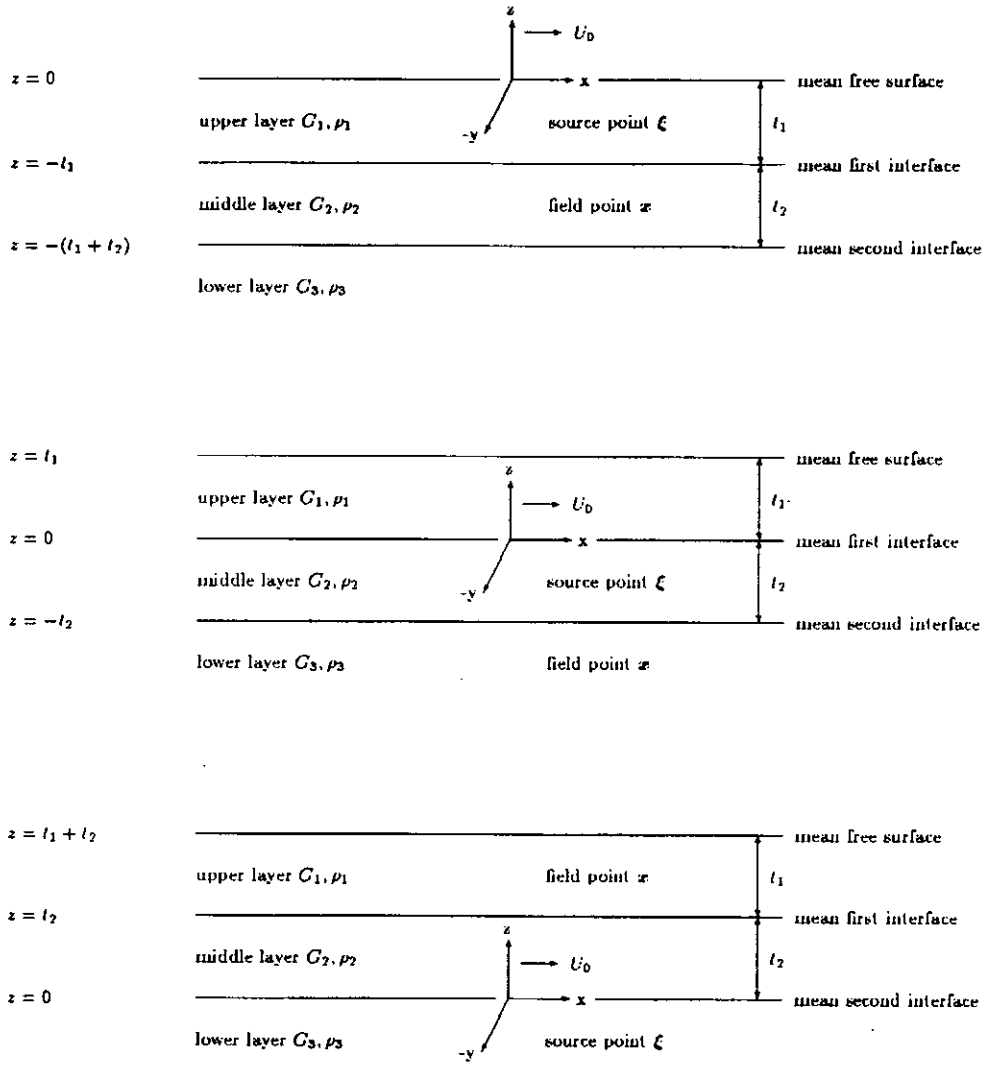

Figure 1: Configuration of the coordinate system.

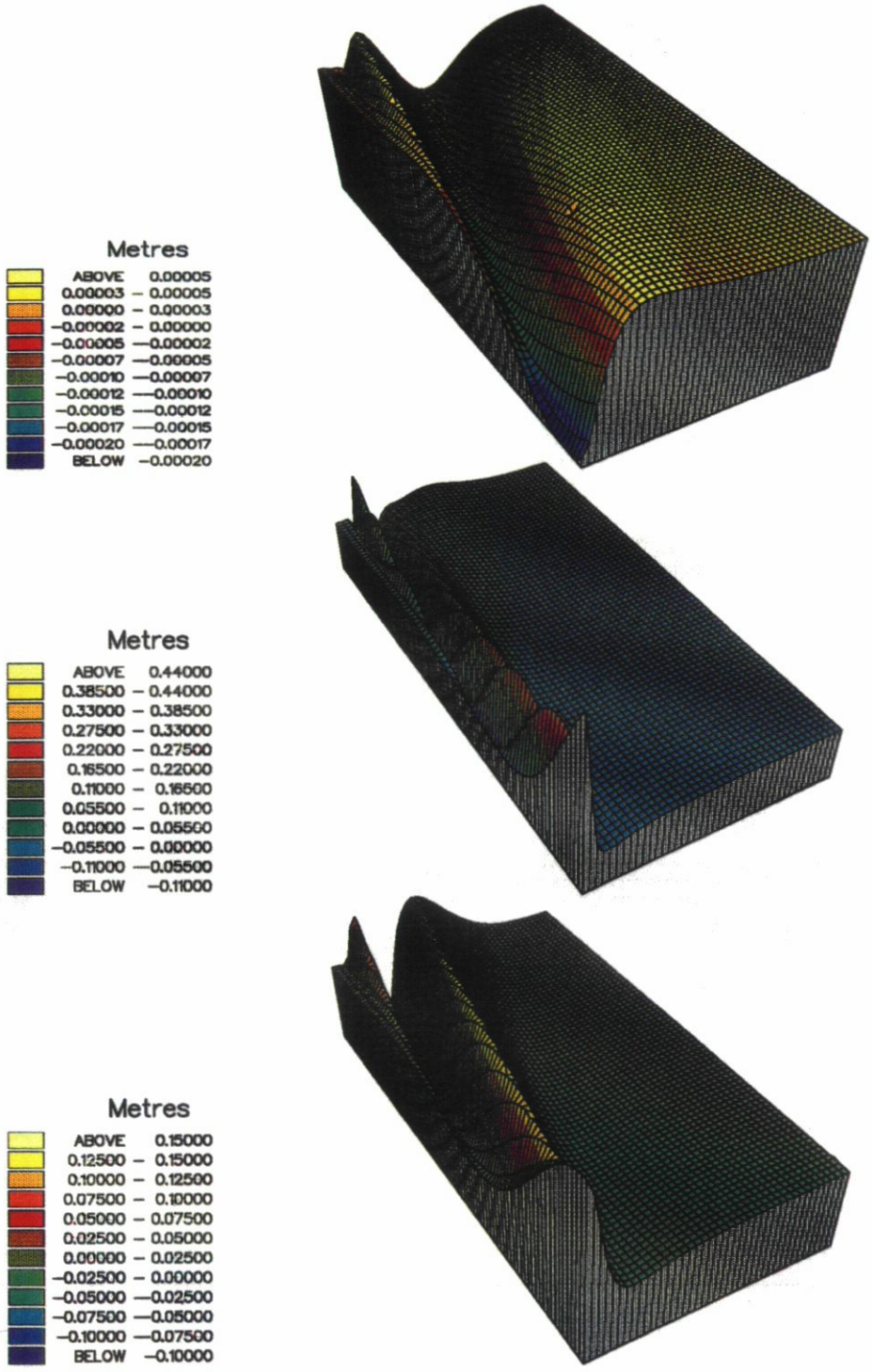

Figure 2: Free surface and interface wave systems when the body is in the upper layer. $U_0 = 2.0\ m/s$ $(F_n = 0.064)\ L = 100.0\ m\ d = 10.0\ m\ \rho_1 = 1025.0\ Kg/m^3\ \rho_2 = 1026.5\ Kg/m^3\ \rho_3 = 1028.0\ Kg/m^3$ $t_1 = 30.0\ m\ t_2 = 30.0\ m\ f = 15\ m$

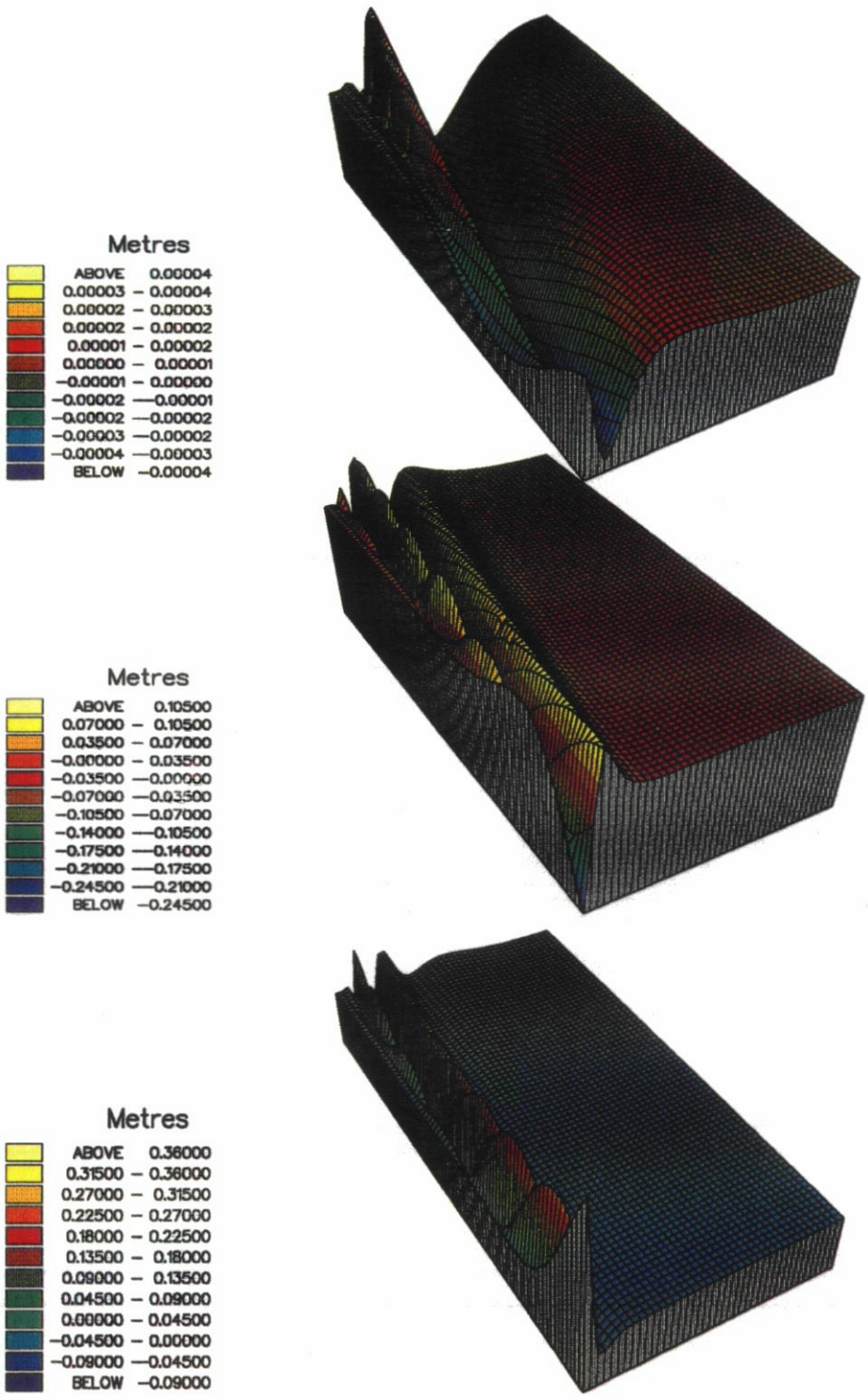

Figure 3: Free surface and interface wave systems when the body is in the middle layer. $U_0 = 2.0\ m/s$ $(F_n = 0.064)\ L = 100.0\ m\ d = 10.0\ m\ \rho_1 = 1025.0\ Kg/m^3\ \rho_2 = 1026.5\ Kg/m^3\ \rho_3 = 1028.0\ Kg/m^3$ $t_1 = 30.0\ m\ t_2 = 30.0\ m\ f = 45\ m$

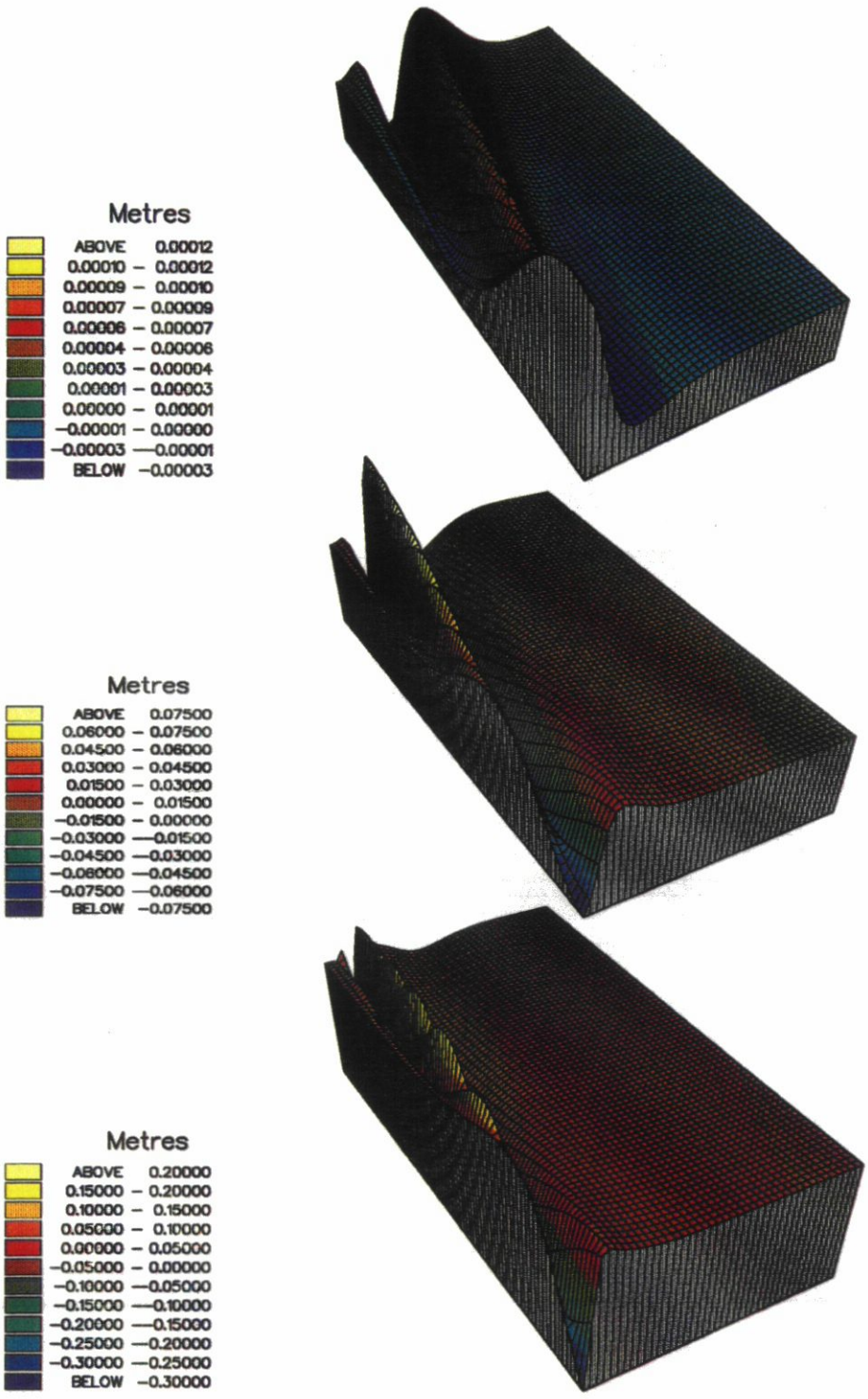

Figure 4: Free surface and interface wave systems when the body is in the lower layer. $U_0 = 2.0\ m/s$ $(F_n = 0.064)\ L = 100.0\ m\ d = 10.0\ m\ \rho_1 = 1025.0\ Kg/m^3\ \rho_2 = 1026.5\ Kg/m^3\ \rho_3 = 1028.0\ Kg/m^3$ $t_1 = 30.0\ m\ t_2 = 30.0\ m\ f = 75\ m$

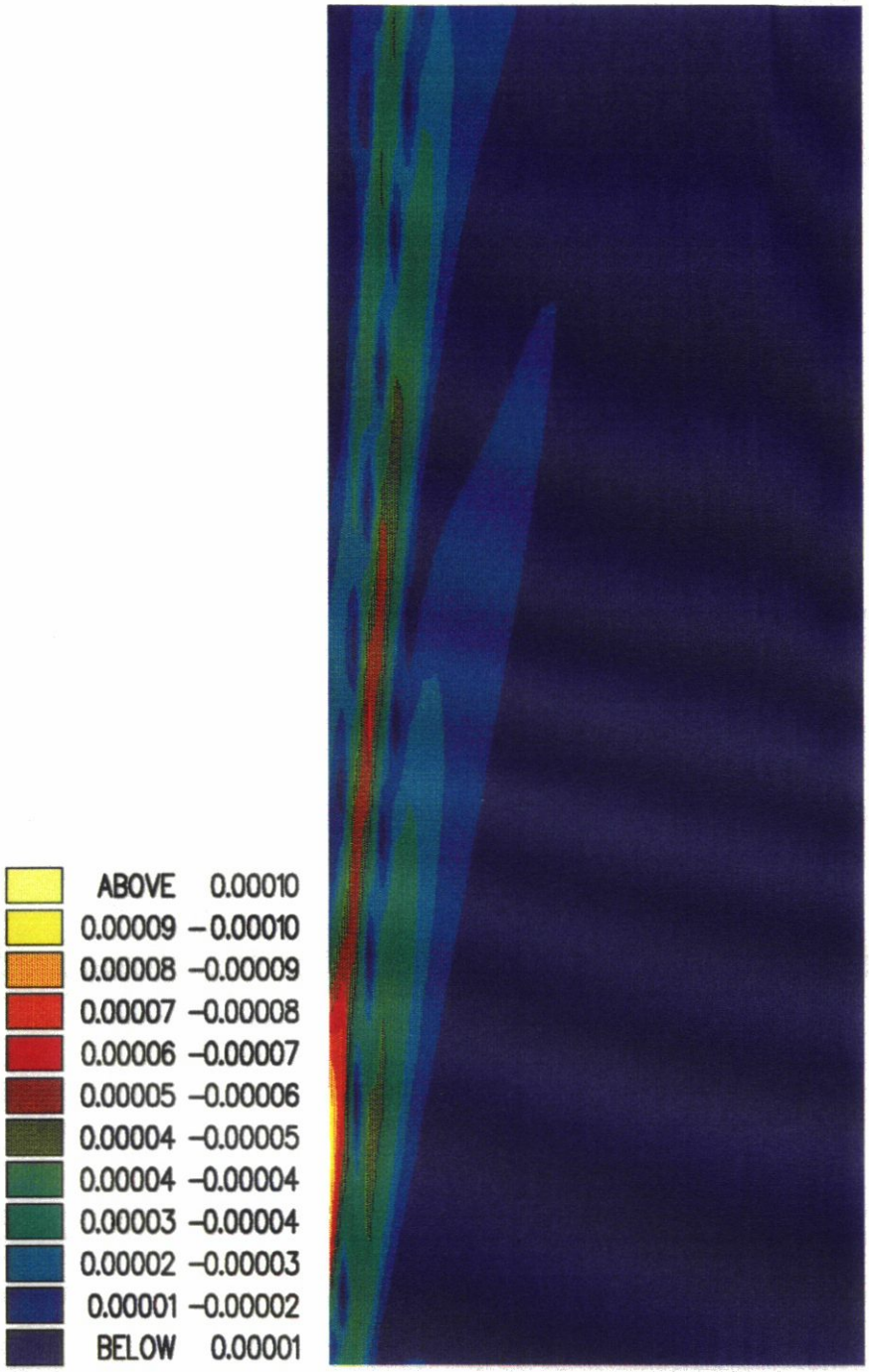

Figure 5: Free surface shear when the body is in the upper layer. $U_0 = 2.0\ m/s$ ($F_n = 0.064$) $L = 100.0\ m$ $d = 10.0\ m$ $\rho_1 = 1025.0\ Kg/m^3$ $\rho_2 = 1026.5\ Kg/m^3$ $\rho_3 = 1028.0\ Kg/m^3$ $t_1 = 30.0\ m$ $t_2 = 30.0\ m$ $f = 15\ m$

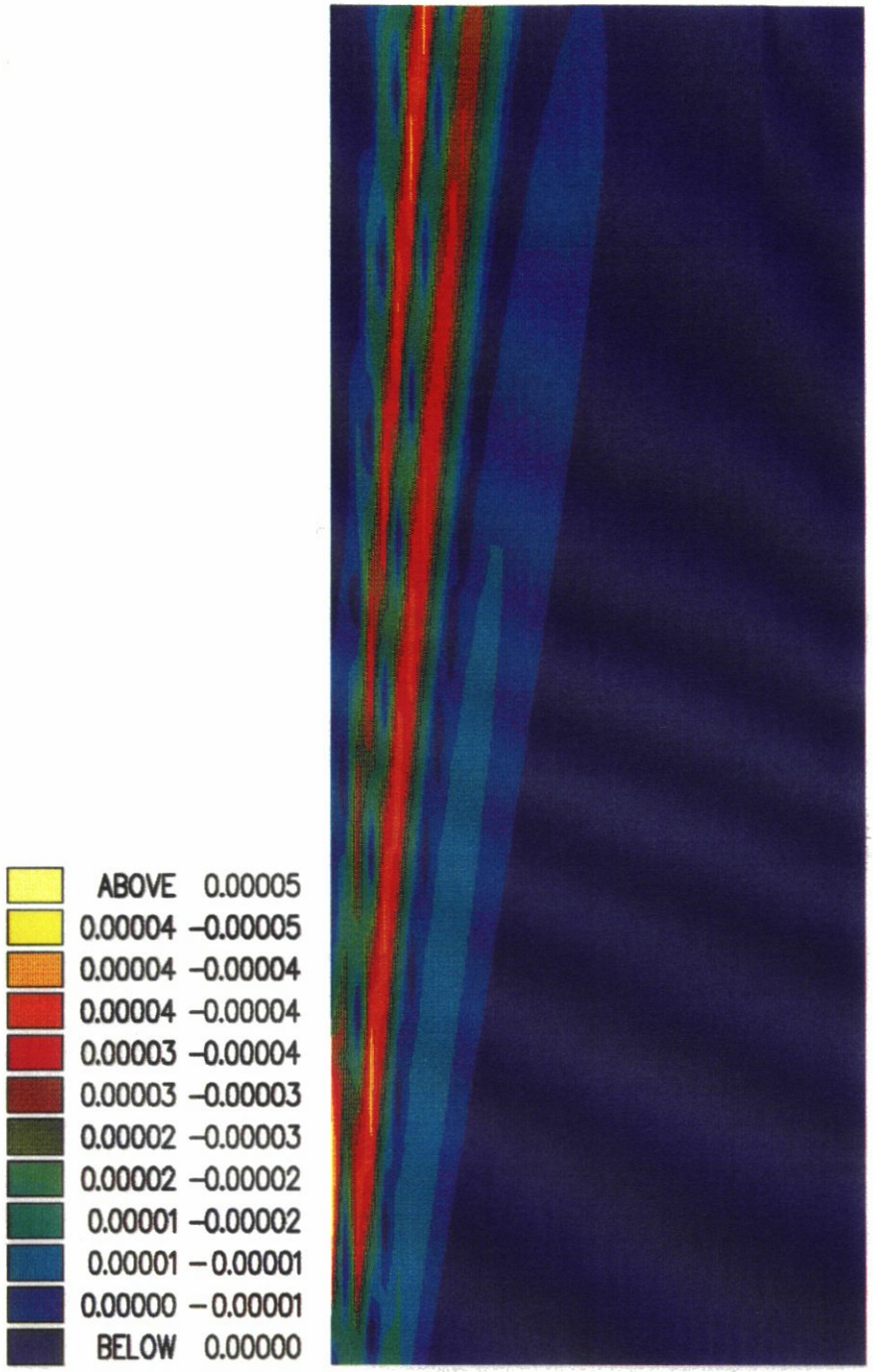

Figure 6: Free surface shear when the body is in the middle layer. $U_0 = 2.0\ m/s$ ($F_n = 0.064$) $L = 100.0\ m$ $d = 10.0\ m$ $\rho_1 = 1025.0\ Kg/m^3$ $\rho_2 = 1026.5\ Kg/m^3$ $\rho_3 = 1028.0\ Kg/m^3$ $t_1 = 30.0\ m$ $t_2 = 30.0\ m$ $f = 45\ m$

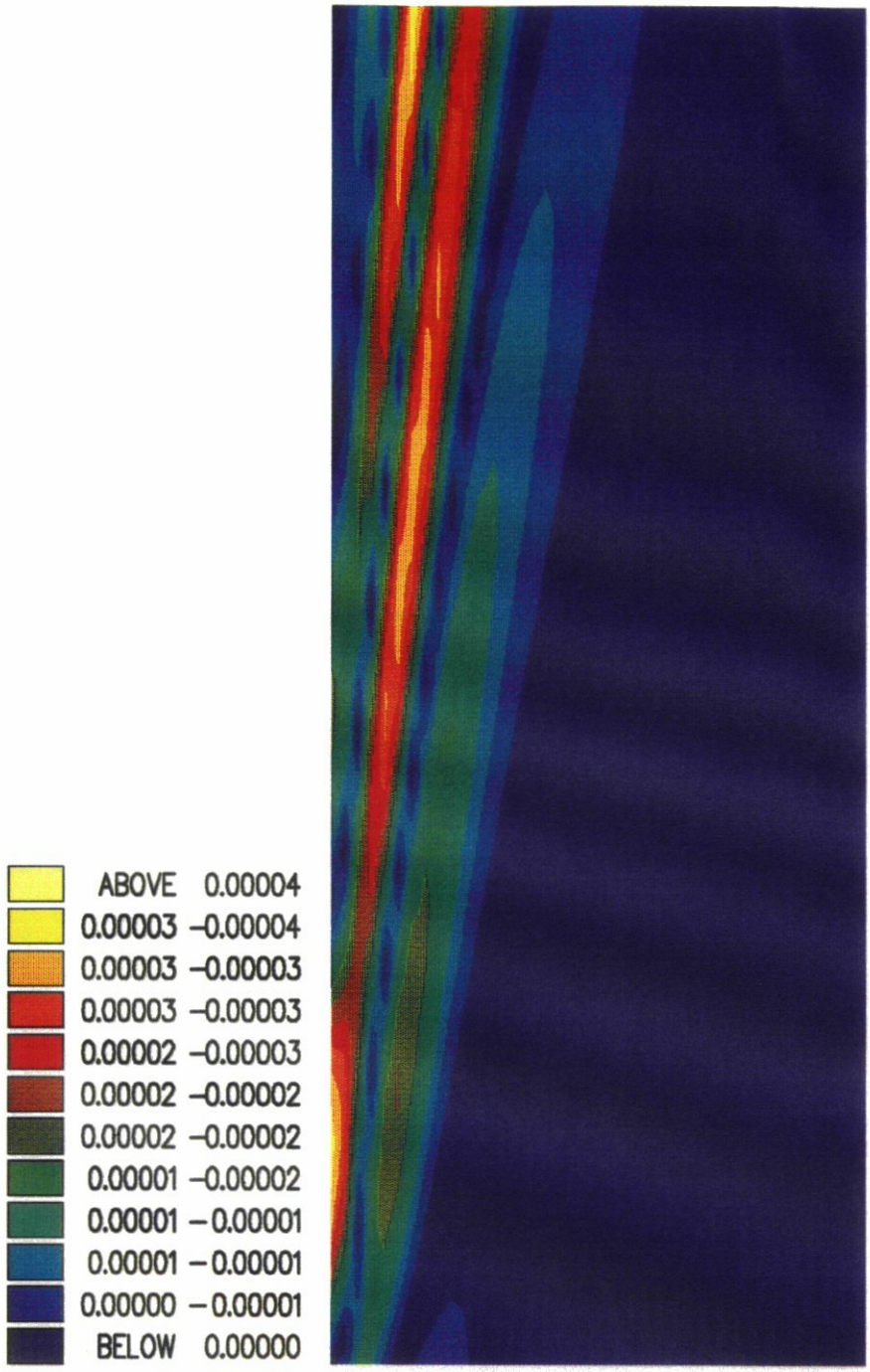

Figure 7: Free surface shear distribution when the body is in the lower layer. $U_0 = 2.0\,m/s$ ($F_n = 0.064$) $L = 100.0\,m$ $d = 10.0\,m$ $\rho_1 = 1025.0\,Kg/m^3$ $\rho_2 = 1026.5\,Kg/m^3$ $\rho_3 = 1028.0\,Kg/m^3$ $t_1 = 30.0\,m$ $t_2 = 30.0\,m$ $f = 75\,m$

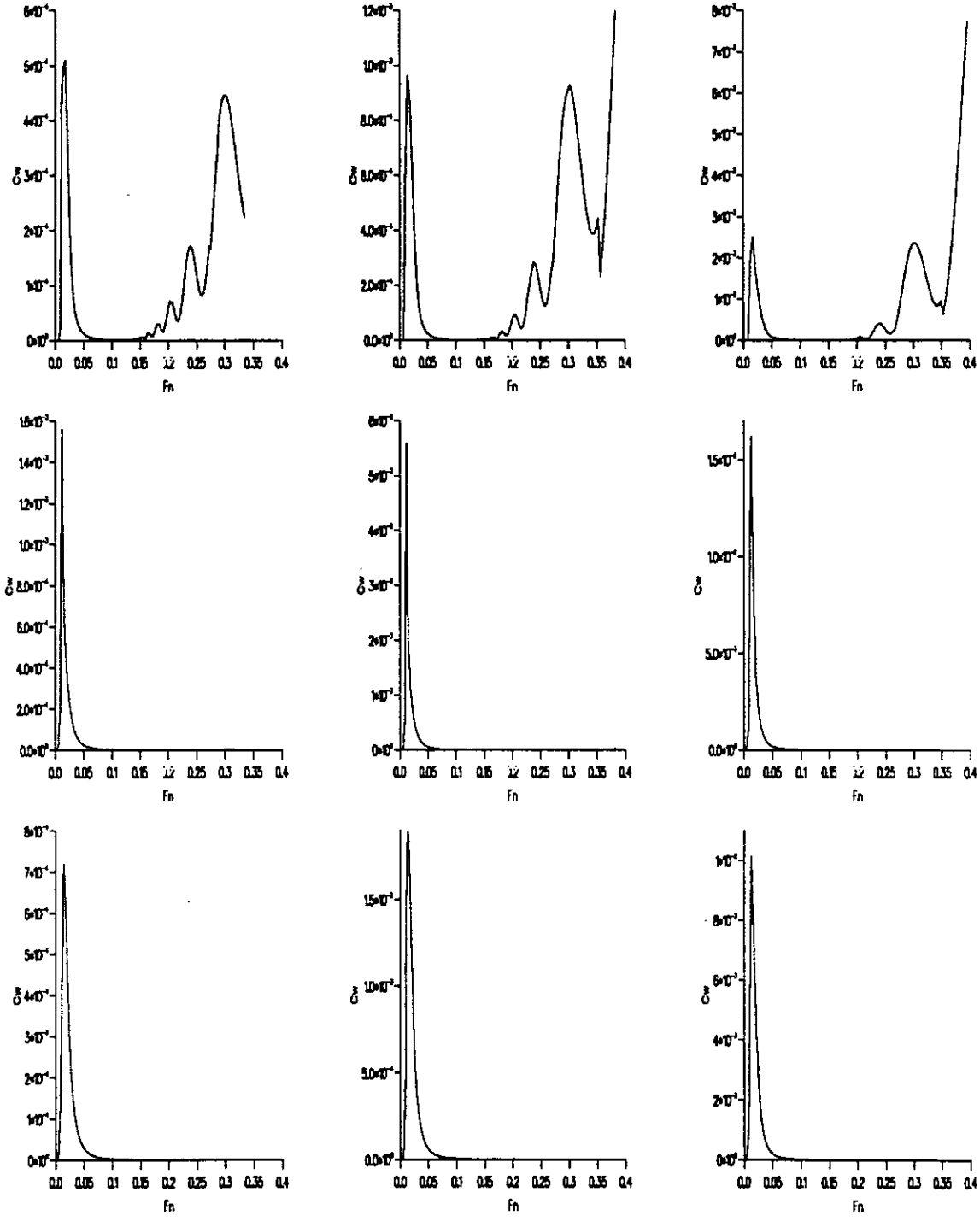

Figure 8: C_w / F_n at a constant displacement when the body is in the upper,middle and lower layers for $\frac{L}{d}$ = 15, 10 and 5. U_0 = 0.5 − 12.0m/s (F_n = 0.016 − 0.383) $\frac{L}{d}$ = 15 L = 131.0 m d = 8.736 m $\frac{L}{d}$ = 10 L = 100.0 m d = 10.000 m $\frac{L}{d}$ = 5 L = 63.0 m d = 12.600 m ρ_1 = 1025.0 Kg/m^3 ρ_2 = 1026.5 Kg/m^3 ρ_3 = 1028.0 Kg/m^3 t_1 = 30.0 m t_2 = 30.0 m f = 15, 45 *and* 75 m

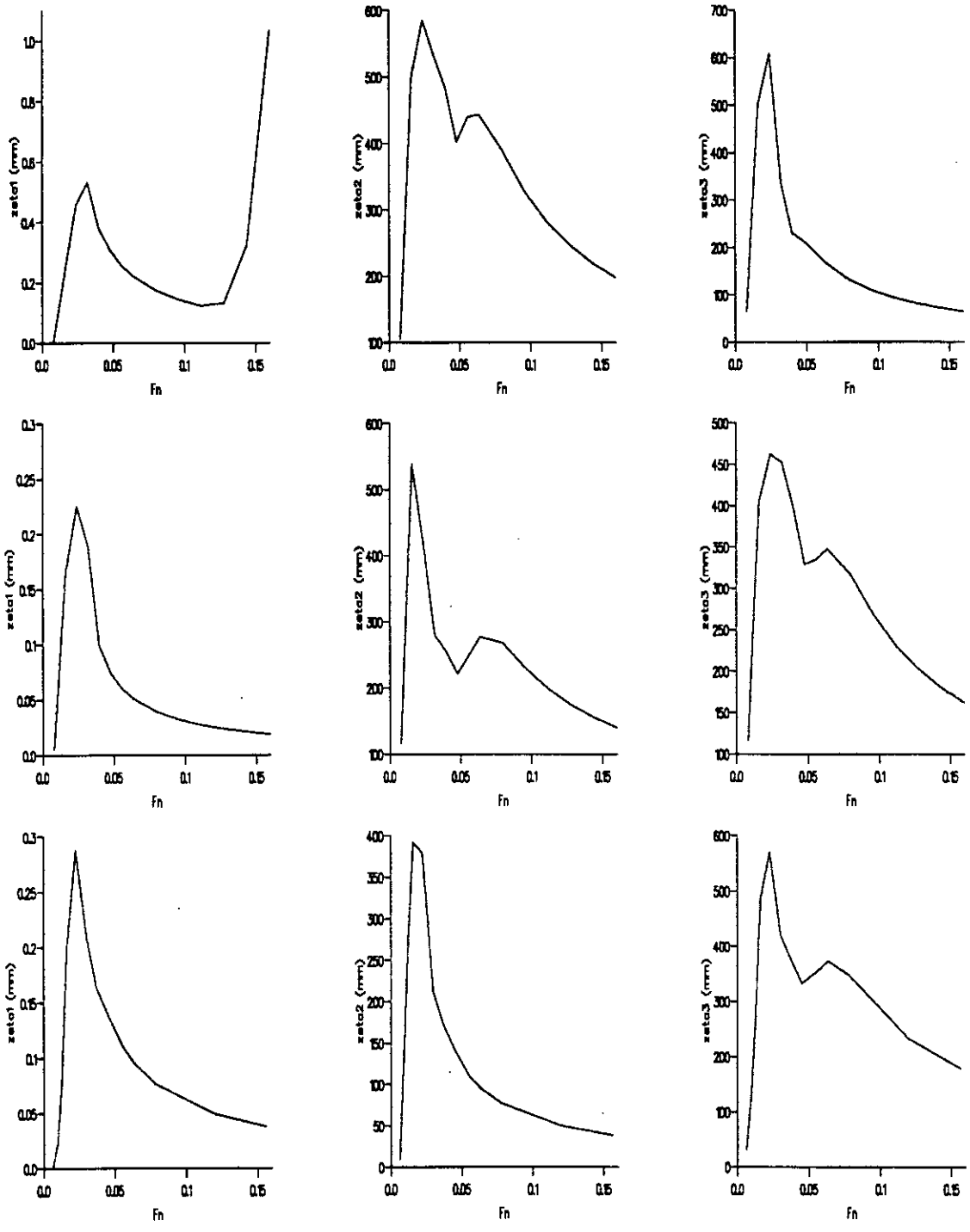

Figure 9: Maximum values of free surface, first and second interface elevations / F_n when the body is in the upper,middle and lower layers. $U_0 = 0.25 - 5.0\ m/s$ $(F_n = 0.008 - 0.160)$ $L = 100.0\ m$ $d = 10.000\ m$ $\rho_1 = 1025.0\ Kg/m^3$ $\rho_2 = 1026.5\ Kg/m^3$ $\rho_3 = 1028.0\ Kg/m^3$ $t_1 = 30.0\ m$ $t_2 = 30.0\ m$ $f = 15, 45\ and\ 75\ m$

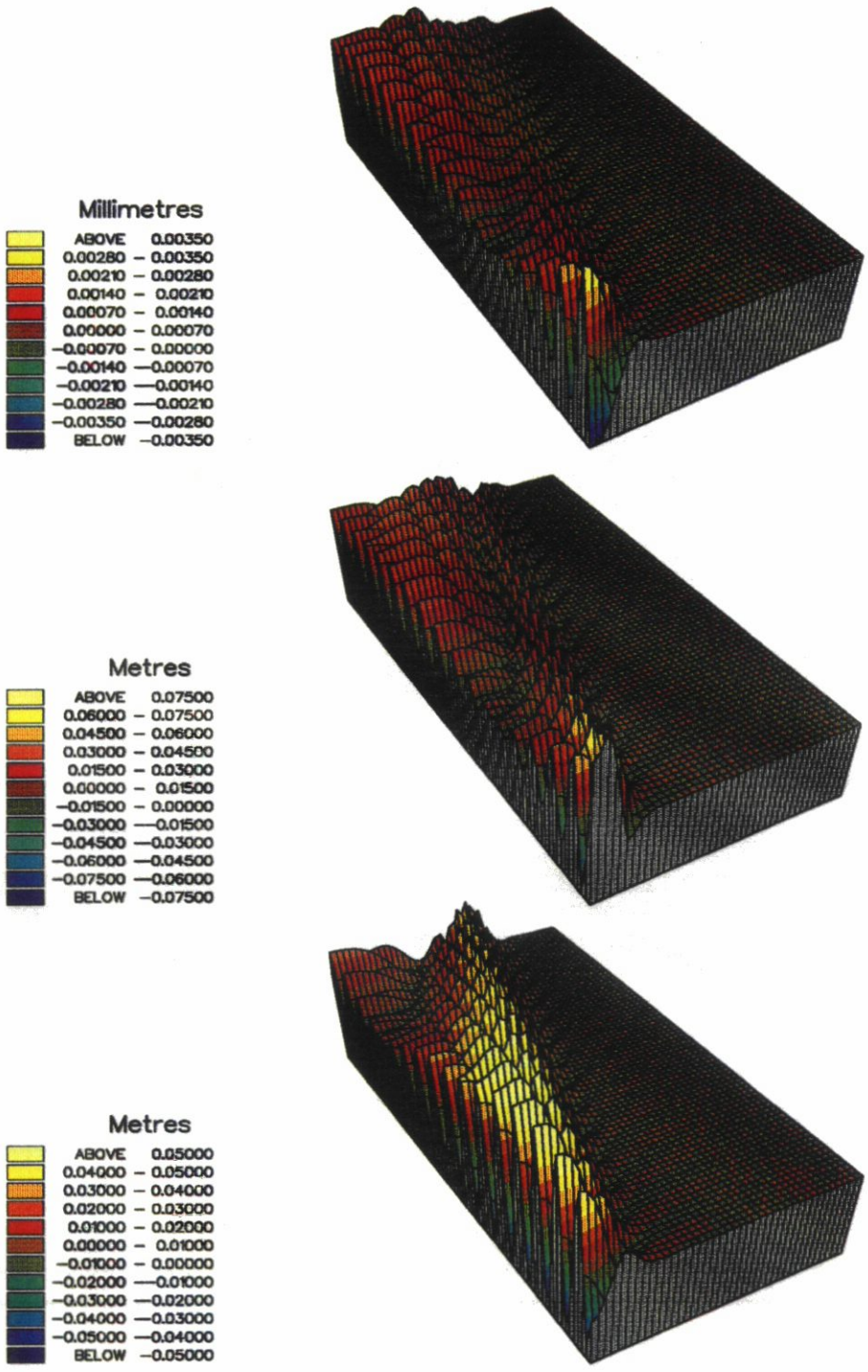

Figure 10: Free surface and interface wave systems for $U_0 = 0.25\ m/s$ ($F_n = 0.008$) when the body is in the upper layer. $L = 100.0\ m$ $d = 10.000\ m$ $\rho_1 = 1025.0\ Kg/m^3$ $\rho_2 = 1026.5\ Kg/m^3$ $\rho_3 = 1028.0\ Kg/m^3$ $t_1 = 30.0\ m$ $t_2 = 30.0\ m$ $f = 15\ m$

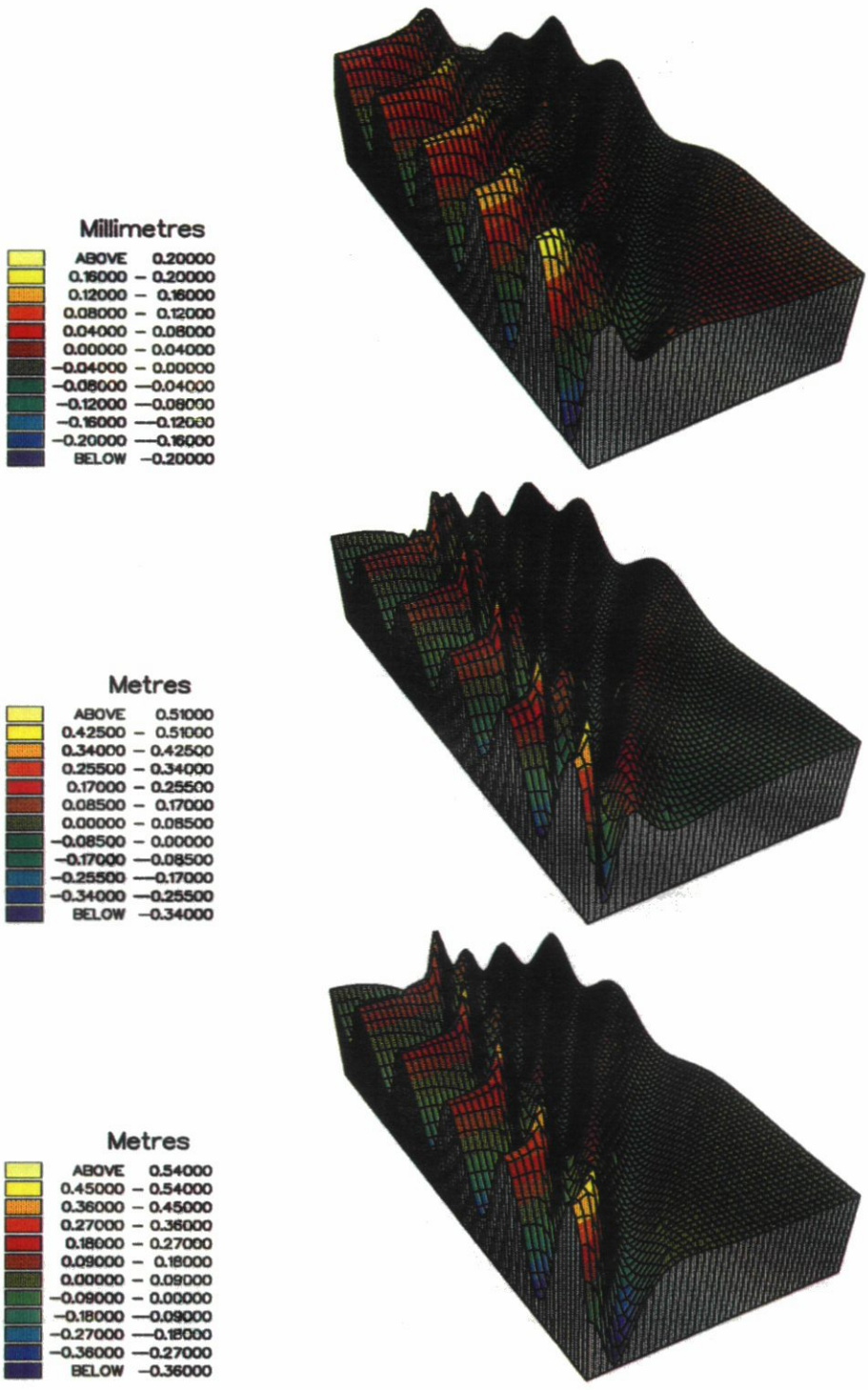

Figure 11: Free surface and interface wave systems for $U_0 = 0.50\ m/s$ ($F_n = 0.016$) when the body is in the upper layer. $L = 100.0\ m$ $d = 10.000\ m$ $\rho_1 = 1025.0\ Kg/m^3$ $\rho_2 = 1026.5\ Kg/m^3$ $\rho_3 = 1028.0\ Kg/m^3$ $t_1 = 30.0\ m$ $t_2 = 30.0\ m$ $f = 15\ m$

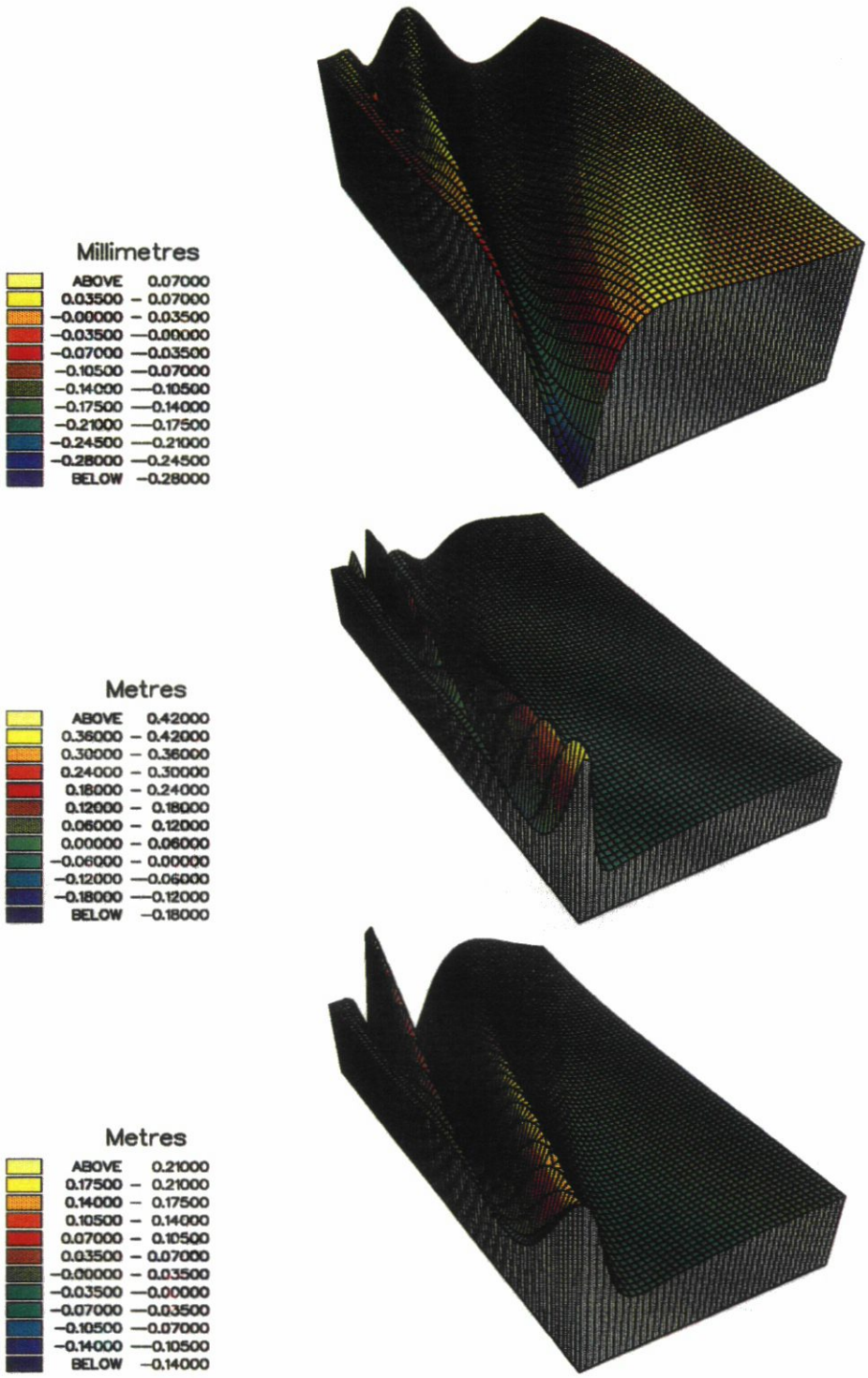

Figure 12: Free surface and interface wave systems for $U_0 = 1.50\ m/s$ ($F_n = 0.048$) when the body is in the upper layer. $L = 100.0\ m$ $d = 10.000\ m$ $\rho_1 = 1025.0\ Kg/m^3$ $\rho_2 = 1026.5\ Kg/m^3$ $\rho_3 = 1028.0\ Kg/m^3$ $t_1 = 30.0\ m$ $t_2 = 30.0\ m$ $f = 15\ m$

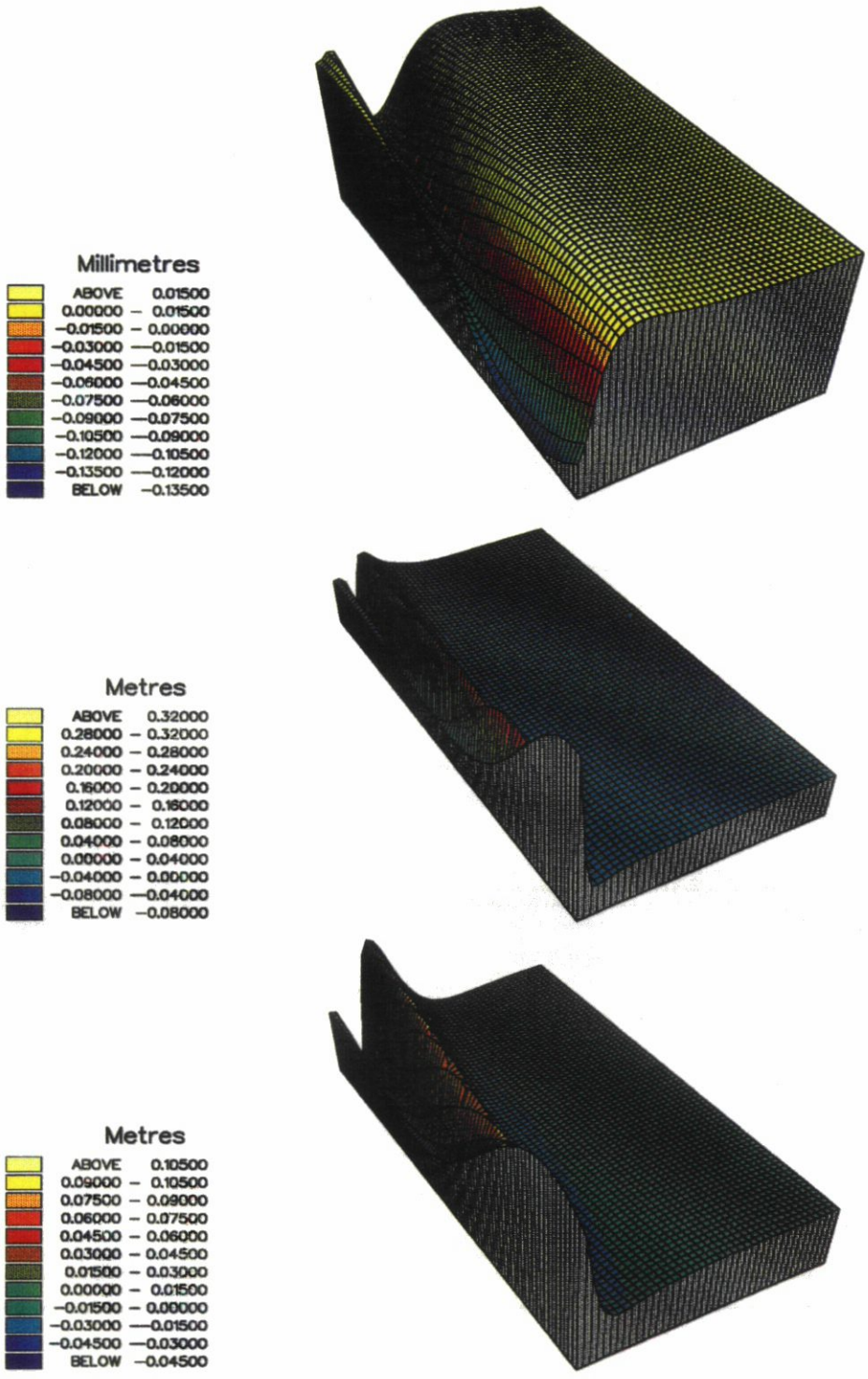

Figure 13: Free surface and interface wave systems for $U_0 = 3.00\ m/s$ ($F_n = 0.096$) when the body is in the upper layer. $L = 100.0\ m$ $d = 10.000\ m$ $\rho_1 = 1025.0\ Kg/m^3$ $\rho_2 = 1026.5\ Kg/m^3$ $\rho_3 = 1028.0\ Kg/m^3$ $t_1 = 30.0\ m$ $t_2 = 30.0\ m$ $f = 15\ m$

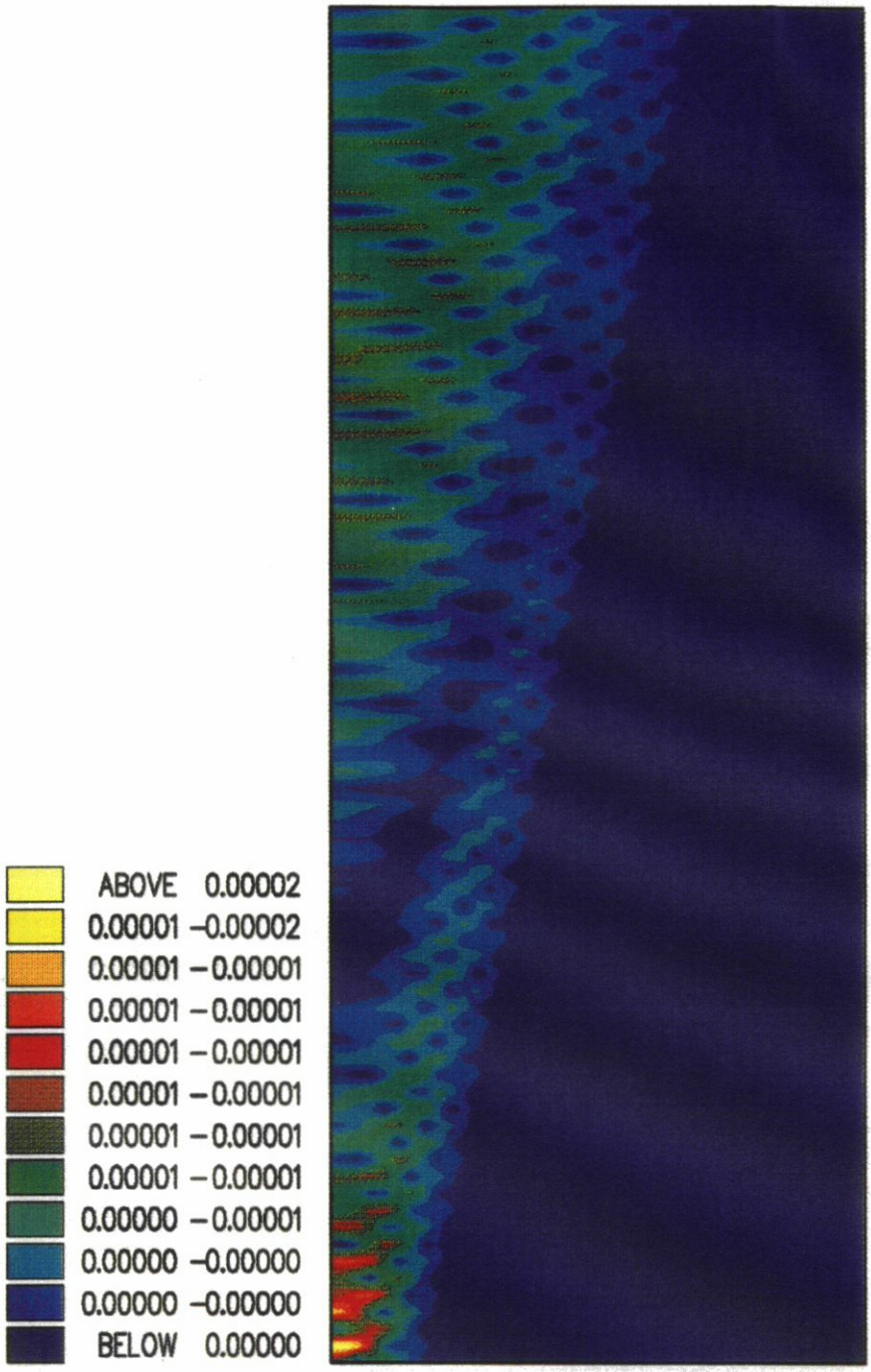

Figure 14: Free surface shear for $U_0 = 0.25\ m/s$ when the body is in the upper layer. $L = 100.0\ m$ $d = 10.000\ m$ $\rho_1 = 1025.0\ Kg/m^3$ $\rho_2 = 1026.5\ Kg/m^3$ $\rho_3 = 1028.0\ Kg/m^3$ $t_1 = 30.0\ m$ $t_2 = 30.0\ m$ $f = 15\ m$

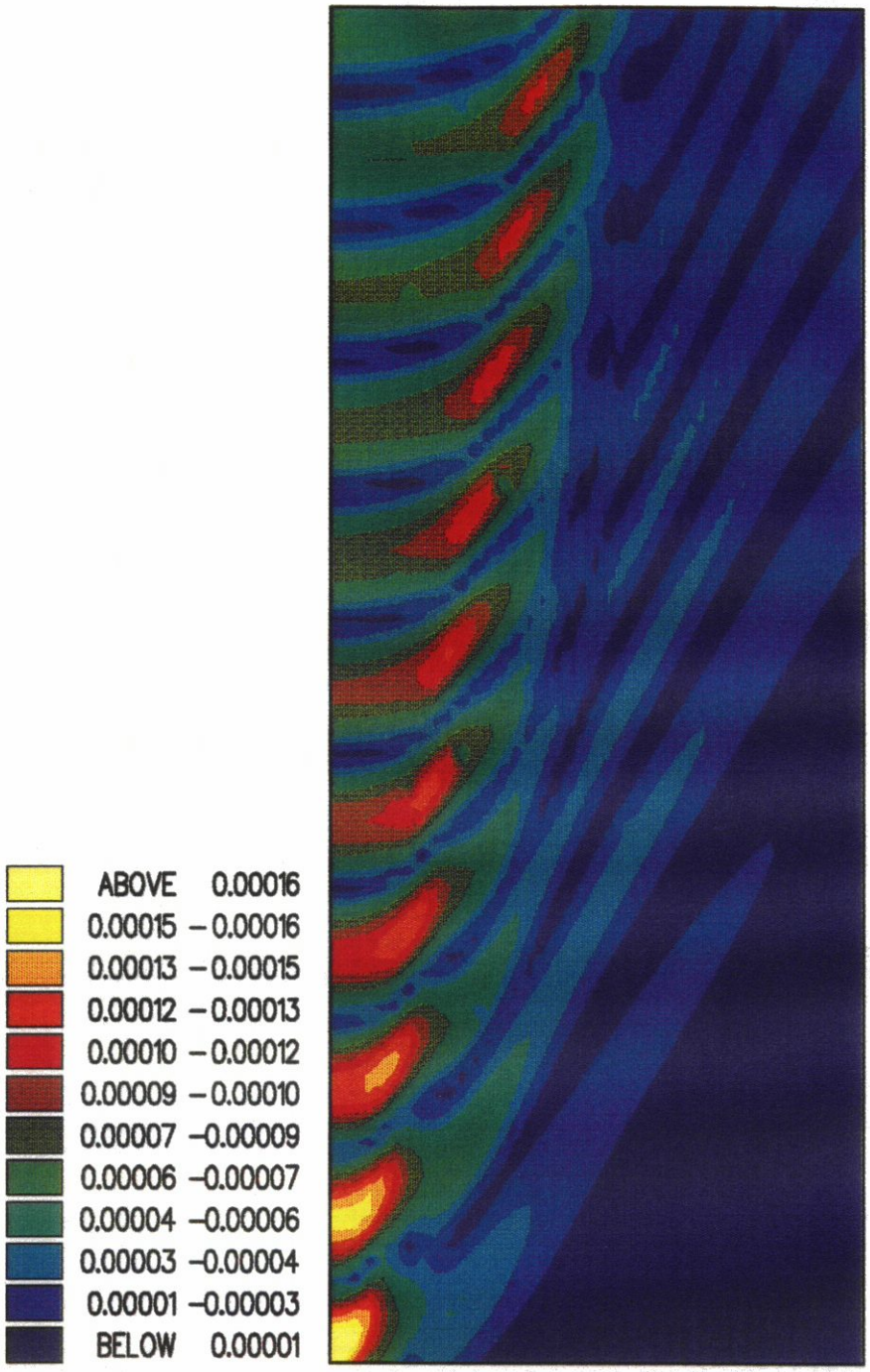

Figure 15: Free surface shear for $U_0 = 0.50\ m/s$ when the body is in the upper layer. $L = 100.0\ m$ $d = 10.000\ m$ $\rho_1 = 1025.0\ Kg/m^3$ $\rho_2 = 1026.5\ Kg/m^3$ $\rho_3 = 1028.0\ Kg/m^3$ $t_1 = 30.0\ m$ $t_2 = 30.0\ m$ $f = 15\ m$

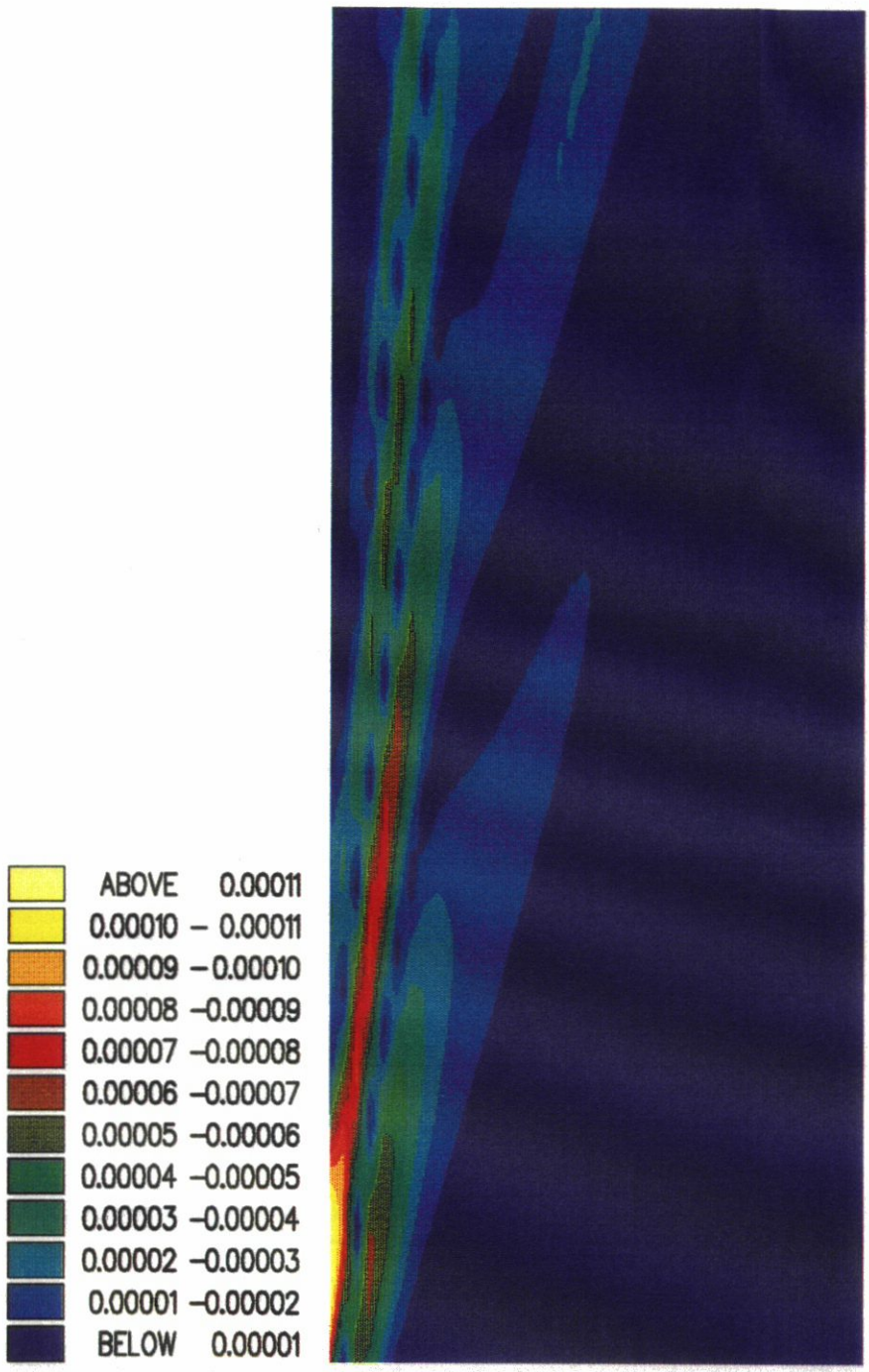

Figure 16: Free surface shear for $U_0 = 1.50\ m/s$ when the body is in the upper layer. $L = 100.0\ m$ $d = 10.000\ m$ $\rho_1 = 1025.0\ Kg/m^3$ $\rho_2 = 1026.5\ Kg/m^3$ $\rho_3 = 1028.0\ Kg/m^3$ $t_1 = 30.0\ m$ $t_2 = 30.0\ m$ $f = 15\ m$

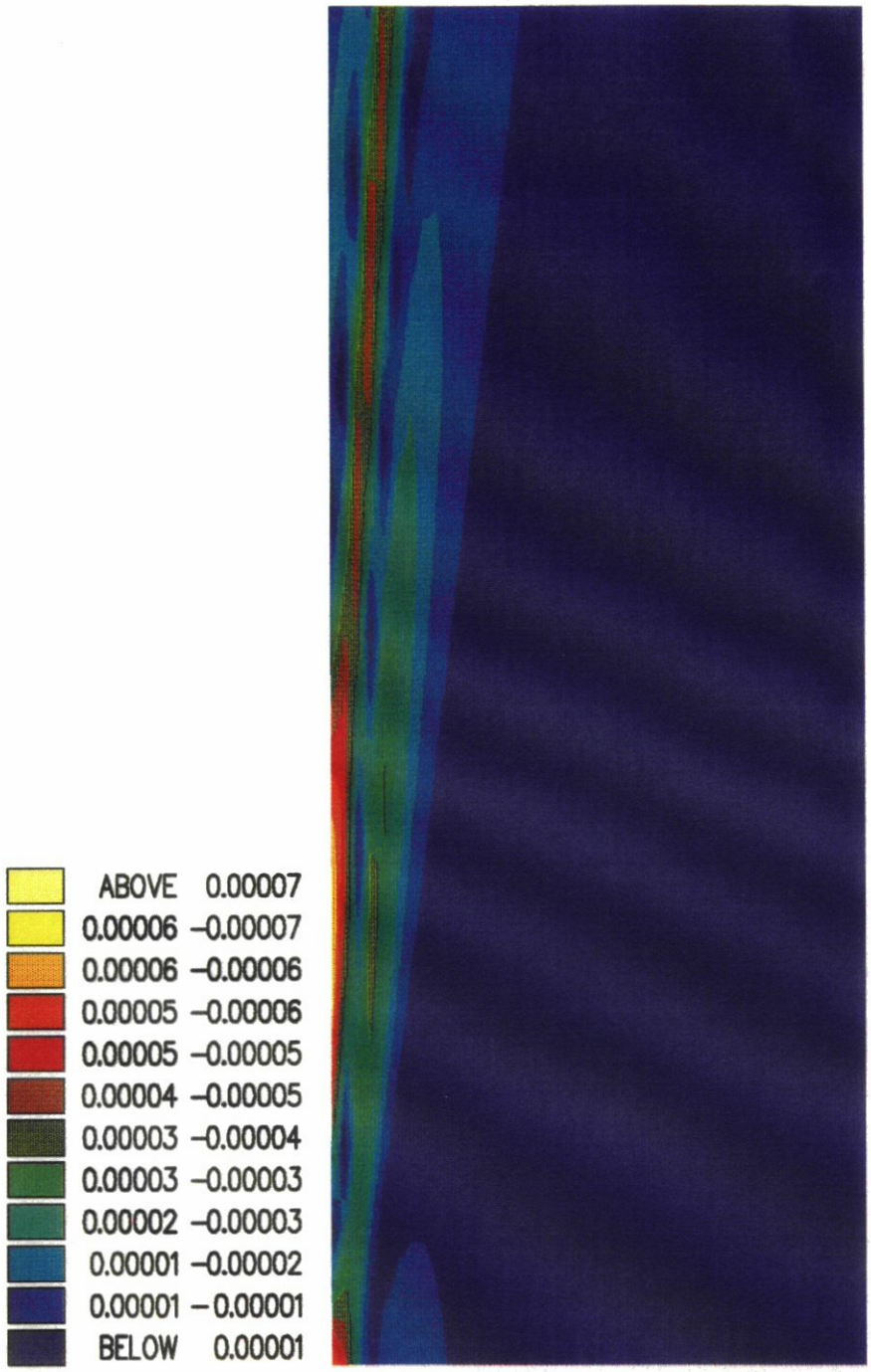

Figure 17: Free surface shear for $U_0 = 3.00\ m/s$ when the body is in the upper layer. $L = 100.0\ m$ $d = 10.000\ m$ $\rho_1 = 1025.0\ Kg/m^3$ $\rho_2 = 1026.5\ Kg/m^3$ $\rho_3 = 1028.0\ Kg/m^3$ $t_1 = 30.0\ m$ $t_2 = 30.0\ m$ $f = 15\ m$

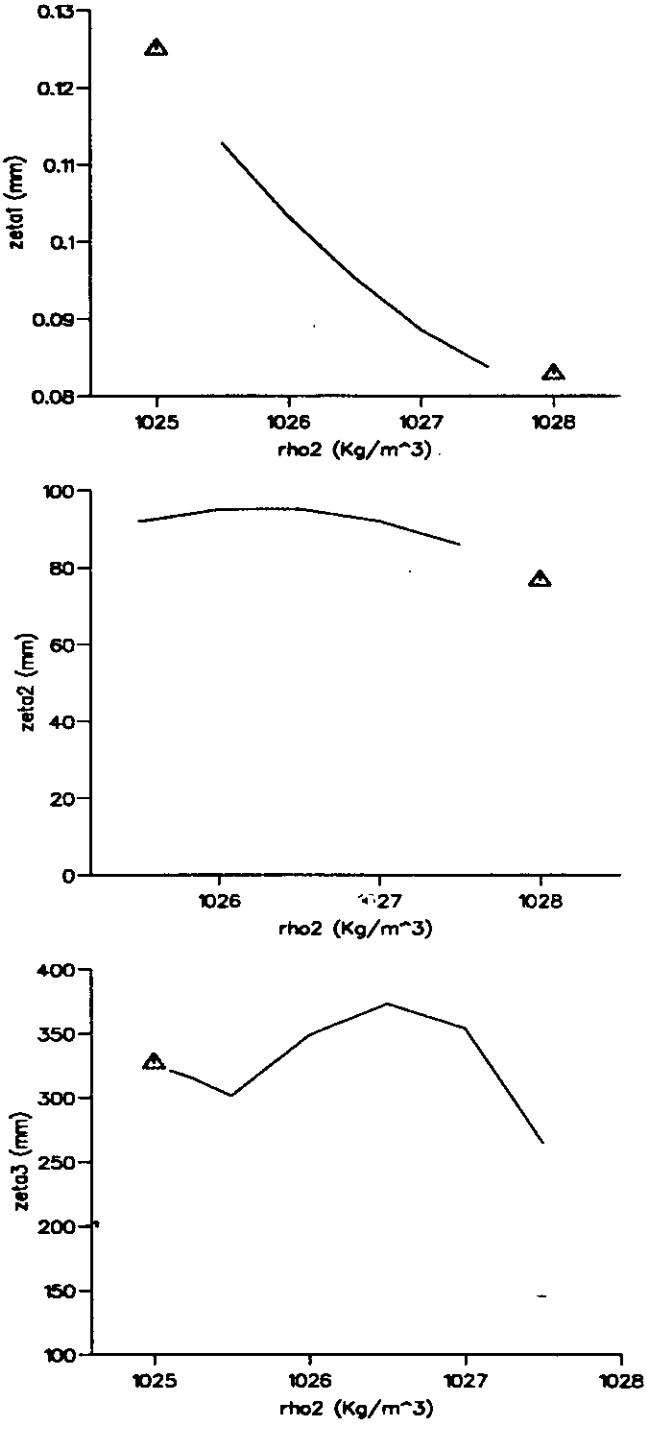

Figure 18: Maximum values of free surface and interface elevations for a variation of ρ_2 when the body is in the lower layer. $U_0 = 2.0\ m/s$ ($F_n = 0.064$) $L = 100.0\ m$ $d = 10.000\ m$ $\rho_1 = 1025.0\ Kg/m^3$ $\rho_3 = 1028.0\ Kg/m^3$ $t_1 = 30.0\ m$ $t_2 = 30.0\ m$ $f = 75\ m$

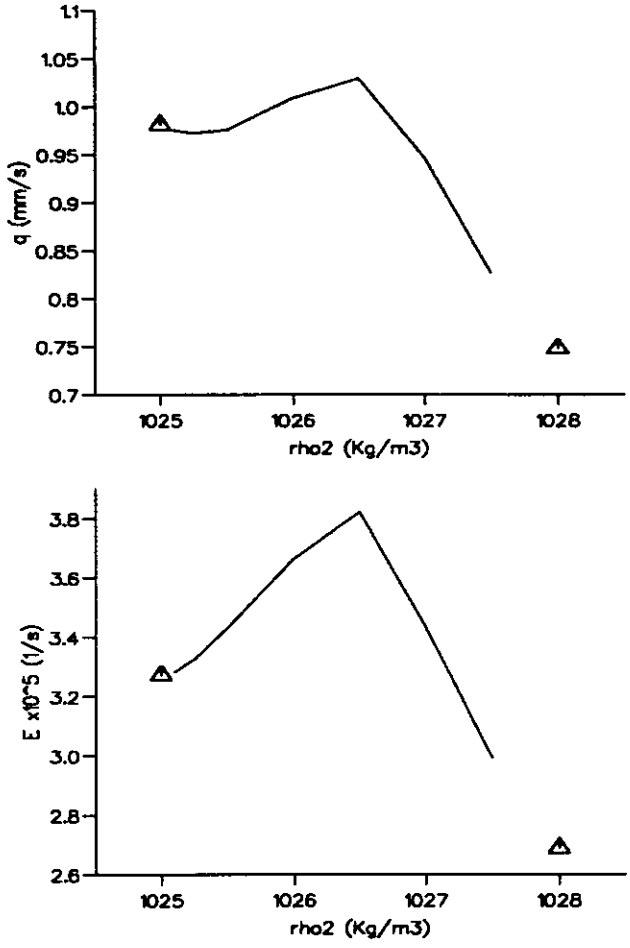

Figure 19: Maximum values of the free surface velocity (q) and shear (E) for a variation of ρ_2 when the body is in the lower layer. $U_0 = 2.0\ m/s$ ($F_n = 0.064$) $L = 100.0\ m$ $d = 10.000\ m$ $\rho_1 = 1025.0\ Kg/m^3$ $\rho_3 = 1028.0\ Kg/m^3$ $t_1 = 30.0\ m$ $t_2 = 30.0\ m$ $f = 75\ m$

SSSU 62
ISSN 0140 3818

UNIVERSITY OF SOUTHAMPTON

DEPARTMENT OF SHIP SCIENCE

FACULTY OF ENGINEERING AND APPLIED SCIENCE

INTERFACIAL WAVES PRODUCED BY A SUBMERGED BODY MOVING IN A LAYERED FLUID

W. G. Price
P. C. Westlake

Ship Science Report No. 62

July 1993

Interfacial waves produced by a submerged body moving in a layered fluid
Ship Science Report No. 62

W.G.Price
P.C.Westlake

July 20, 1993

Contents

Nomenclature

$A(\xi)$	Longitudinal sectional area function of the body
C_w	Nondimensional wave resistance coefficient $= \frac{R_w}{\frac{1}{2}\rho_j s U_0^2}$
d	Maximum diameter of the body
$E(x,y)$	Magnitude of the free surface strain vector $= \sqrt{u_x^2 + v_y^2}$
F_n	Froude number $= \frac{U_0}{\sqrt{gL}}$
f	Depth of the axis of revolution of the prolate spheroid from the undisturbed free surface $= -\zeta$
$G_{ij}(\boldsymbol{x},\boldsymbol{\xi})$	Greens function in Oxyz
g	Gravity acceleration
$H(z)$	Heaviside unit step function
h_i	Vertical separation of the i^{th} interface and free surface
h_j	Vertical separation of the origin and free surface
i	Layer number, 1^{st} layer = upper layer
j	Layer number in which the body is located
L	Length of body
l	Summation index $(1 \leq l \leq N_r)$
$N(z)$	Brunt-Väisälä frequency
N_r	Number of roots of nonzero $D(k,\theta) = 0$
$Oxyz$	Moving reference coordinate system located vertically above the body's centroid on the undisturbed free surface or interface
$O(x)$	Landau order symbol
$o(x)$	Landau order symbol
$P.V.$	Cauchy's principal value integral
$Q(\xi)$	Longitudinal source strength distribution representing the body
$q(x,y)$	Magnitude of the free surface velocity vector $= \sqrt{u^2 + v^2}$
R_w	Wave resistance
s	Surface area of body, for a prolate spheroid $s = \frac{1}{2}\pi(d^2 + \frac{Ld}{\epsilon}\arcsin\epsilon)$
t_1	Thickness of upper layer
t_2	Thickness of middle layer
U_{cl}	Lower critical velocity of the fluid system
U_{cu}	Upper critical velocity of the fluid system
U_0	Velocity of body
$\boldsymbol{u}(x,y,z)$	Disturbance velocity vector in $Oxyz = (u,v,w)$
$\boldsymbol{x}$	Position vector of the field point (x,y,z) in $Oxyz$
α_l	l^{th} non zero root of k from $D(k,\theta) = 0$
δ_1	Upper density ratio $= \frac{\rho_1}{\rho_2}$
δ_2	Lower density ratio $= \frac{\rho_2}{\rho_3}$
δ_{ij}	Kronecker delta function
ϵ	$= \sqrt{1 - \left(\frac{d}{L}\right)^2}$
$\zeta_1(x,y)$	Free surface elevation
$\zeta_2(x,y)$	Upper interface elevation
$\zeta_3(x,y)$	Lower interface elevation
$\boldsymbol{\xi}$	Position vector of source point (ξ,η,ζ) in $Oxyz$
ρ_1	Density of fluid in the upper layer
ρ_2	Density of fluid in the middle layer
ρ_3	Density of fluid in the lower layer
$\phi_{ij}(\boldsymbol{x},\boldsymbol{\xi})$	Disturbance velocity potential in $Oxyz$
$\psi_{ij}(\boldsymbol{x},\boldsymbol{\xi})$	Disturbance stream function in $Oxyz$

Abstract

Velocity potential solutions are derived for an arbitrary shaped body moving horizontally in a fluid system consisting of three layers, the lower layer of infinite depth. The body may be located in any one of the three layers. The boundary conditions on the free surface and interface are linearised and a radiation condition imposed. Expressions for the far field free surface and interface elevations are derived. A three dimensional extension of Lagally's theory provides a method which allows the wave resistance of the body to be determined. The application of a slender body approximation permits the derivation of analytical expressions for the elevations and wave resistance. Plots of the far field free surface and interface wave systems are presented when the body is located in each layer. The wave resistance of a prolate spheroid length L to diameter d for a series of L/d ratios is calculated over a Froude number range. The "dead water" effect being apparent in every case. The results of other parametric studies are also included.

1 Introduction

Generally the fluid in which vessels navigate is not homogeneous, a degree of stratification is present. This stratification may be weak, one or two parts in one thousand occur in the ocean; in estuaries and fjords stratification may reach thirty parts in one thousand. The presence of stratification is due to a variation of density, temperature or salinity with depth. Stratifications due to a change in density, temperature or salinity are known as pynoclines, thermoclines and haloclines respectively. The effects of stratification on the forward motion and control of ships has been recorded by many mariners, many compiled by Ekman (1904). The most noticeable effect observed was a decrease in the forward speed of the vessel caused by an increase in resistance due to the additional energy expended creating waves within the fluid. This effect initiated research into the generation of ship waves in a stratified fluid. More recently the application of remote sensing techniques to the oceans surface has revealed 'v' shape images in the wake of ships, the cause of which is suspected to be due to internal wave generation. Experimenters have reproduced these images under controlled conditions (Apel and Gjessing, 1989). Accurate mathematical models of the fluid pertabations caused by the body are required in order that the mechanism which produces these images can be fully explained.

Although stratification in the ocean is continuous with depth, many theoretical studies idealise this continuous medium by a series of discrete layers each of finite depth and of constant fluid density. The overall fluid density profile is not constant and discontinuities occur at the layer interfaces. Stratified fluid models have been considered previously, see for example, Hudimac (1961), Sabuncu (1961), Crapper (1967), Rarity (1967), Keller and Monk (1970) , Miles (1971), Hughes (1986), Price et al (1988), Dysthe and Trulsen (1989), Wang (1989) and Tulin and Miloh (1990) but many of these studies concentrate on the description of the wave patterns generated on the free surface and interface(s) by an isolated source rather than detailed descriptions of the interaction between a defined body shape and the surrounding medium. Because of fluid stratification, internal waves occur naturally in oceans and these can be generated locally by turbulence or externally by a distant storm. A body moving in a stratified fluid produces a pressure field within the fluid creating internal and free surface disturbances. Since waves always radiate energy away from the region where they are being formed, the stratification of the fluid provides an additional outlet for this radiation to occur.

For a ship or submerged body moving horizontally with constant forward speed in a constant density fluid medium which is assumed "idealised", Baar and Price (1988) developed numerical procedures to determine solutions of the steady body motion problem. That is, predictions of wavemaking resistance, wave patterns generated on the free surface, pressure fields within the fluid, etc. These were derived from a linearised three dimensional flow formulation and they describe the disturbance potential of the steady perturbed flow about the moving body. The solutions were obtained by means of a Kelvin wave source distribution method. This is based on an integral identity for the Neumann-Kelvin potential involving an integral distribution of Kelvin wave sources over the body's surface and waterline contour (if the vessel is surface piercing). The unknown source strength is determined by solving the Fredholm integral equation of the second kind which ensures that the kinematic condition at the hull surface is satisfied. This theoretical approach and iterative numerical approximation procedure were applied to six different

hull forms and the calculated results showed good agreement with experimental data in both a qualitative and quantative manner. see for example, Andrew et al (1988).

This approach was extended by Price et al (1988) to solve the similar problem in a stratified fluid. A panel method was developed allowing the modelling of the geometric shape of an arbitrary shaped body. This method was, applied to a prolate spheroid and the predicted results were compared with those derived using a slender body approach. A comparison of the predicted values revealed only minor variations thus justifying the use of the slender body approach for this body shape. This has the advantage of reducing the computational effort significantly without diminishing the description of the physical processes arising in the stratified fluid - structure interaction. For these reasons, the slender body approach is used in the calculations described herein.

2 Model definition

This report describes the first stage of an investigation into the problem of a body moving in a stratified fluid. Here the mathematical model describing a stably stratified fluid is discretised into three layers. In each layer the density of the fluid is constant and the lower layer is of infinite depth. A prolate spheroid, which is completely contained in any one of the three layers, moves with constant horizontal velocity along a straight track extending from its axis of revolution. The disturbance created within the fluid is described by velocity potential functions.

2.1 Fluid Model

The fluid in each layer is assumed inviscid, incompressible and the fluids are immiscible at the interfaces. The disturbance produced in each layer by the moving body may therefore be represented by a velocity potential flow theory.

The density profile can be expressed as:

$$\rho(z) = \rho_1 H(-z) + (\rho_2 - \rho_1)H[-(z+t_1)] + (\rho_3 - \rho_2)H[-(z+t_1+t_2)] \quad \rho_1 < \rho_2 < \rho_3 \tag{1}$$

where the plane $z = 0$ denotes the undisturbed free surface. The coordinate z is defined negative pointing into the fluid and $H(z)$ denotes the Heaviside unit step function.

The Brunt-Väisälä frequency, $N(z)$ is defined as

$$N^2(z) = -\frac{g}{\rho(z)}\frac{d\rho(z)}{dz} \tag{2}$$

which for this model is discontinuous across the interfaces and zero within each layer.

2.2 Body Model

In general, a submarine, idealised here by a prolate spheroid, has a streamline form with a maximum diameter, d, substantially smaller than its length, L. A slender body approximation may therefore be employed to simplify the hydrodynamic analysis. The disturbance velocity potential is represented by a source distribution along the longitudinal axis of the body, the strength $Q(\xi)$ of a source at position ξ , $-\frac{L}{2} \leq \xi \leq \frac{L}{2}$ is given by:

$$Q(\xi) = -\frac{U_0}{4\pi}\frac{dA(\xi)}{d\xi} \tag{3}$$

For a prolate spheroid this becomes:

$$Q(\xi) = \frac{U_0}{2}\left(\frac{d}{L}\right)^2 \xi \tag{4}$$

The achievement of exact body shape cannot be fully realised using this method due to the proximity of the free surface and interface wave systems which modify the streamline $\psi_{jj}(\boldsymbol{x}, \boldsymbol{\xi}) = 0$. An accurate

description of the shape of the body can only be achieved using an additional boundary condition ensuring no fluid particles penetrate the wetted surface of the body. The problem can then be regarded as a Neumann-Kelvin problem, a solution of which can be obtained using panel methods and numerical computation. However, it has been shown that for slender bodies the discrepancy between the two methods does not merit the increase in computational effort required for the Neumann-Kelvin theory, see Price et al (1988).

2.3 Coordinate System

Figure 1 illustrates the location and orientation of the orthogonal, right handed, coordinate axis system chosen to simplify the mathematics of the three layer system. For example, for a body in the upper layer the undisturbed free surface is the plane $z = 0$, the x-axis lies along the direction of motion of the body and the positive y-axis is chosen to satisfy the orthogonality condition. The origin of the coordinate system lies vertically above the body's centroid. For a body in one of the lower layers the undisturbed interface above the body becomes the plane $z = 0$.

3 Statement and solution of the boundary value problem

3.1 Boundary Conditions

Using a body fixed coordinate system the linearised boundary conditions imposed to describe the velocity potential disturbance $\phi_{ij}(\boldsymbol{x}, \boldsymbol{\xi})$ in the i^{th} layer created by the steady motion of the body moving in the j^{th} layer of a three layer fluid system are given by (Wang, 1989, pages 51-62) :

(1) The continuity equation

$$\nabla^2 \phi_{ij} = 0 \quad \text{for } i = 1, 2, 3 \tag{5}$$

(2) The free surface condition

$$\phi_{1j_{xx}} + k_0 \phi_{1j_x} = 0 \quad \text{on } z = h_j \tag{6}$$

(3) The interface condition

$$\phi_{(i-1)j_z} = \phi_{ij_z} \quad \text{on } z = h_j - h_i \quad \text{for } i = 2, 3 \tag{7}$$

$$\rho_{(i-1)}[\phi_{(i-1)j_{xx}} + k_0 \phi_{(i-1)j_z}] = \rho_i[\phi_{ij_{xx}} + k_0 \phi_{ij_z}] \quad \text{on } z = h_j - h_i \quad \text{for } i = 2, 3 \tag{8}$$

(4) The radiation condition

$$\phi_{ij} = \begin{cases} O(\frac{1}{|\boldsymbol{x}|}) & \text{for } x > 0 \\ o(1) & \text{for } x < 0 \end{cases} \quad \text{as } |\boldsymbol{x}| \to \infty \quad \text{for } i = 1, 2, 3 \tag{9}$$

(5) The bottom condition

$$\nabla \phi_{3j} \to 0 \quad \text{as } z \to -\infty \tag{10}$$

where $k_0 = \frac{g}{U_0^2}$, $O(x)$ and $o(x)$ denote the Landau order symbols as defined by Erdelyi (1956). Here h_i is the vertical separation of the free surface and i^{th} interface, h_j is the vertical separation of the origin and the free surface.

Equation 5 ensures the fluid disturbance can be described by potential flow theory. Equation 6 describes a combination of the kinematic and dynamic conditions applied on the free surface. The kinematic condition ensures that the fluid particles cannot pass through the disturbed free surface, the dynamic condition constrains the pressure in the fluid at the disturbed free surface to be atmospheric. The application of this boundary condition allows the presence of wave systems on the free surface. Equation 7 ensures the vertical velocity is continuous across the interfaces. Equation 8 describes a similar condition to equation 6 but applied at the interfaces. Equation 9 requires that the waves only exist behind the body and there are no waves upstream. Equation 10 imposes the condition that the disturbance velocity potential decays with increasing depth.

3.2 Derivation of Green's Functions

The disturbance velocity potential solution can be obtained from the summation of a Green's function solution, $G_{ij}(\boldsymbol{x}\ ,\boldsymbol{\xi})$. That is, the Green's function solution is an expression modelling a single source of unit strength in the fluid system.

$$\phi_{ij}(\boldsymbol{x}\ ,\boldsymbol{\xi}) = \int_{-\frac{L}{2}}^{\frac{L}{2}} Q(\xi) G_{ij}(\boldsymbol{x};\xi,0,\zeta=-f)d\xi \tag{11}$$

This implies that $\phi_{ij}(\boldsymbol{x}\ ,\boldsymbol{\xi})$ in the boundary conditions 5 - 10 can be replaced by $G_{ij}(\boldsymbol{x}\ ,\boldsymbol{\xi})$

To ensure that equation 5 is satisfied, it is assumed that the Green's functions are of the form

$$G_{ij}(\boldsymbol{x}\ ,\boldsymbol{\xi}\ ) = -\frac{\delta_{ij}}{2\pi}\int_{-\pi}^{\pi}\int_{0}^{\infty} e^{k[iw\pm(z-\zeta)]}dkd\theta \qquad \begin{matrix} + & z-\zeta<0 \\ - & z-\zeta>0 \end{matrix}$$

$$+\int_{-\pi}^{\pi}\int_{0}^{\infty}\left[A_{ij}(k,\theta)e^{kz}+B_{ij}(k,\theta)e^{-kz}\right]e^{ikw}dkd\theta \tag{12}$$

for j=1,2,3 and i=1,2,3. Here δ_{ij} denotes the Kronecker delta function,

$$w = (x-\xi)\cos\theta + (y-\eta)\sin\theta \tag{13}$$

and $B_{3j}(k,\theta)=0$ to comply with the condition stated in equation 10.

The method of solution involves the substitution of the Green's functions into the free surface and interface conditions, thus forming a system of equations from which the unknown coefficients $A_{ij}(k,\theta)$ and $B_{ij}(k,\theta)$ can be determined.

3.3 Derivation of Greens Functions for the body in the upper layer

Substituting equation 12 into the boundary conditions 5-8 when $j = 1$ produces the system of equations

$$\begin{bmatrix} 1 & a & 0 & 0 & 0 \\ \delta_1 e^{-kt_1} & a\delta_1 e^{kt_1} & -e^{-kt_1} & -ae^{kt_1} & 0 \\ e^{-kt_1} & -e^{kt_1} & -e^{-kt_1} & e^{kt_1} & 0 \\ 0 & 0 & \delta_2 e^{-k(t_1+t_2)} & a\delta_2 e^{k(t_1+t_2)} & -e^{-k(t_1+t_2)} \\ 0 & 0 & e^{-k(t_1+t_2)} & -e^{k(t_1+t_2)} & -e^{-k(t_1+t_2)} \end{bmatrix} \begin{Bmatrix} A_{11} \\ B_{11} \\ A_{21} \\ B_{21} \\ A_{31} \end{Bmatrix} = \frac{1}{2\pi} \begin{Bmatrix} ae^{k\zeta} \\ \delta_1 e^{-k(t_1+\zeta)} \\ e^{-k(t_1+\zeta)} \\ 0 \\ 0 \end{Bmatrix} \tag{14}$$

where $\delta_1 = \frac{\rho_1}{\rho_2}$, $\delta_2 = \frac{\rho_2}{\rho_3}$, $k_f = \frac{k_0}{\cos^2\theta}$ and $a = \frac{k+k_f}{k-k_f}$.

Solving for $A_{i1}(k,\theta)$ and $B_{i1}(k,\theta)$ then substituting into equation 12, we obtain the results:

$$G_{11}(\boldsymbol{x}\ ,\boldsymbol{\xi}) = -\frac{1}{2\pi}\int_{-\pi}^{\pi}\int_{0}^{\infty} e^{k[iw\pm(z-\zeta)]}dkd\theta$$

$$+\frac{1}{2\pi}\int_{-\pi}^{\pi}\int_{0}^{\infty} \frac{ae^{k(iw+z)}\left\{(1+a\delta_2)e^{kt_2}\left[(1+a\delta_1)e^{k(t_1+\zeta)}+(1-\delta_1)e^{-k(t_1+\zeta)}\right]+(1-\delta_2)e^{-kt_2}\left[a(1-\delta_1)e^{k(t_1+\zeta)}+(a+\delta_1)e^{-k(t_1+\zeta)}\right]\right\}}{(1+a\delta_2)e^{kt_2}\left[(1+a\delta_1)e^{kt_1}+a(1-\delta_1)e^{-kt_1}\right]+a(1-\delta_2)e^{-kt_2}\left[(1-\delta_1)e^{kt_1}+(a+\delta_1)e^{-kt_1}\right]}dkd\theta$$

$$+\frac{1}{2\pi}\int_{-\pi}^{\pi}\int_{0}^{\infty} \frac{e^{k(iw-z)}(ae^{k(\zeta-t_1)}-e^{-k(\zeta+t_1)})\left[(1-\delta_1)(1+a\delta_2)e^{kt_2}+(a+\delta_1)(1-\delta_2)e^{-kt_2}\right]}{(1+a\delta_2)e^{kt_2}\left[(1+a\delta_1)e^{kt_1}+a(1-\delta_1)e^{-kt_1}\right]+a(1-\delta_2)e^{-kt_2}\left[(1-\delta_1)e^{kt_1}+(a+\delta_1)e^{-kt_1}\right]}dkd\theta \quad 0 \geq z \geq -t_1 \tag{15}$$

$$G_{21}(\boldsymbol{x}\ ,\boldsymbol{\xi}) = -\frac{1}{2\pi}\int_{-\pi}^{\pi}\int_{0}^{\infty} \frac{\delta_1(1+a)(e^{-k\zeta}-ae^{k\zeta})\left[(1+a\delta_2)e^{k(z+t_1+t_2)}+(1-\delta_2)e^{-k(z+t_1+t_2)}\right]e^{ikw}}{(1+a\delta_2)e^{kt_2}\left[(1+a\delta_1)e^{kt_1}+a(1-\delta_1)e^{-kt_1}\right]+a(1-\delta_2)e^{-kt_2}\left[(1-\delta_1)e^{kt_1}+(a+\delta_1)e^{-kt_1}\right]}dkd\theta \quad -t_1 \geq z \geq -(t_1+t_2) \tag{16}$$

$$G_{31}(\boldsymbol{x}\ ,\boldsymbol{\xi}) = -\frac{1}{2\pi}\int_{-\pi}^{\pi}\int_{0}^{\infty} \frac{\delta_1\delta_2(1+a)^2(e^{-k\zeta}-ae^{k\zeta})e^{k(iw+z+t_1+t_2)}}{(1+a\delta_2)e^{kt_2}\left[(1+a\delta_1)e^{kt_1}+a(1-\delta_1)e^{-kt_1}\right]+a(1-\delta_2)e^{-kt_2}\left[(1-\delta_1)e^{kt_1}+(a+\delta_1)e^{-kt_1}\right]}dkd\theta \quad -(t_1+t_2) \geq z > -\infty \tag{17}$$

3.4 Derivation of Greens Functions for the body in the middle layer

Substituting equation 12 into the boundary conditions 5-8 when $j = 2$ produces the system of equations

$$\begin{bmatrix} e^{kt_1} & ae^{-kt_1} & 0 & 0 & 0 \\ 1 & -1 & -1 & 1 & 0 \\ -\delta_1 & -a\delta_1 & 1 & a & 0 \\ 0 & 0 & e^{-kt_2} & -e^{kt_2} & -e^{-kt_2} \\ 0 & 0 & \delta_2 e^{-kt_2} & a\delta_2 e^{kt_2} & -e^{-kt_2} \end{bmatrix} \begin{Bmatrix} A_{12} \\ B_{12} \\ A_{22} \\ B_{22} \\ A_{32} \end{Bmatrix} = \frac{1}{2\pi} \begin{Bmatrix} 0 \\ e^{k\zeta} \\ ae^{k\zeta} \\ e^{-k(t_2+\zeta)} \\ \delta_2 e^{-k(t_2+\zeta)} \end{Bmatrix} \tag{18}$$

Solving for $A_{i2}(k,\theta)$ and $B_{i2}(k,\theta)$ then substituting into equation 12, we obtain the results:

$$G_{12}(\boldsymbol{x}\ ,\boldsymbol{\xi}) = \frac{1}{2\pi}\int_{-\pi}^{\pi}\int_{0}^{\infty} \frac{(1+a)e^{ikw}\left[(1+a\delta_2)e^{k(t_2+\zeta)}+(1-\delta_2)e^{-k(t_2+\zeta)}\right]\left(ae^{k(z-t_1)}-e^{-k(z-t_1)}\right)}{(1+a\delta_2)e^{kt_2}\left[(1+a\delta_1)e^{kt_1}+a(1-\delta_1)e^{-kt_1}\right]+a(1-\delta_2)e^{-kt_2}\left[(1-\delta_1)e^{kt_1}+(a+\delta_1)e^{-kt_1}\right]}dkd\theta \quad t_1 \geq z \geq 0 \tag{19}$$

$$G_{22}(\boldsymbol{x}\ ,\boldsymbol{\xi}) = -\frac{1}{2\pi}\int_{-\pi}^{\pi}\int_{0}^{\infty} e^{k[iw\pm(z-\zeta)]}dkd\theta$$

$$+\frac{1}{2\pi}\int_{-\pi}^{\pi}\int_{0}^{\infty} \frac{ae^{k(iw+z)}\left\{(1-\delta_1)e^{kt_1}\left[(1+a\delta_2)e^{k(t_2+\zeta)}+(1-\delta_2)e^{-k(t_2+\zeta)}\right]+(a+\delta_1)e^{-kt_1}\left[(1+a\delta_2)e^{k(t_2+\zeta)}+(1-\delta_2)e^{-k(t_2+\zeta)}\right]\right\}}{(1+a\delta_2)e^{kt_2}\left[(1+a\delta_1)e^{kt_1}+a(1-\delta_1)e^{-kt_1}\right]+a(1-\delta_2)e^{-kt_2}\left[(1-\delta_1)e^{kt_1}+(a+\delta_1)e^{-kt_1}\right]}dkd\theta$$

$$-\frac{1}{2\pi}\int_{-\pi}^{\pi}\int_{0}^{\infty} \frac{(1-\delta_2)e^{k(iw-z-t_2)}\left\{e^{kt_1}\left[(1+a\delta_1)e^{-k\zeta}-a(1-\delta_1)e^{k\zeta}\right]+ae^{-kt_1}\left[(1-\delta_1)e^{-k\zeta}-(a+\delta_1)e^{k\zeta}\right]\right\}}{(1+a\delta_2)e^{kt_2}\left[(1+a\delta_1)e^{kt_1}+a(1-\delta_1)e^{-kt_1}\right]+a(1-\delta_2)e^{-kt_2}\left[(1-\delta_1)e^{kt_1}+(a+\delta_1)e^{-kt_1}\right]}dkd\theta \quad 0 \geq z \geq -t_2 \tag{20}$$

$$G_{32}(\boldsymbol{x}\ ,\boldsymbol{\xi}) = \frac{1}{2\pi}\int_{-\pi}^{\pi}\int_{0}^{\infty} \frac{\delta_2(1+a)e^{k(iw+z+t_2)}\left\{e^{kt_1}\left[a(1-\delta_1)e^{k\zeta}-(1+a\delta_1)e^{-k\zeta}\right]+ae^{-kt_1}\left[(a+\delta_1)e^{k\zeta}-(1-\delta_1)e^{-k\zeta}\right]\right\}}{(1+a\delta_2)e^{kt_2}\left[(1+a\delta_1)e^{kt_1}+a(1-\delta_1)e^{-kt_1}\right]+a(1-\delta_2)e^{-kt_2}\left[(1-\delta_1)e^{kt_1}+(a+\delta_1)e^{-kt_1}\right]}dkd\theta \quad -t_2 \geq z > -\infty \tag{21}$$

3.5 Derivation of Greens Functions for the body in the lower layer

Substituting equation 12 into the boundary conditions 5-8 when $j = 3$ with the body in the lower layer produces the system of equations

$$\begin{bmatrix} e^{k(t_1+t_2)} & ae^{-k(t_1+t_2)} & 0 & 0 & 0 \\ \delta_1 e^{kt_2} & a\delta_1 e^{-kt_2} & -e^{-kt_2} & -ae^{-kt_2} & 0 \\ e^{kt_2} & -e^{-kt_2} & -e^{-kt_2} & e^{-kt_2} & 0 \\ 0 & 0 & -\delta_2 & -a\delta_2 & 1 \\ 0 & 0 & 1 & -1 & -1 \end{bmatrix} \begin{Bmatrix} A_{13} \\ B_{13} \\ A_{23} \\ B_{23} \\ A_{33} \end{Bmatrix} = \frac{e^{k\zeta}}{2\pi} \begin{Bmatrix} 0 \\ 0 \\ 0 \\ a \\ 1 \end{Bmatrix} \tag{22}$$

Solving for $A_{i3}(k,\theta)$ and $B_{i3}(k,\theta)$ then substituting into equation 12, we obtain the results:

$$G_{13}(\boldsymbol{x}\ ,\boldsymbol{\xi}) = \frac{1}{2\pi}\int_{-\pi}^{\pi}\int_{0}^{\infty} \frac{(1+a)^2 e^{k(iw+\zeta)}(ae^{k(z-t_1-t_2)} - e^{-k(z-t_1-t_2)})}{(1+a\delta_2)e^{kt_2}\left[(1+a\delta_1)e^{kt_1} + a(1-\delta_1)e^{-kt_1}\right] + a(1-\delta_2)e^{-kt_2}\left[(1-\delta_1)e^{kt_1} + (a+\delta_1)e^{-kt_1}\right]} dkd\theta \quad t_1+t_2 \geq z \geq t_2 \tag{23}$$

$$G_{23}(\boldsymbol{x}\ ,\boldsymbol{\xi}) = \frac{1}{2\pi}\int_{-\pi}^{\pi}\int_{0}^{\infty} \frac{(1+a)e^{k(iw+\zeta)}\left\{ae^{k(z-t_2)}\left[(1-\delta_1)e^{kt_1} + (a+\delta_1)e^{-kt_1}\right] - e^{-k(z-t_2)}\left[(1+a\delta_1)e^{kt_1} + a(1-\delta_1)e^{-kt_1}\right]\right\}}{(1+a\delta_2)e^{kt_2}\left[(1+a\delta_1)e^{kt_1} + a(1-\delta_1)e^{-kt_1}\right] + a(1-\delta_2)e^{-kt_2}\left[(1-\delta_1)e^{kt_1} + (a+\delta_1)e^{-kt_1}\right]} dkd\theta \quad t_2 \geq z \geq 0 \tag{24}$$

$$G_{33}(\boldsymbol{x}\ ,\boldsymbol{\xi}) = -\frac{1}{2\pi}\int_{-\pi}^{\pi}\int_{0}^{\infty} e^{k[iw\pm(z-\zeta)]} dkd\theta$$

$$+\frac{1}{2\pi}\int_{-\pi}^{\pi}\int_{0}^{\infty} \frac{ae^{k(iw+z+\zeta)}\left\{e^{kt_1}\left[(1+a\delta_1)(1-\delta_2)e^{kt_2} + (1-\delta_1)(a+\delta_2)e^{-kt_2}\right] + e^{-kt_1}\left[a(1-\delta_1)(1-\delta_2)e^{kt_2} + (a+\delta_1)(a+\delta_2)e^{-kt_2}\right]\right\}}{(1+a\delta_2)e^{kt_2}\left[(1+a\delta_1)e^{kt_1} + a(1-\delta_1)e^{-kt_1}\right] + a(1-\delta_2)e^{-kt_2}\left[(1-\delta_1)e^{kt_1} + (a+\delta_1)e^{-kt_1}\right]} dkd\theta \quad 0 \geq z > -\infty \tag{25}$$

3.6 Application of the radiation condition

The Green's functions 15 - 17, 19 - 21 and 23 - 25 now satisfy the boundary conditions 5-8 and 10, the radiation condition however has yet to be addressed. The wavenumber integration, involving the circumvention of the singularities present in the Green's functions, provides an opportunity to examine the functions as $x \rightarrow \infty$. The upstream expressions are then subtracted from the Green's functions to provide equations satisfying all boundary conditions. An example of this process for a body located in the upper layer of a two layer fluid is given by Wang (1989), pages 70-78.

3.7 Complete velocity potentials

The following Green's functions comply with all the boundary conditions described in 3.1

$$G_{ij}(\boldsymbol{x}\ ,\boldsymbol{\xi}) = -\delta_{ij}\left(\frac{1}{r_1}+\frac{1}{r_2}\right)+\frac{1}{\pi}\int_0^{\frac{\pi}{2}} P.V.\int_0^{\infty}\frac{F_{ij}(k,\theta)C(k,\theta)}{(k-k_f)D(k,\theta)}dkd\theta+\int_0^{\frac{\pi}{2}}\frac{F_{0_j}(\theta)S(k_f,\theta)}{D_0(\theta)}d\theta$$

$$+\sum_{l=1}^{N_r}\int_{\theta_0}^{\frac{\pi}{2}}\frac{F_{ij}(\alpha_l,\theta)S(\alpha_l,\theta)}{(\alpha_l-k_f)D_k(\alpha_l,\theta)}d\theta \tag{26}$$

here *P.V.* denotes Cauchy's principal value integral, α_l is the l^{th} root of k determined from the equation $D(k,\theta)=0$ and N_r is the number of non zero roots of $D(k,\theta)=0$,

$$C(k,\theta) = \cos[k(x-\xi)\cos\theta]\cos[k(y-\eta)\sin\theta] \tag{27}$$

$$D(k,\theta) = \delta_1 k(1-\delta_2)(k+k_f)e^{-kt_2}\sinh(kt_1)$$

$$-[\cosh(kt_1)+\delta_1\sinh(kt_1)][\cosh(kt_2)+\delta_2\sinh(kt_2)][k-\frac{k(1-\delta_1)\tanh(kt_1)}{1+\delta_1\tanh(kt_1)}][k-\frac{k(1-\delta_2)\tanh(kt_2)}{1+\delta_2\tanh(kt_2)}] \tag{28}$$

$$D_0(k,\theta) = -[\delta_1\delta_2+(1-\delta_1)\delta_2 e^{-2k_f t_1}+(1-\delta_2)e^{-2k(t_1+t_2)}] \tag{29}$$

$$D_k(k,\theta) = \frac{\partial\{D(k,\theta)\}}{\partial k}e^{-k(t_1+t_2)} \tag{30}$$

$$F_{0_1}(\theta) = -4\delta_1\delta_2 k_f e^{k_f(z+\zeta)} \tag{31}$$

$$F_{0_2}(\theta) = -4\delta_2 k_f e^{k_f(z+\zeta-2t_1)} \tag{32}$$

$$F_{0_3}(\theta) = -4k_f e^{k_f(z+\zeta-2t_1-2t_2)} \tag{33}$$

$$r_1 = \sqrt{(x-\xi)^2+(y-\eta)^2+(z-\zeta)^2} \tag{34}$$

$$r_2 = \sqrt{(x-\xi)^2+(y-\eta)^2+(z+\zeta)^2} \tag{35}$$

$$S(k,\theta) = \sin[k(x-\xi)\cos\theta]\cos[k(y-\eta)\sin\theta] \tag{36}$$

and the 'F' functions are defined as

$$F_{11}(k,\theta) = -\frac{1}{2}(k+k_f)e^{kz}\left[(k-k_f)+\delta_2(k+k_f)\right]\left\{\left[(k-k_f)+\delta_1(k+k_f)\right]e^{k\zeta}+(k-k_f)(1-\delta_1)e^{-k(2t_1+\zeta)}\right\}$$

$$-\frac{1}{2}(k+k_f)(k-k_f)(1-\delta_2)e^{k(z-2t_2)}\left\{(k+k_f)(1-\delta_1)e^{k\zeta}+\left[(k+k_f)+\delta_1(k-k_f)\right]e^{-k(2t_1+\zeta)}\right\}$$

$$-\frac{1}{2}(k-k_f)e^{-k(2t_1+z)}\left[(k+k_f)e^{k\zeta}-(k-k_f)e^{-k\zeta}\right]\left\{(1-\delta_1)\left[(k-k_f)+\delta_2(k+k_f)\right]+(1-\delta_2)\left[(k+k_f)+\delta_1(k-k_f)\right]e^{-2kt_2}\right\} \tag{37}$$

$$F_{12}(k,\theta) = -k\left\{\left[(k-k_f)+\delta_2(k+k_f)\right]e^{k\zeta}+(1-\delta_2)(k-k_f)e^{-k(2t_2+\zeta)}\right\}\left[(k+k_f)e^{k(z-2t_1)}-(k-k_f)e^{-kz}\right] \tag{38}$$

$$F_{13}(k,\theta) = -2k^2e^{k\zeta}\left[(k+k_f)e^{(z-2t_1-2t_2)}-(k-k_f)e^{-kz}\right] \tag{39}$$

$$F_{21}(k,\theta) = -\delta_1 k\left[(k+k_f)e^{k\zeta}-(k-k_f)e^{-k\zeta}\right]\left\{\left[(k-k_f)+\delta_2(k+k_f)\right]e^{kz}+(1-\delta_2)(k-k_f)e^{-k(z+2t_1+2t_2)}\right\} \tag{40}$$

$$F_{22}(k,\theta) = -\frac{1}{2}(k+k_f)e^{kz}\left\{\left[(k-k_f)+\delta_2(k+k_f)\right]e^{k\zeta}+(1-\delta_2)(k-k_f)e^{-k(2t_2+\zeta)}\right\}\left[(1-\delta_1)(k+k_f)+\left[(k+k_f)+\delta_1(k-k_f)\right]e^{-2kt_1}\right]$$

$$-\frac{1}{2}(1-\delta_2)(k-k_f)e^{-k(z+2t_2)}\left\{(k-k_f)\left[(1-\delta_1)(k+k_f)e^{k\zeta}-\left[(k-k_f)+\delta_1(k+k_f)\right]e^{-k\zeta}\right]+(k+k_f)e^{-2kt_1}\left[\left[(k+k_f)+\delta_1(k-k_f)\right]e^{k\zeta}-(1-\delta_1)(k+k_f)e^{-k\zeta}\right]\right\} \tag{41}$$

$$F_{23}(k,\theta) = -ke^{k\zeta}\left\{(k+k_f)e^{k(z-2t_2)}\left[(1-\delta_1)(k-k_f)+\left[(k+k_f)+\delta_1(k-k_f)\right]e^{-2kt_1}\right]-(k-k_f)e^{-kz}\left[(k-k_f)+\delta_1(k+k_f)+(1-\delta_1)(k+k_f)e^{-2kt_1}\right]\right\} \tag{42}$$

$$F_{31}(k,\theta) = -2\delta_1\delta_2k^2\left[(k+k_f)e^{k\zeta}-(k-k_f)e^{-k\zeta}\right]e^{kz} \tag{43}$$

$$F_{32}(k,\theta) = -\delta_2 ke^{kz}\left\{(k-k_f)\left[(1-\delta_1)(k+k_f)e^{k\zeta}-\left[(k-k_f)+\delta_1(k+k_f)\right]e^{-k\zeta}\right]+(k+k_f)e-2kt_1\left\{\left[(k+k_f)+\delta_1(k-k_f)\right]e^{k\zeta}-(1-\delta_1)(k-k_f)e^{-k\zeta}\right]\right\} \tag{44}$$

$$F_{33}(k,\theta) = -\frac{1}{2}(k+k_f)(k-k_f)e^{k(z+\zeta)}\left\{(1-\delta_2)\left[(k-k_f)+\delta_1(k+k_f)\right]+(1-\delta_1)\left[(k+k_f)+\delta_2(k-k_f)\right]e^{-2kt_2}\right\}$$

$$-\frac{1}{2}(k+k_f)e^{k(z+\zeta-2kt_1)}\left\{(1-\delta_1)(1-\delta_2)(k-k_f)(k+k_f)+\left[(k+k_f)+\delta_1(k-k_f)\right]\left[(k+k_f)+\delta_2(k-k_f)\right]e^{-2kt_2}\right\} \tag{45}$$

In these expressions the lower limit of the theta integral, θ_0, is given by

$$\theta_0 = \begin{cases} 0 & N_r = 2 & & U_0 \le U_{cl} \\ 0 & N_r = \begin{cases} 1 & 0 \le \theta < \theta_1 \\ 2 & \theta_1 \le \theta \le \frac{\pi}{2} \end{cases} & & U_{cl} < U_0 \le U_{cu} \\ \theta_2 & N_r = \begin{cases} 1 & \theta_2 \le \theta < \theta_1 \\ 2 & \theta_1 \le \theta \le \frac{\pi}{2} \end{cases} & & U_0 > U_{cu} \end{cases} \tag{46}$$

where

$$\theta_1 = \cos^{-1}\left(\frac{U_{cl}}{U_0}\right) \tag{47}$$

$$\theta_2 = \cos^{-1}\left(\frac{U_{cu}}{U_0}\right) \tag{48}$$

$$U_{cl} = \left(\frac{g}{s_+}\right)^{\frac{1}{2}} \tag{49}$$

$$U_{cu} = \left(\frac{g}{s_-}\right)^{\frac{1}{2}} \tag{50}$$

$$s_\pm = \frac{b \pm (b^2 - 4a)^{\frac{1}{2}}}{2a} \tag{51}$$

$$a = (1-\delta_1)(1-\delta_2)t_1 t_2 \tag{52}$$

$$b = (1-\delta_1)t_1 + (1-\delta_2)t_2 + \delta_1(1-\delta_2)t_1 \tag{53}$$

Substituting the Green's functions into equation 11 and completing the ξ integration produces the velocity potential for the i^{th} layer we find that when the body is moving in the j^{th} layer

$$\phi_{ij}(\boldsymbol{x}\ ,\boldsymbol{\xi}) = -\frac{\xi^2\delta_{ij}}{2}\left(\frac{1}{r_1}+\frac{1}{r_2}\right) + \frac{1}{\pi}\int_0^{\frac{\pi}{2}} P.V.\int_0^\infty \frac{F_{ij}(k,\theta)P_1(k,\theta)}{(k-k_f)D(k,\theta)}dk\,d\theta + \int_0^{\frac{\pi}{2}} \frac{F_{0_j}(\theta)P_2(k_f,\theta)}{D_0(\theta)}d\theta$$

$$\sum_{l=1}^{N_r}\int_{\theta_0}^{\frac{\pi}{2}} \frac{F_{ij}(\alpha_l,\theta)P_2(\alpha_l,\theta)}{(\alpha_l-k_f)D_k(\alpha_l,\theta)}d\theta \tag{54}$$

where

$$P_1(k,\theta) = \sin(kx\cos\theta)\cos\left[k(y-\eta)\sin\theta\right]P_3(k,\theta) \tag{55}$$

$$P_2(k,\theta) = -\cos(kx\cos\theta)\cos\left[k(y-\eta)\sin\theta\right]P_3(k,\theta) \tag{56}$$

$$P_3(k,\theta) = U_0\left(\frac{d}{kL\cos\theta}\right)^2\left[\sin\left(\frac{kL\cos\theta}{2}\right) - \frac{kL}{2}\cos\theta\cos\left(\frac{kL\cos\theta}{2}\right)\right] \tag{57}$$

and the far field expressions for the velocity potentials are

$$\phi_{ij}(\boldsymbol{x}\ ,\boldsymbol{\xi}) = \int_0^{\frac{\pi}{2}} \frac{F_{0_j}(\theta)P_2(k_f,\theta)}{D_0(\theta)}d\theta$$

$$+\sum_{l=1}^{N_r}\int_{\theta_0}^{\frac{\pi}{2}} \frac{F_{ij}(\alpha_l,\theta)P_2(\alpha_l,\theta)}{(\alpha_l-k_f)D_k(\alpha_l,\theta)}d\theta \tag{58}$$

The velocity potentials defined in equation 54 reduce to the velocity potentials describing a body moving in a two layer fluid when either of the density ratios δ_1 or δ_2 is equated to unity. The reduction also occurs when either of the layer thicknesses is zero. Finally the velocity potential for a body moving in a homogeneous fluid can be obtained when an appropriate combination of two of the four options above are applied to equation 54.

4 Far field free surface and interface disturbances

The linearised disturbance on the free surface, ζ_1, is given by

$$\zeta_1(x,y) = \frac{U_0}{g}\phi_{1j_x} \tag{59}$$

and on the i^{th} interface

$$\zeta_i(x,y) = \frac{1}{\rho_i - \rho_{i-1}}\frac{U_0}{g}[\rho_i\phi_{ij_x} - \rho_{i-1}\phi_{(i-1)j_x}] \quad \text{for } i = 2,3 \tag{60}$$

Substituting equation 58 into equation 59 yields the far field surface elevation caused by the moving prolate spheroid and this may be written in the form

$$\zeta_1(x,y) = \frac{2U_0}{g}\int_0^{\frac{\pi}{2}} \frac{F_{0_j}(\theta)P_4(k_f,\theta)}{D_0(\theta)}d\theta$$

$$+ \frac{2U_0}{g}\sum_{l=1}^{N_r}\int_{\theta_0}^{\frac{\pi}{2}} \frac{F_{1j}(\alpha_l,\theta)P_4(\alpha_l,\theta)}{(\alpha_l - k_f)D_k(\alpha_l,\theta)}d\theta \tag{61}$$

and the far field interface elevation on the i^{th} interface is given by

$$\zeta_i(x,y) = \frac{2U_0}{g}\int_0^{\frac{\pi}{2}} \frac{F_{0_j}(\theta)P_4(k_f,\theta)}{D_0(\theta)}d\theta$$

$$+ \frac{2U_0}{g}\sum_{l=1}^{N_r}\int_{\theta_0}^{\frac{\pi}{2}} \frac{F_{ij}(\alpha_l,\theta)P_4(\alpha_l,\theta)}{(\alpha_l - k_f)D_k(\alpha_l,\theta)}d\theta \quad \text{for } i = 2,3 \tag{62}$$

where

$$P_4(k,\theta) = \frac{\partial\{P_2(k,\theta)\}}{\partial x} \tag{63}$$

5 Wave resistance

An expression for the wave resistance of the body can be derived using a three dimensional extension of Lagally's method (Sabuncu, 1961; Wang, 1989). In an ideal fluid a singularity $\boldsymbol{x} = (\xi', \eta', \zeta')$ experiences a resultant force due to the free stream and other singularities. The summation of these forces is equal to the wave resistance. Mathematically for a slender body this can be written in the form

$$R_w = -4\pi\rho_j \int_{-\frac{L}{2}}^{\frac{L}{2}} Q(\xi')\phi_{jj_x}(\boldsymbol{x},\boldsymbol{\xi})\Big|_{\boldsymbol{x}=(\xi',\eta,\zeta)} d\xi' \tag{64}$$

The substitution of equations 4, 11 and 26 into equation 64 gives

$$R_w = -4\pi\rho_j \left[2\pi U_0\left(\frac{d}{L}\right)^2\right]^2 \int_{-\frac{L}{2}}^{\frac{L}{2}}\int_{-\frac{L}{2}}^{\frac{L}{2}} \xi'\xi G_{jj_x}(\boldsymbol{x},\boldsymbol{\xi})\Big|_{\boldsymbol{x}=(\xi',\eta,\zeta)} d\xi d\xi' \tag{65}$$

and with the substitution of $G_{jj}(\boldsymbol{x},\boldsymbol{\xi})$ together with the results

$$\int_{-\frac{L}{2}}^{\frac{L}{2}}\int_{-\frac{L}{2}}^{\frac{L}{2}} \xi^{'}\xi \sin[k(\xi^{'}-\xi)\cos\theta]d\xi d\xi^{'} = 0 \tag{66}$$

$$\int_{-\frac{L}{2}}^{\frac{L}{2}}\int_{-\frac{L}{2}}^{\frac{L}{2}} \xi^{'}\xi(\xi^{'}-\xi)\left(\frac{1}{r_1}+\frac{1}{r_2}\right)_x\Big|_{\boldsymbol{x}=(\xi^{'},\eta,\zeta)} d\xi d\xi^{'} = 0 \tag{67}$$

we find that

$$R_w = -\rho_j\left[2\pi U_0\left(\frac{d}{L}\right)^2\right]^2\int_0^{\frac{\pi}{2}}\frac{k_f\cos\theta F_{0_j}(\theta)T(k_f,\theta)}{D_0(\theta)}d\theta$$

$$+\sum_{l=1}^{N_r}\int_{\theta_0}^{\frac{\pi}{2}}\frac{\alpha_l\cos\theta F_{jj}(\alpha_l,\theta)T(\alpha_l,\theta)}{(\alpha_l-k_f)D_k(\alpha_l,\theta)}d\theta \tag{68}$$

where

$$T(k,\theta) = \left\{\frac{L}{k\cos\theta}\left(\frac{1}{\frac{kL}{2}\cos\theta}\sin(\frac{kL}{2}\cos\theta)-\cos(\frac{kL}{2}\cos\theta)\right)\right\}^2 \tag{69}$$

The wave resistance of a body moving in a two layer or homogeneous fluid may be obtained through reducing the number of fluid layers as detailed in section 3.7.

6 Discussion of results

Figures 2, 3 and 4 are the free surface and interface elevations generated by a prolate spheroid moving in the upper, middle and lower layers respectively. Only the port half of the disturbance is plotted as the wave system is symmetrical about the body centreplane (ie the plane $y = 0$). The area shown commences one body length behind the stern and extends nine body lengths longitudinally and six body lengths transversely from the centreline. The direction of motion of the body is towards the lower right hand side of the page. In all three cases the density of the upper layer, $\rho_1 = 1025\ Kg/m^3$, the density of the middle layer, $\rho_2 = 1026.5\ Kg/m^3$ and the density of the lower layer, $\rho_3 = 1028\ Kg/m^3$. The speed of the body is 2 m/s which lies in the supercritical region ($U_0 > U_{cu}$) for this fluid system. Therefore only the divergent part of the wave system is present. Additional information relevent to the each figure can be found in the captions.

The free surface shears corresponding to figures 2, 3 and 4 are the figures 5, 6 and 7 respectively. As previously, only the port half of the disturbance is plotted and the area shown is the $9L$ x $6L$ rectangle described in the paragraph above. The direction of motion of the body is towards the bottom of the page.

Figure 8 demonstrates the effect of the ratio L/d on the wave resistance experienced by the body. Here $L/d = 15$, 10 and 5 whilst a constant displacement is maintained. The effect of the diameter can readily be seen in equation 68, for the diameter dimension appears only outside the integral as a fourth power, the effect of length cannot be so easily determined as L also appears in the function $T(k,\theta)$. The non dimensional wave resistance coefficient is defined as $R_w/\frac{1}{2}\rho_j sU_0^2$. When the body is in the upper layer the effect of the free surface on C_w can clearly be observed. The presence of the stratification in the form of fluid layers produces a large spike at low Froude numbers when the body is moving in any layer. It is this spike which causes the "dead water" effect.

Figure 9 reveals how the maximum values of free surface and interface elevations are related to the speed of the body when the body is located in each layer. The maximum values of free surface and interface elevations are the maximum values present in the area behind the body (ie $9L$ x $6L$) as

previously described. The interfaces closest to the body display two maxima and a minimum, other interface disturbances have single peaks then decay monotonically with increasing speed.

Figures 10, 11, 12 and 13 display the change in the appearance of the free surface and interface wave patterns when the speed of the body is increased. At $U_0 = 0.25\ m/s$ the speed of the body is below the lower critical speed. The wave system consists of transverse waves and no divergent waves are present. As U_0 increases to $0.50\ m/s$, a speed which is between the lower and upper critical speeds a transition appears, a divergent contribution to the wave system is also apparent. Above the upper critical speed the tranverse portion of the wave system disappears and the disturbance consists of only the divergent waves. Any further increase in U_0 causes the disturbance to be contained within a decreasingly small angle given by $\frac{\pi}{2} - \theta_0$. These transitions are continuous, the divergent part of the wave system gradually becomes more prominent whilst the transverse part slowly decays. This implies that as the speed of the body increases the energy in the wave system shifts from a conc entration at low frequency to a concentration at high frequency.

The free surface shears corresponding to the wave systems generated at $U_0 = 0.25, 0.50, 1.50$ and $3.00\ m/s$, ie the figures 10, 11, 12 and 13 are the figures 14, 15, 16 and 17 respectively.

Figures 18 and 19 display the effect of the variation of the middle layer density when all other variables remain constant. The maximum values of elevations, currents and strains are the maximum values present in the area behind the body (ie $9L$ x $6L$) as previously described. When $\rho_2 = \rho_1$ or $\rho_2 = \rho_3$ the three layer fluid system reduces to a two layer fluid system. The points marked by triangles are the maximum values of the disturbance obtained from two layer theory. The trend clearly is towards the two layer results. The free surface disturbance increases when ρ_2 tends to ρ_1 whilst the first interface disturbance displays a maximum when ρ_2 is the average of the densities of the fluid from above and below the middle layer. The second interface disturbance has a maximum and minimum value over the density range.

7 Conclusion

The three layer model qualitively and quantitatively predicts the fluid disturbances and body forces produced by a body moving in a three layer fluid. The velocity potential, free surface elevation and wave resistance expressions reduce firstly to two layer expressions then to expressions describing a body in a homogeneous fluid. The "dead water" effect popularised by Ekman has been demonstrated to exist, its magnitude now calculable from a velocity potential solution. The results of the three layer fluid system will provide a useful comparison when the second stage of this investigation, a continuously stratified fluid, requires validation.

From a **submarine operational viewpoint**, if we assume a correlation between wavemaking resistance and wave pattern characteristics, there is evidence presented herein (e.g figure 8) to suggest that there is a small window of Froude numbers where the wavemaking resistance is a minimum and hence the wave pattern generated within the stratified fluid is less detectable. However before this operational benefit can be substantiated, more theoretical and experimental studies are needed.

References

Andrew, R. N., Baar, J. J. M., and Price, W. G. (1988). Prediction of ship wavemaking resistance and other steady flow parameters using neumann-kelvin theory. *Trans R.I.N.A.*, 130:119–133.

Apel, J. R. and Gjessing, D. T. (1989). Internal wave measurements in a Norwegian fjord using multi-frequency radars. *John Hopkins APL technical digest*, 10(4):295–306.

Baar, J. J. M. and Price, W. G. (1988). Developments in the calculation of the wavemaking resistance of ships. *Proc. R. Soc., London*, A416:115–147.

Crapper, G. D. (1967). Ship waves in a stratified ocean. *J. Fluid Mech*, 29(4):667–672.

Dysthe, K. B. and Trulsen, J. (1989). Internal waves from moving point sources. *John Hopkins APL technical digest*, 10(4):307–317.

Ekman, V. W. (1904). On dead water. *Scientific results of the Norwegian North Polar expedition 1893 - 1896*, 5(15):1–152. Publisher Kristiania, Editor Fridtjof Nansen.

Erdelyi, A. (1956). *Asymptotic expansions.* Dover.

Hudimac, A. A. (1961). Ship waves in a stratified ocean. *J. Fluid Mech*, 11:229–243.

Hughes, B. A. (1986). Surface wave wakes and internal wave wakes produced by surface ships. In *Proc. 16th Symp. on Naval Hydrodynamics*, pages 1–17, University of California, Berkeley. National Academy Press.

Keller, J. B. and Monk, W. H. (1970). Internal wave wakes of a body moving in a stratified fluid. *Phys. Fluids*, 13(6):1425–1431.

Miles, J. W. (1971). Internal waves generated by a horizontally moving point source. *Geophys. Fluid Dyn*, 2:63–87.

Price, W. G., Wang, Y., and Baar, J. J. M. (1988). Influence of fluid density on steady ship wave characteristics. In *Proc. 17th Symp. on Naval Hydrodynamics*, pages 63–78, The Hague. National Academy Press.

Rarity, B. S. H. (1967). The two dimensional wave pattern produced by a disturbance moving in an arbitrary direction in a density stratified liqiud. *J. Fluid Mech*, 30(2):329–336.

Sabuncu, T. (1961). The thoeretical wave resistance of a ship travelling under interfacial wave conditions. Norwegian ship model experiment tank publication 63, The Technical University of Norway.

Tulin, M. and Miloh, T. (1990). Ship internal waves in a shallow thermocline : the supersonic case. In *Proc. 18th Symp. on Naval Hydrodynamics*, pages 567–581, The University of Michigan, Ann Arbor. National Academy Press. I.S.B.N. 0-309-04575-4.

Wang, Y. (1989). *The influence of fluid stratification on wave making resistance and other steady flow parameters.* PhD thesis, Brunel University.

List of Figures

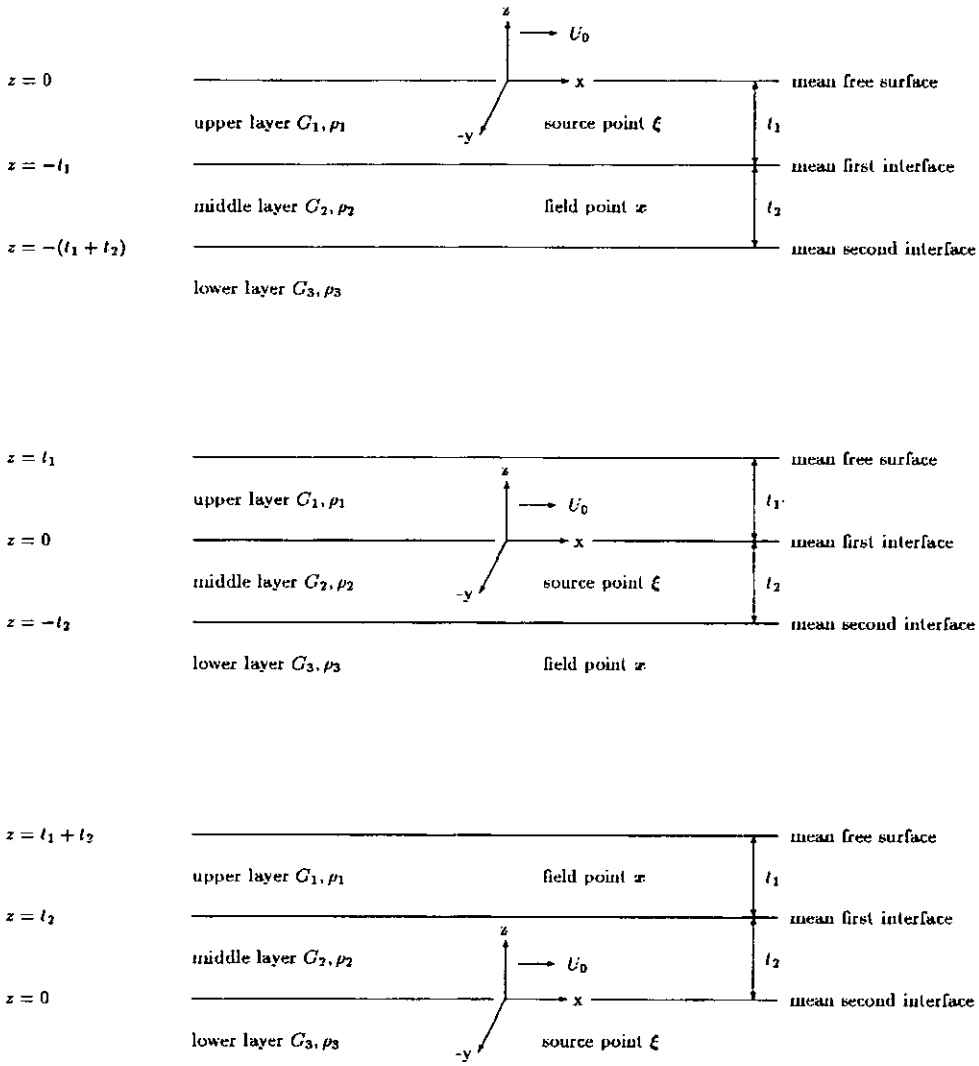

Figure 1: Configuration of the coordinate system.

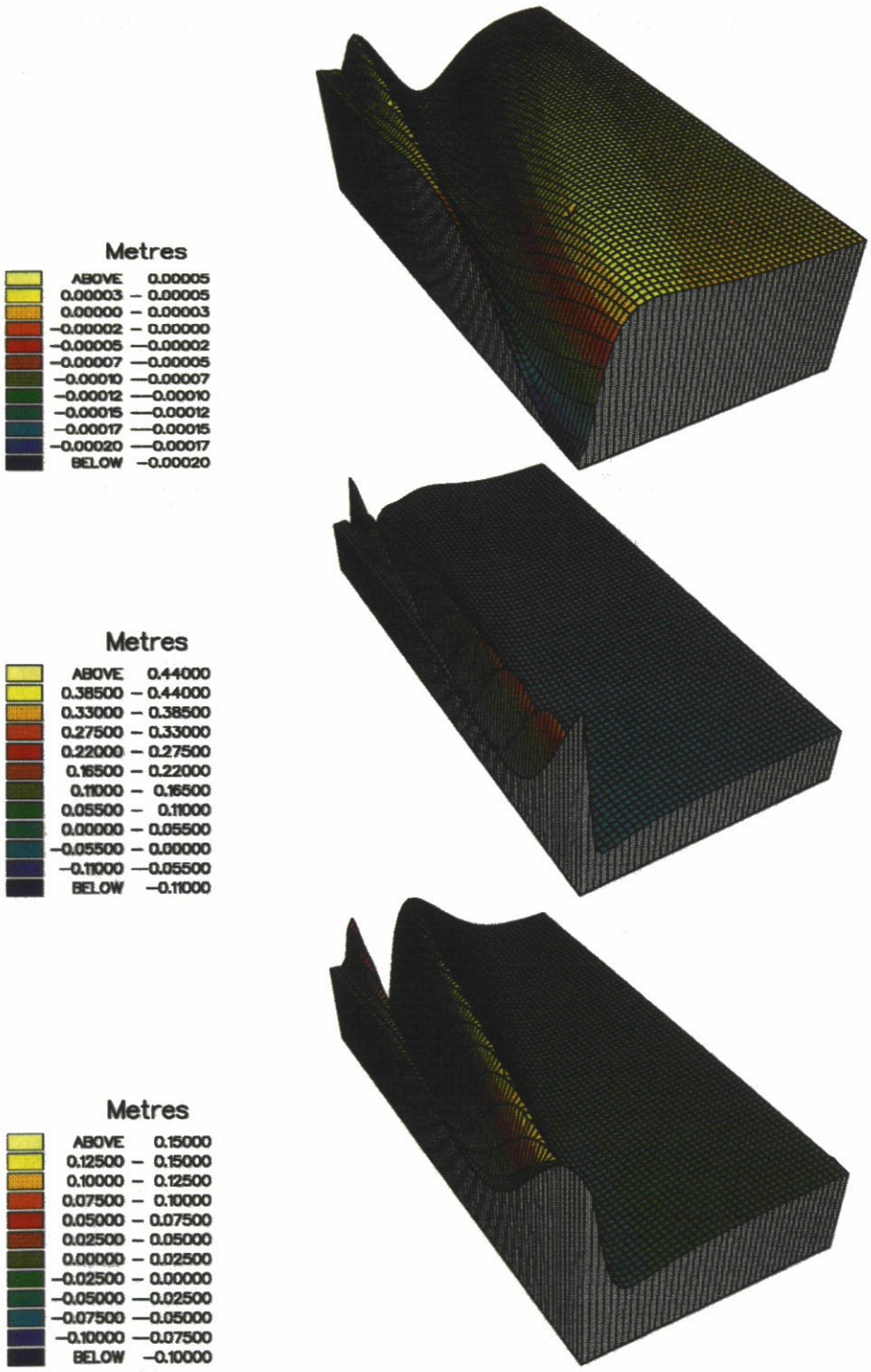

Figure 2: Free surface and interface wave systems when the body is in the upper layer. $U_0 = 2.0\ m/s$ $(F_n = 0.064)\ L = 100.0\ m\ d = 10.0\ m\ \rho_1 = 1025.0\ Kg/m^3\ \rho_2 = 1026.5\ Kg/m^3\ \rho_3 = 1028.0\ Kg/m^3$ $t_1 = 30.0\ m\ t_2 = 30.0\ m\ f = 15\ m$

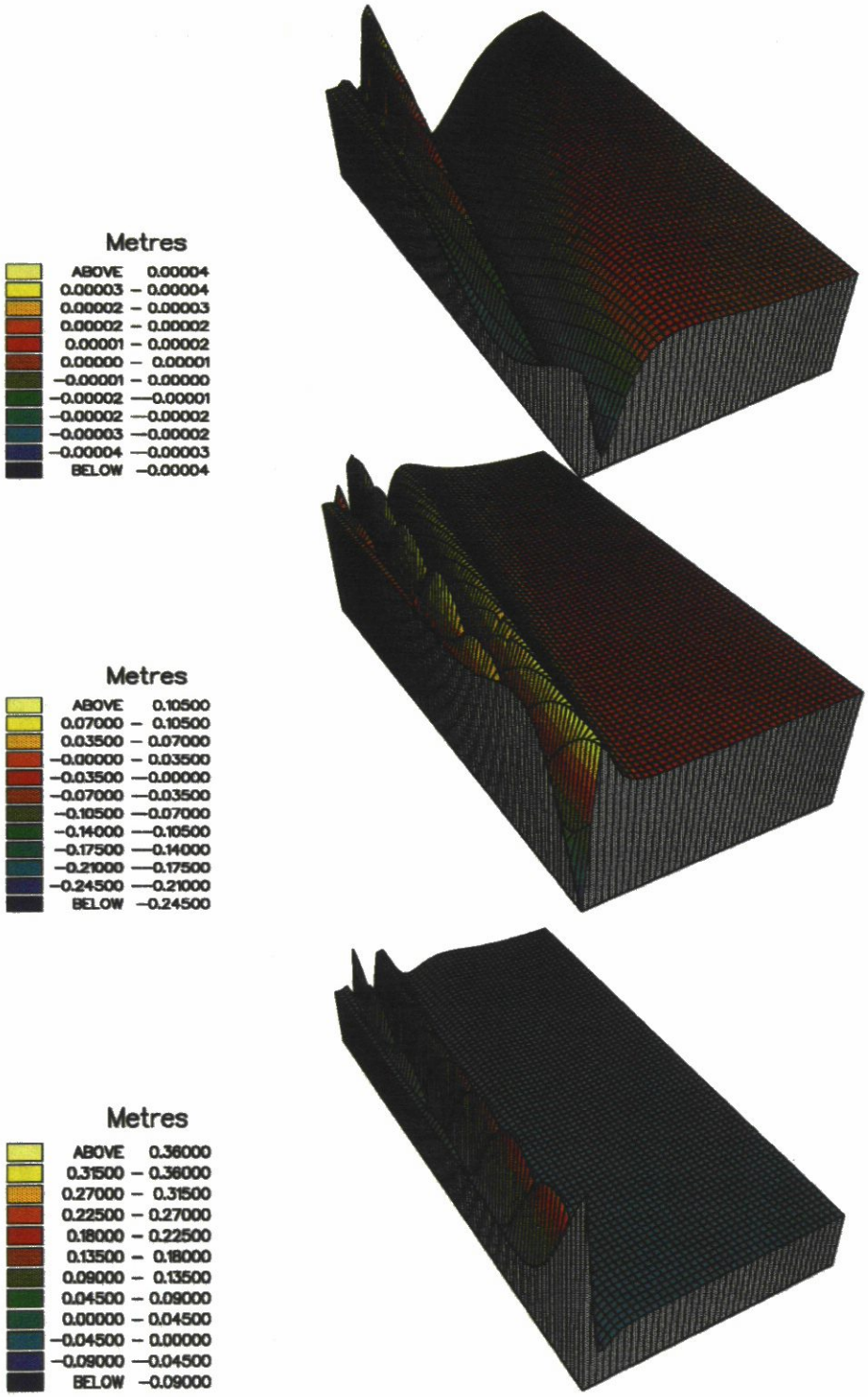

Figure 3: Free surface and interface wave systems when the body is in the middle layer. $U_0 = 2.0\ m/s$ $(F_n = 0.064)\ L = 100.0\ m\ d = 10.0\ m\ \rho_1 = 1025.0\ Kg/m^3\ \rho_2 = 1026.5\ Kg/m^3\ \rho_3 = 1028.0\ Kg/m^3$ $t_1 = 30.0\ m\ t_2 = 30.0\ m\ f = 45\ m$

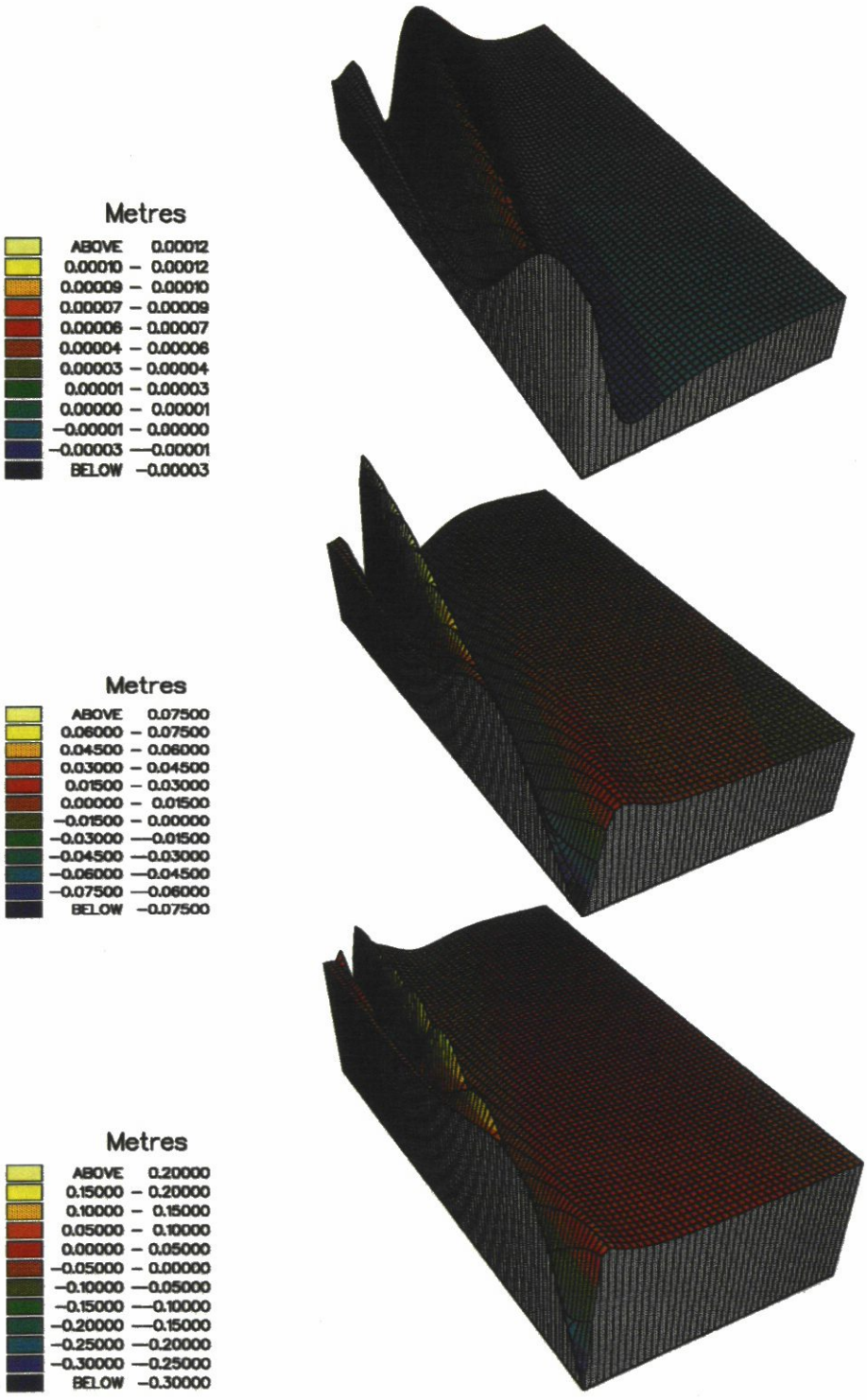

Figure 4: Free surface and interface wave systems when the body is in the lower layer. $U_0 = 2.0\ m/s$ $(F_n = 0.064)\ L = 100.0\ m\ d = 10.0\ m\ \rho_1 = 1025.0\ Kg/m^3\ \rho_2 = 1026.5\ Kg/m^3\ \rho_3 = 1028.0\ Kg/m^3$ $t_1 = 30.0\ m\ t_2 = 30.0\ m\ f = 75\ m$

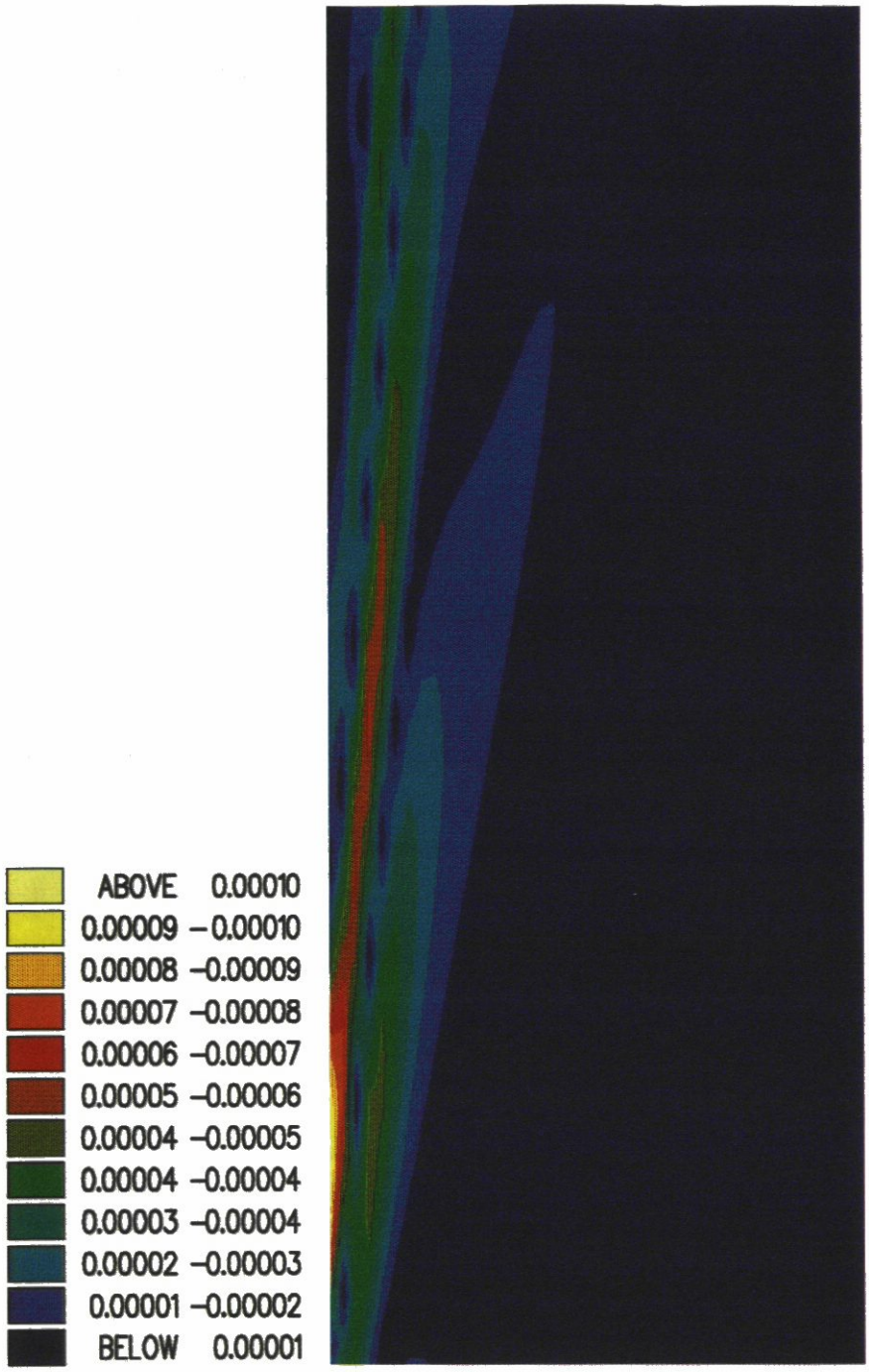

Figure 5: Free surface shear when the body is in the upper layer. $U_0 = 2.0\ m/s$ ($F_n = 0.064$) $L = 100.0\ m$ $d = 10.0\ m$ $\rho_1 = 1025.0\ Kg/m^3$ $\rho_2 = 1026.5\ Kg/m^3$ $\rho_3 = 1028.0\ Kg/m^3$ $t_1 = 30.0\ m$ $t_2 = 30.0\ m$ $f = 15\ m$

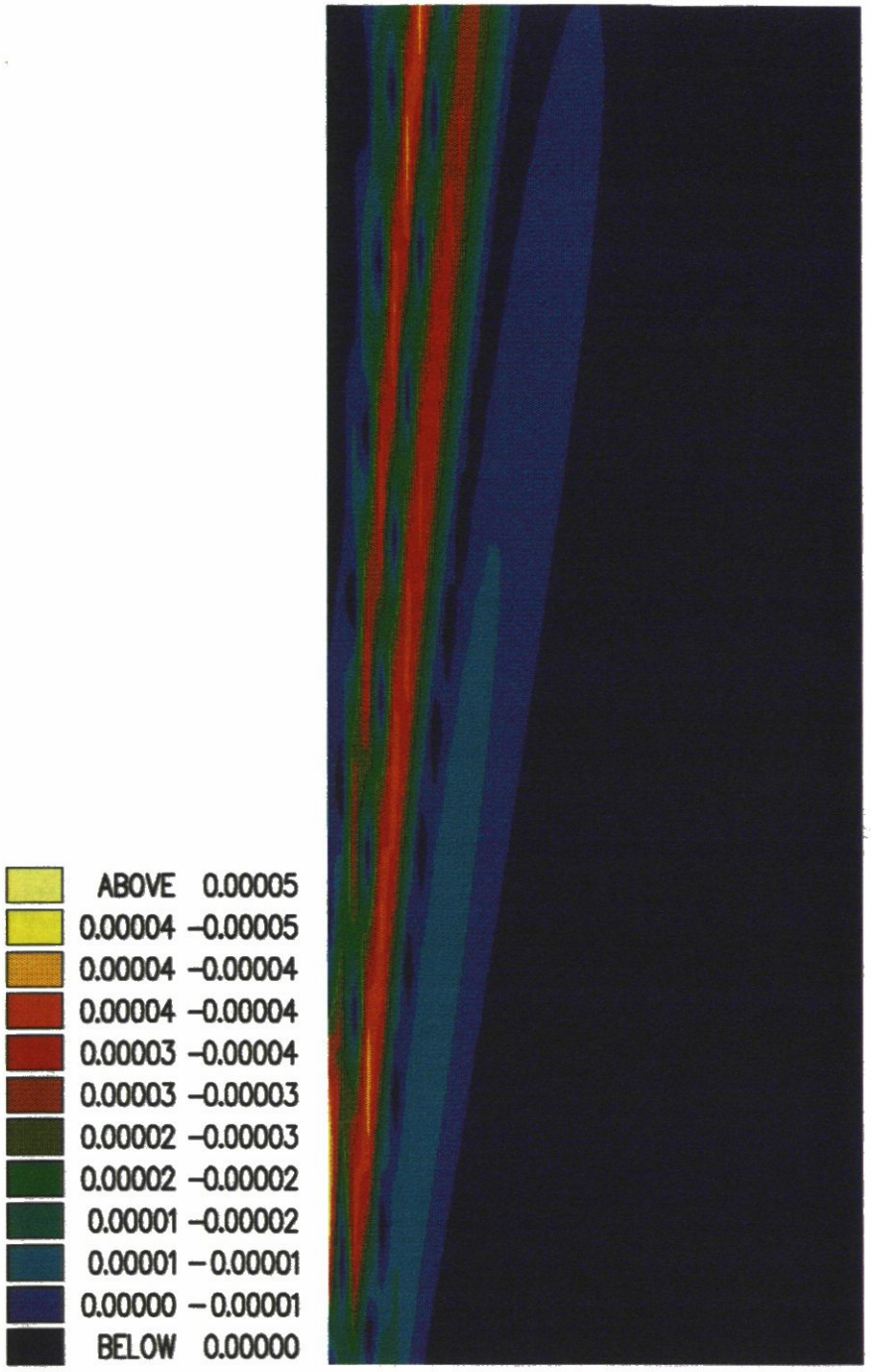

Figure 6: Free surface shear when the body is in the middle layer. $U_0 = 2.0\ m/s$ ($F_n = 0.064$) $L = 100.0\ m$ $d = 10.0\ m$ $\rho_1 = 1025.0\ Kg/m^3$ $\rho_2 = 1026.5\ Kg/m^3$ $\rho_3 = 1028.0\ Kg/m^3$ $t_1 = 30.0\ m$ $t_2 = 30.0\ m$ $f = 45\ m$

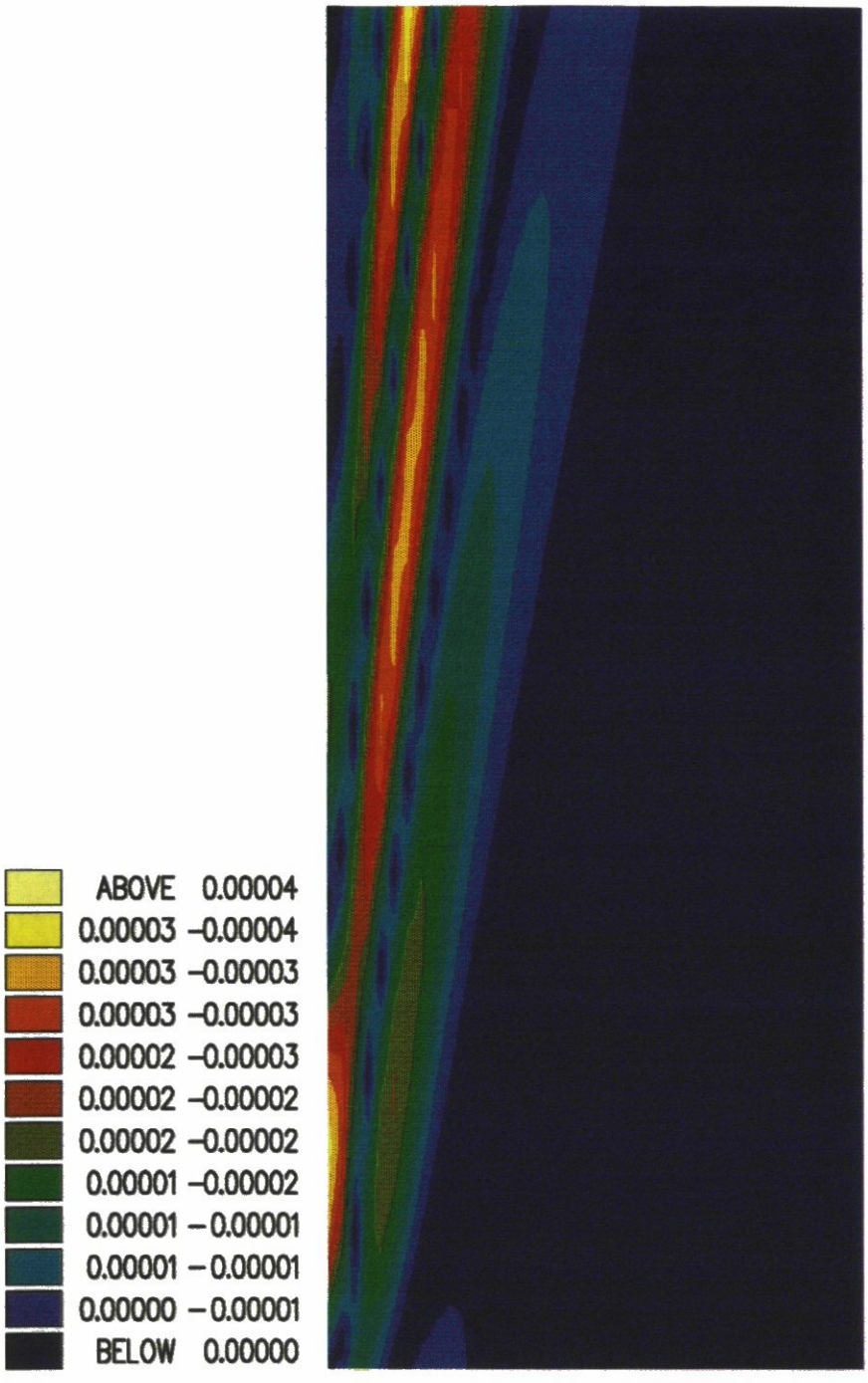

Figure 7: Free surface shear distribution when the body is in the lower layer. $U_0 = 2.0\,m/s$ ($F_n = 0.064$) $L = 100.0\,m$ $d = 10.0\,m$ $\rho_1 = 1025.0\,Kg/m^3$ $\rho_2 = 1026.5\,Kg/m^3$ $\rho_3 = 1028.0\,Kg/m^3$ $t_1 = 30.0\,m$ $t_2 = 30.0\,m$ $f = 75\,m$

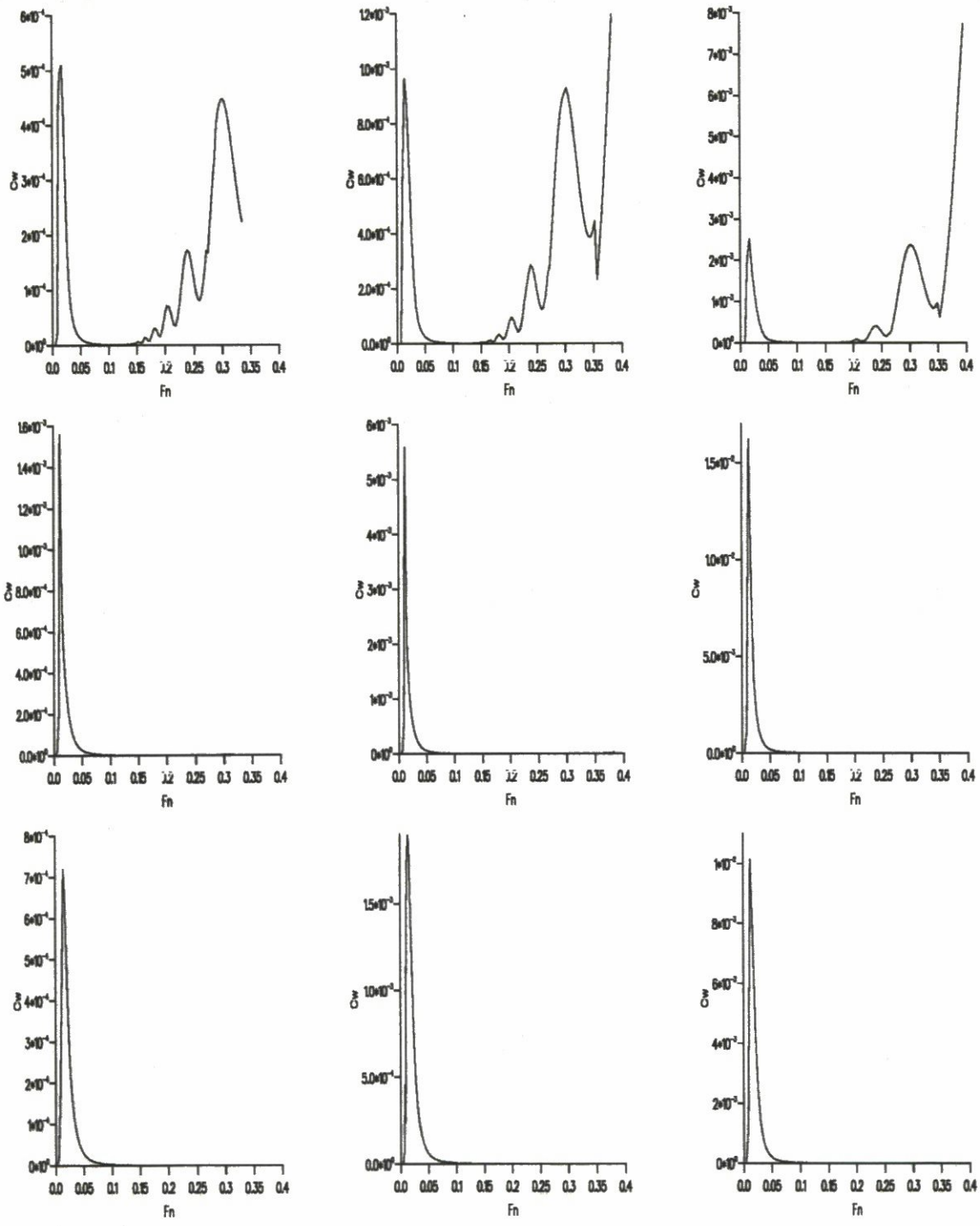

Figure 8: C_w / F_n at a constant displacement when the body is in the upper,middle and lower layers for $\frac{L}{d} = 15$, 10 and 5. $U_0 = 0.5 - 12.0m/s$ ($F_n = 0.016 - 0.383$) $\frac{L}{d} = 15$ $L = 131.0\ m$ $d = 8.736\ m$ $\frac{L}{d} = 10$ $L = 100.0\ m$ $d = 10.000\ m$ $\frac{L}{d} = 5$ $L = 63.0\ m$ $d = 12.600\ m$ $\rho_1 = 1025.0\ Kg/m^3$ $\rho_2 = 1026.5\ Kg/m^3$ $\rho_3 = 1028.0\ Kg/m^3$ $t_1 = 30.0\ m$ $t_2 = 30.0\ m$ $f =$ 15, 45 *and* 75 m

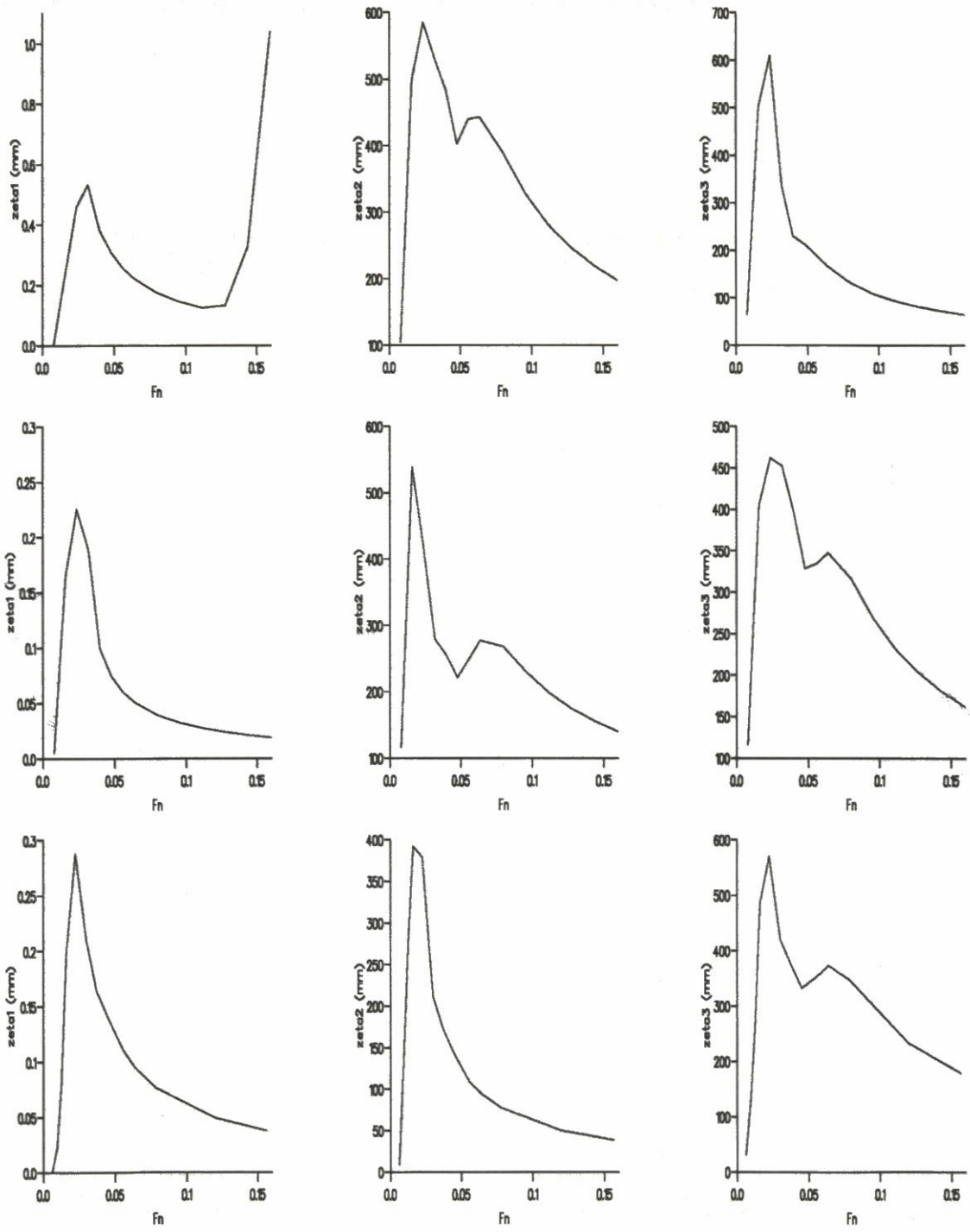

Figure 9: Maximum values of free surface, first and second interface elevations / F_n when the body is in the upper,middle and lower layers. $U_0 = 0.25 - 5.0\ m/s$ ($F_n = 0.008 - 0.160$) $L = 100.0\ m$ $d = 10.000\ m$ $\rho_1 = 1025.0\ Kg/m^3$ $\rho_2 = 1026.5\ Kg/m^3$ $\rho_3 = 1028.0\ Kg/m^3$ $t_1 = 30.0\ m$ $t_2 = 30.0\ m$ $f =$ 15, 45 *and* 75 m

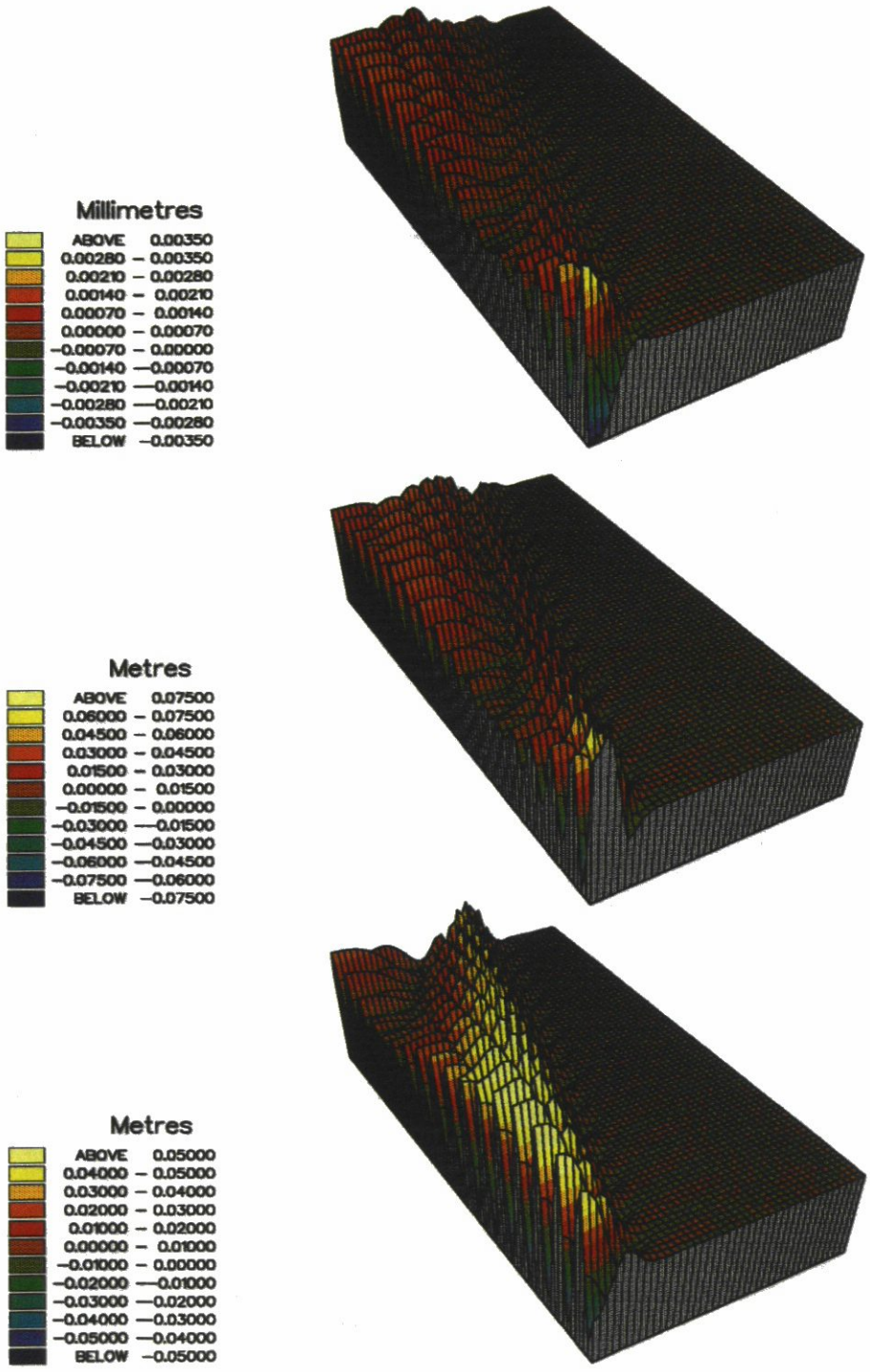

Figure 10: Free surface and interface wave systems for $U_0 = 0.25\ m/s$ ($F_n = 0.008$) when the body is in the upper layer. $L = 100.0\ m$ $d = 10.000\ m$ $\rho_1 = 1025.0\ Kg/m^3$ $\rho_2 = 1026.5\ Kg/m^3$ $\rho_3 = 1028.0\ Kg/m^3$ $t_1 = 30.0\ m$ $t_2 = 30.0\ m$ $f = 15\ m$

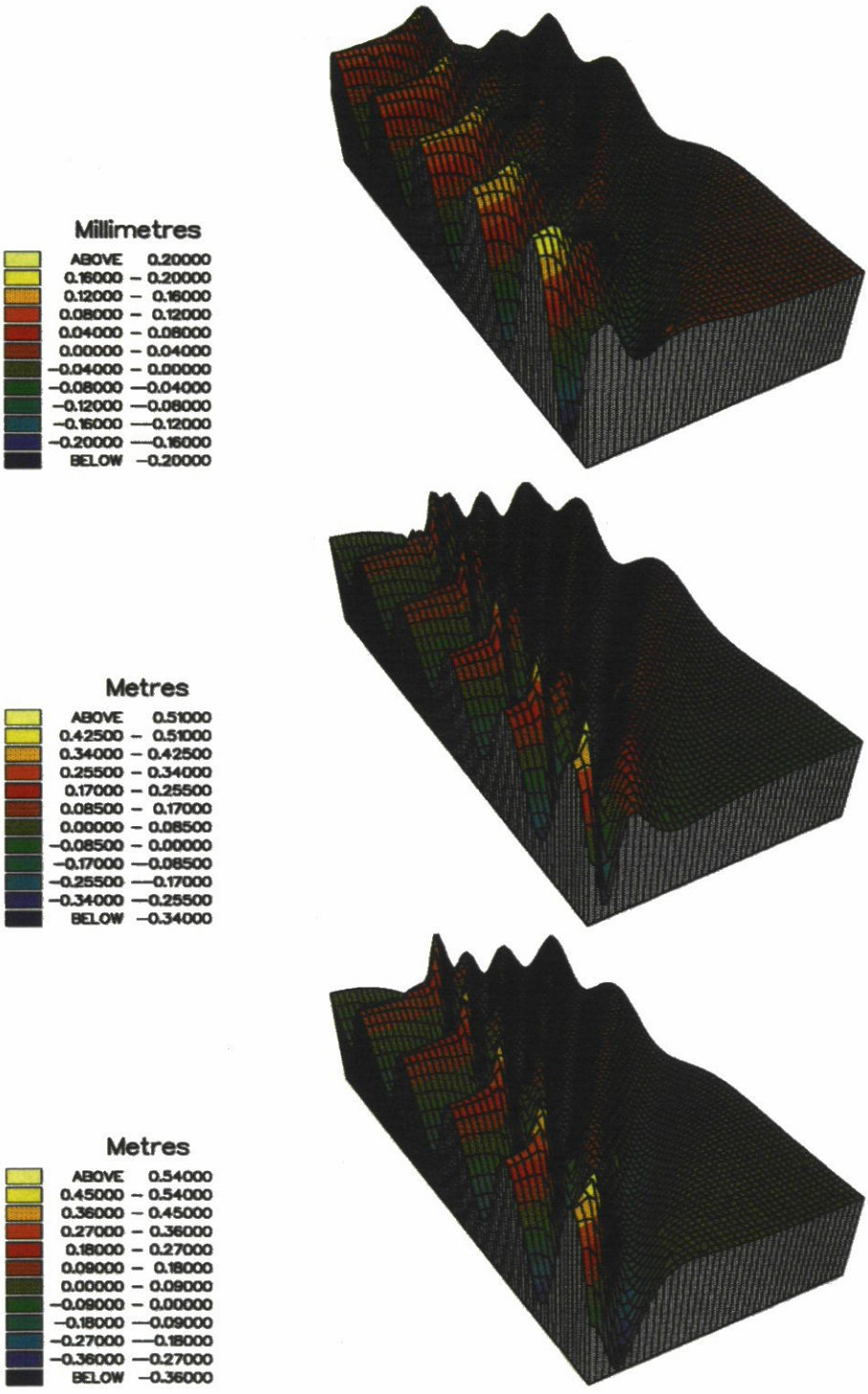

Figure 11: Free surface and interface wave systems for $U_0 = 0.50\ m/s$ ($F_n = 0.016$) when the body is in the upper layer. $L = 100.0\ m$ $d = 10.000\ m$ $\rho_1 = 1025.0\ Kg/m^3$ $\rho_2 = 1026.5\ Kg/m^3$ $\rho_3 = 1028.0\ Kg/m^3$ $t_1 = 30.0\ m$ $t_2 = 30.0\ m$ $f = 15\ m$

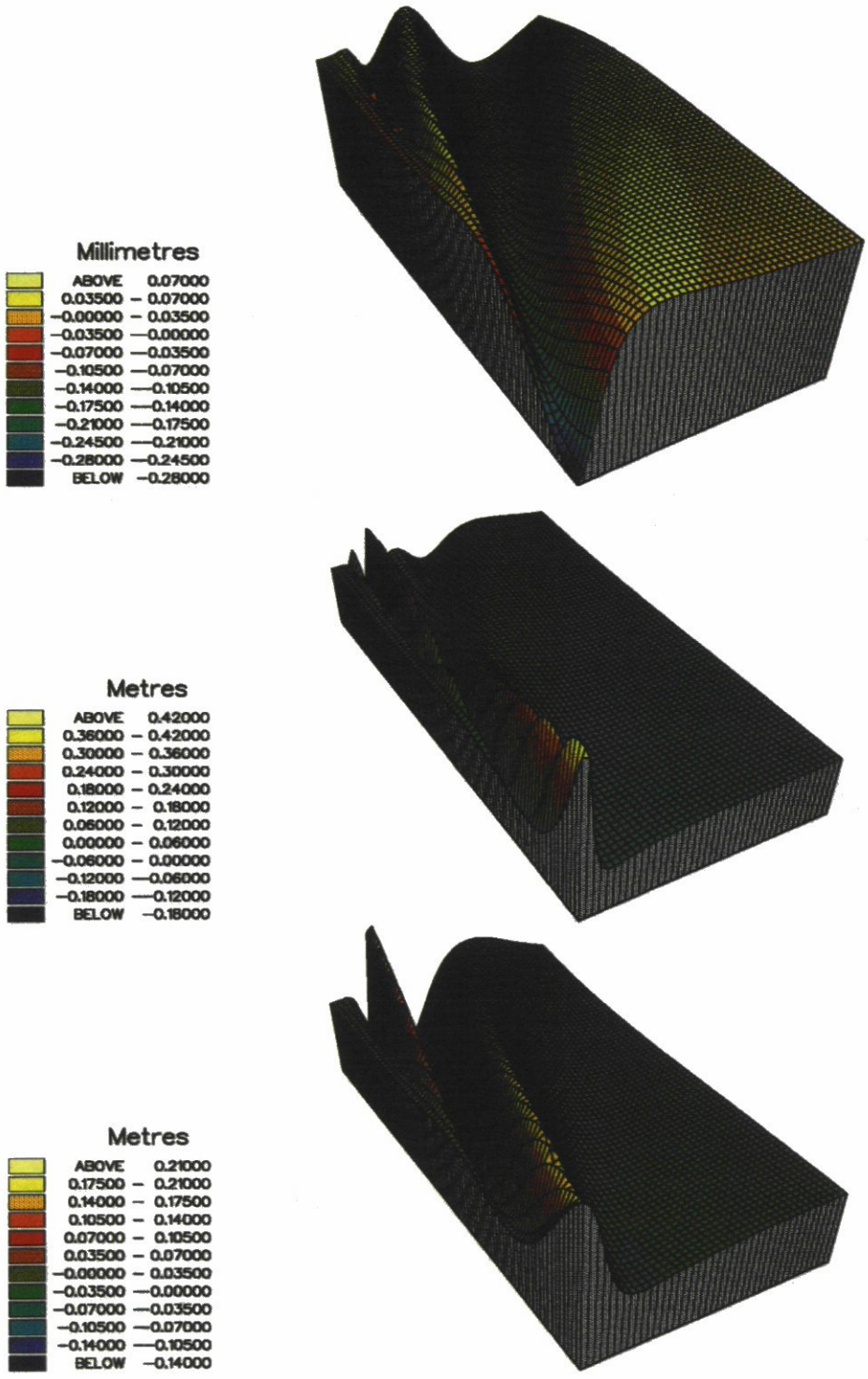

Figure 12: Free surface and interface wave systems for $U_0 = 1.50\ m/s$ ($F_n = 0.048$) when the body is in the upper layer. $L = 100.0\ m$ $d = 10.000\ m$ $\rho_1 = 1025.0\ Kg/m^3$ $\rho_2 = 1026.5\ Kg/m^3$ $\rho_3 = 1028.0\ Kg/m^3$ $t_1 = 30.0\ m$ $t_2 = 30.0\ m$ $f = 15\ m$

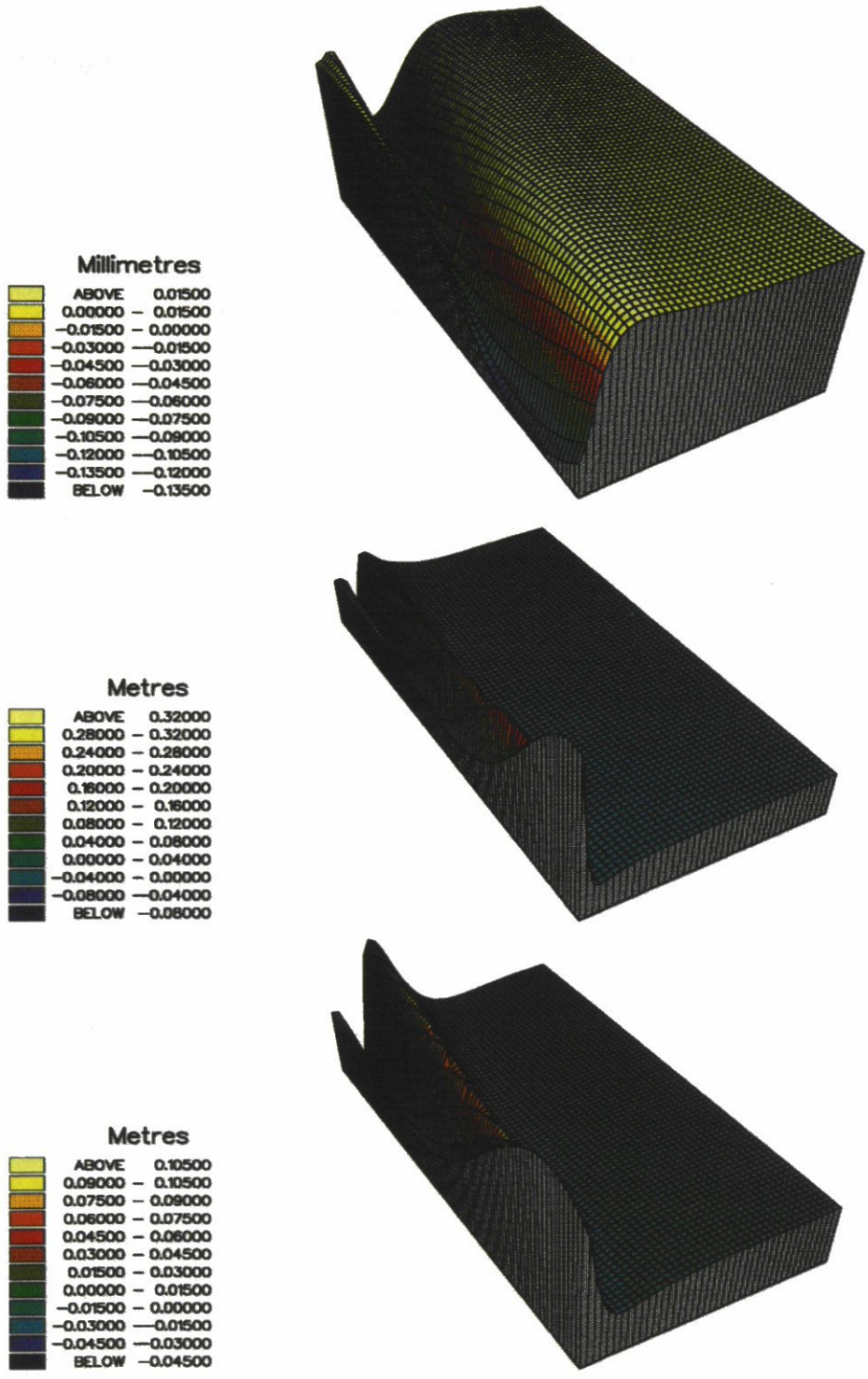

Figure 13: Free surface and interface wave systems for $U_0 = 3.00\ m/s$ ($F_n = 0.096$) when the body is in the upper layer. $L = 100.0\ m$ $d = 10.000\ m$ $\rho_1 = 1025.0\ Kg/m^3$ $\rho_2 = 1026.5\ Kg/m^3$ $\rho_3 = 1028.0\ Kg/m^3$ $t_1 = 30.0\ m$ $t_2 = 30.0\ m$ $f = 15\ m$

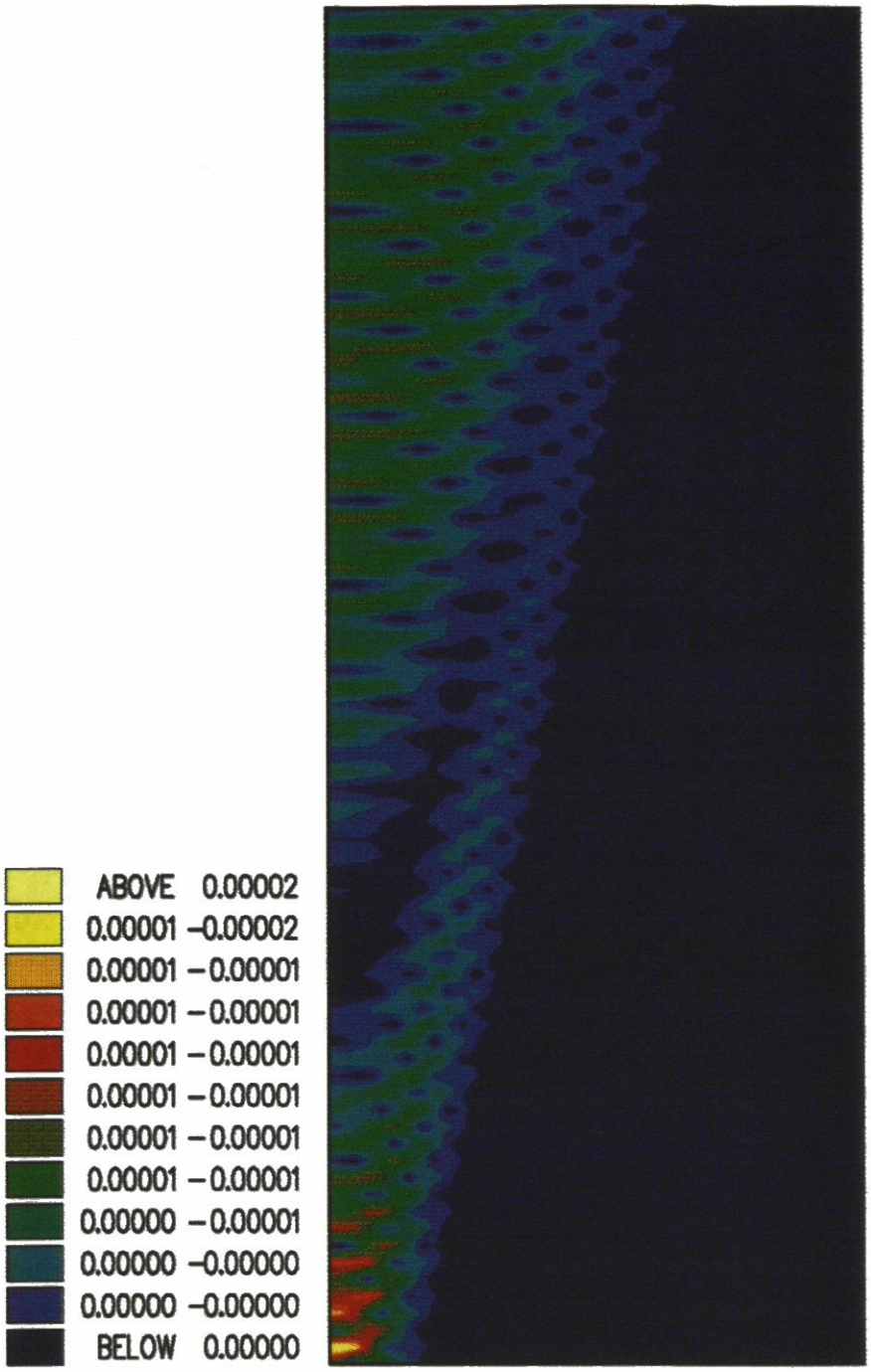

Figure 14: Free surface shear for $U_0 = 0.25\ m/s$ when the body is in the upper layer. $L = 100.0\ m$ $d = 10.000\ m$ $\rho_1 = 1025.0\ Kg/m^3$ $\rho_2 = 1026.5\ Kg/m^3$ $\rho_3 = 1028.0\ Kg/m^3$ $t_1 = 30.0\ m$ $t_2 = 30.0\ m$ $f = 15\ m$

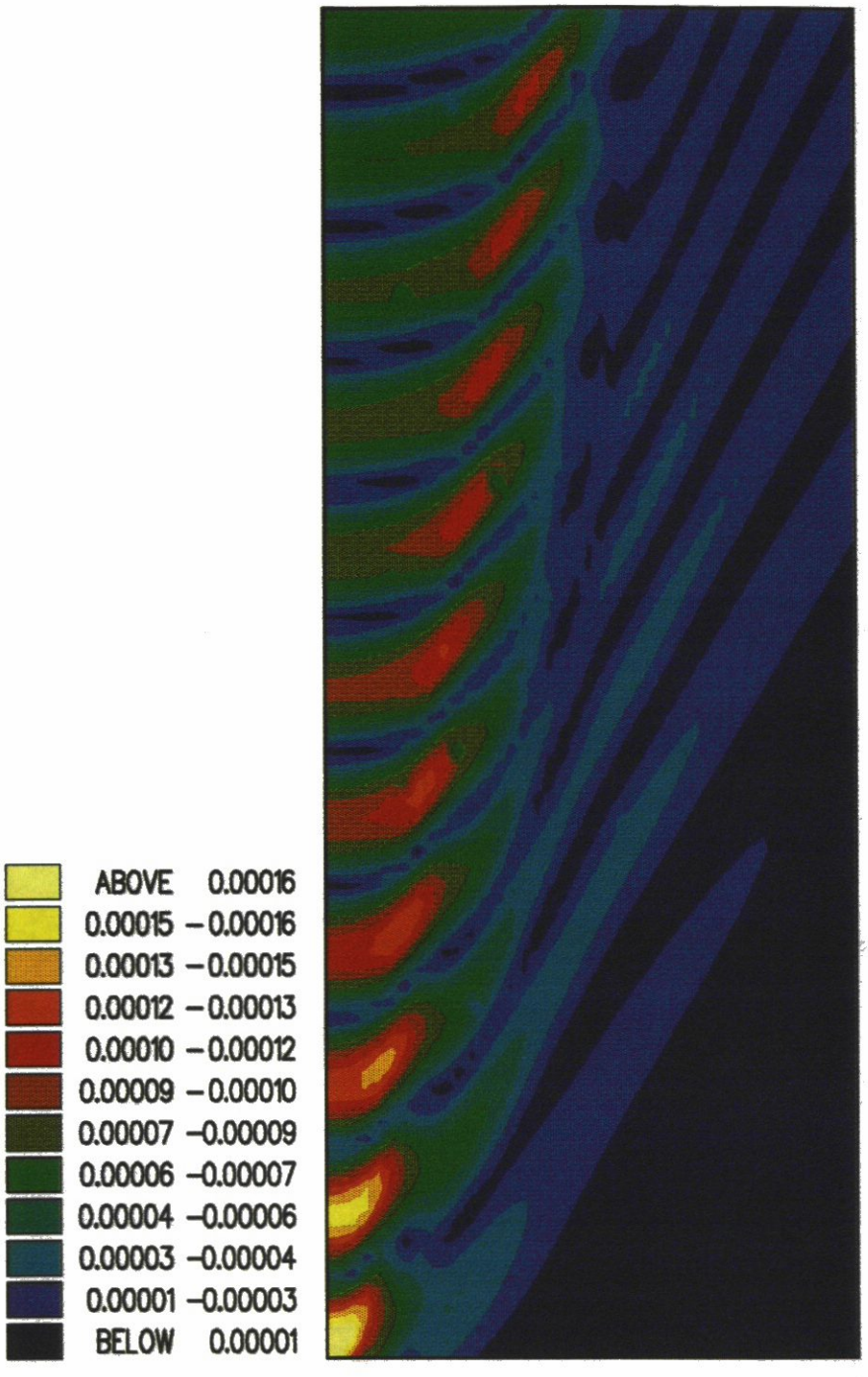

Figure 15: Free surface shear for $U_0 = 0.50\ m/s$ when the body is in the upper layer. $L = 100.0\ m$ $d = 10.000\ m$ $\rho_1 = 1025.0\ Kg/m^3$ $\rho_2 = 1026.5\ Kg/m^3$ $\rho_3 = 1028.0\ Kg/m^3$ $t_1 = 30.0\ m$ $t_2 = 30.0\ m$ $f = 15\ m$

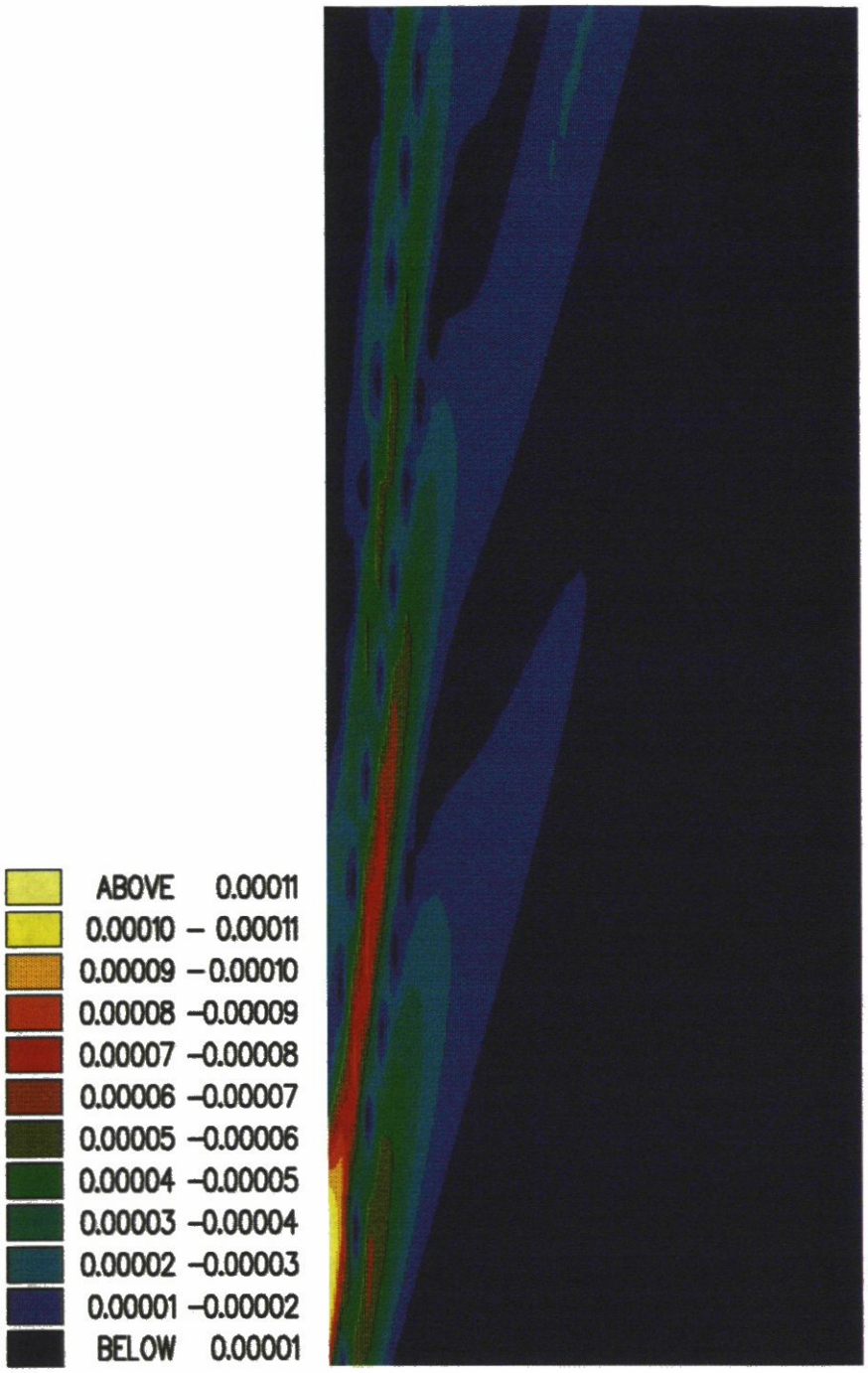

Figure 16: Free surface shear for $U_0 = 1.50\ m/s$ when the body is in the upper layer. $L = 100.0\ m$ $d = 10.000\ m$ $\rho_1 = 1025.0\ Kg/m^3$ $\rho_2 = 1026.5\ Kg/m^3$ $\rho_3 = 1028.0\ Kg/m^3$ $t_1 = 30.0\ m$ $t_2 = 30.0\ m$ $f = 15\ m$

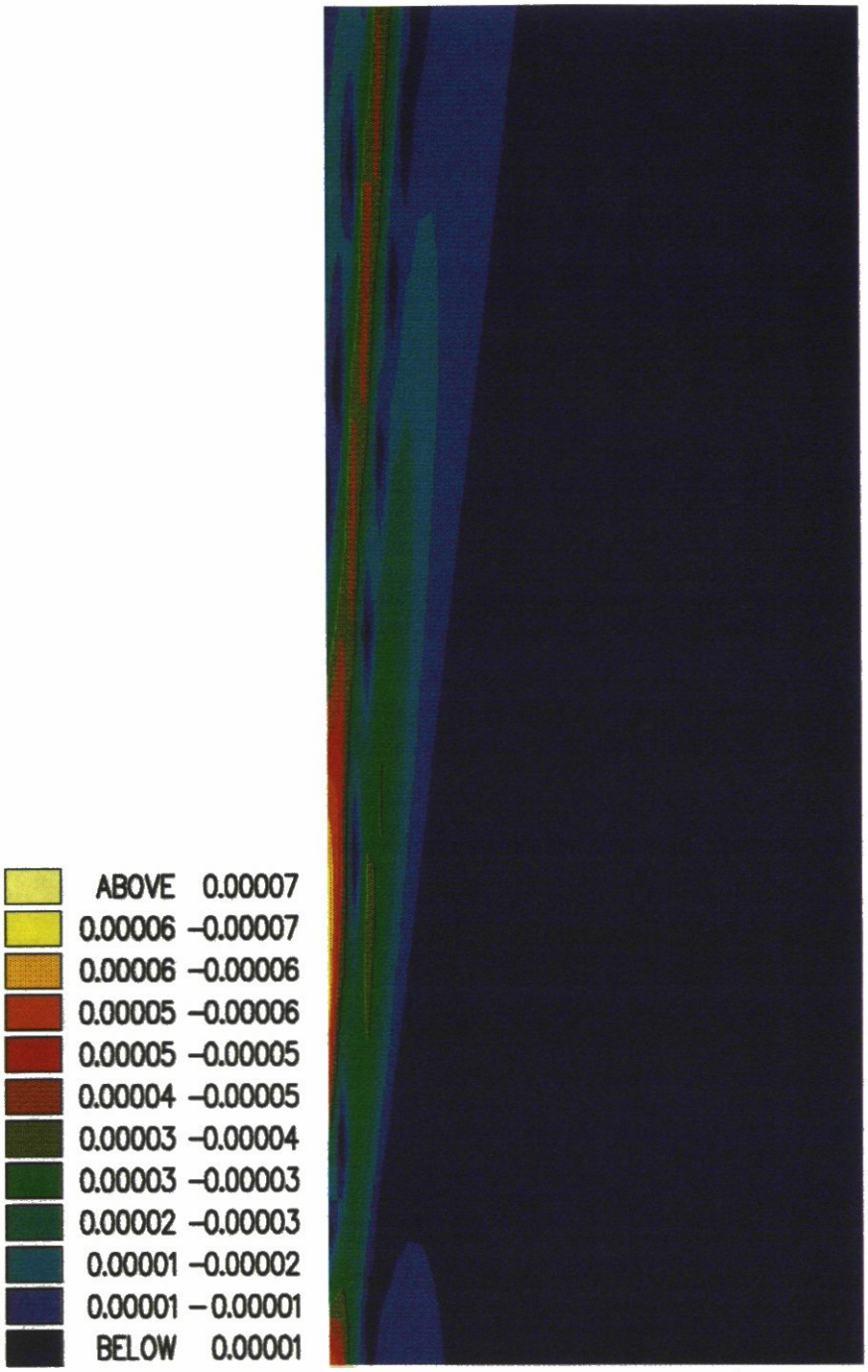

Figure 17: Free surface shear for $U_0 = 3.00\ m/s$ when the body is in the upper layer. $L = 100.0\ m$ $d = 10.000\ m$ $\rho_1 = 1025.0\ Kg/m^3$ $\rho_2 = 1026.5\ Kg/m^3$ $\rho_3 = 1028.0\ Kg/m^3$ $t_1 = 30.0\ m$ $t_2 = 30.0\ m$ $f = 15\ m$

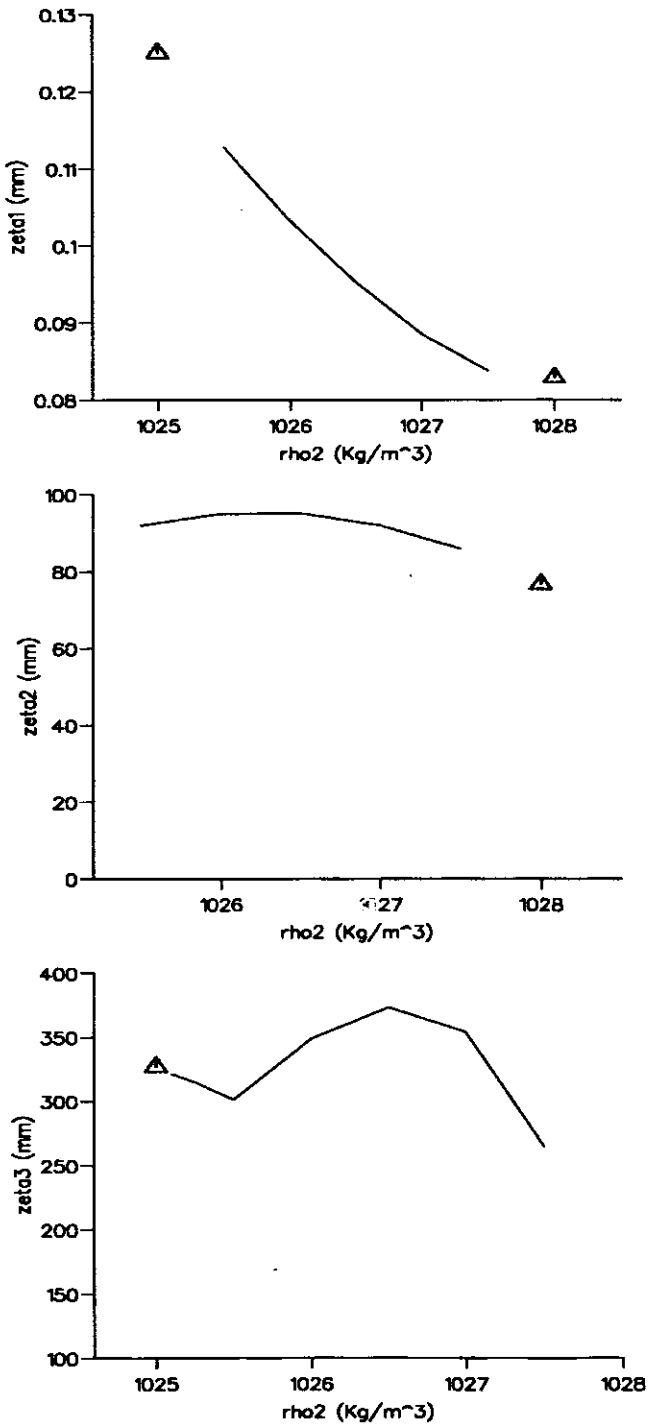

Figure 18: Maximum values of free surface and interface elevations for a variation of ρ_2 when the body is in the lower layer. $U_0 = 2.0\ m/s$ $(F_n = 0.064)$ $L = 100.0\ m$ $d = 10.000\ m$ $\rho_1 = 1025.0\ Kg/m^3$ $\rho_3 = 1028.0\ Kg/m^3$ $t_1 = 30.0\ m$ $t_2 = 30.0\ m$ $f = 75\ m$

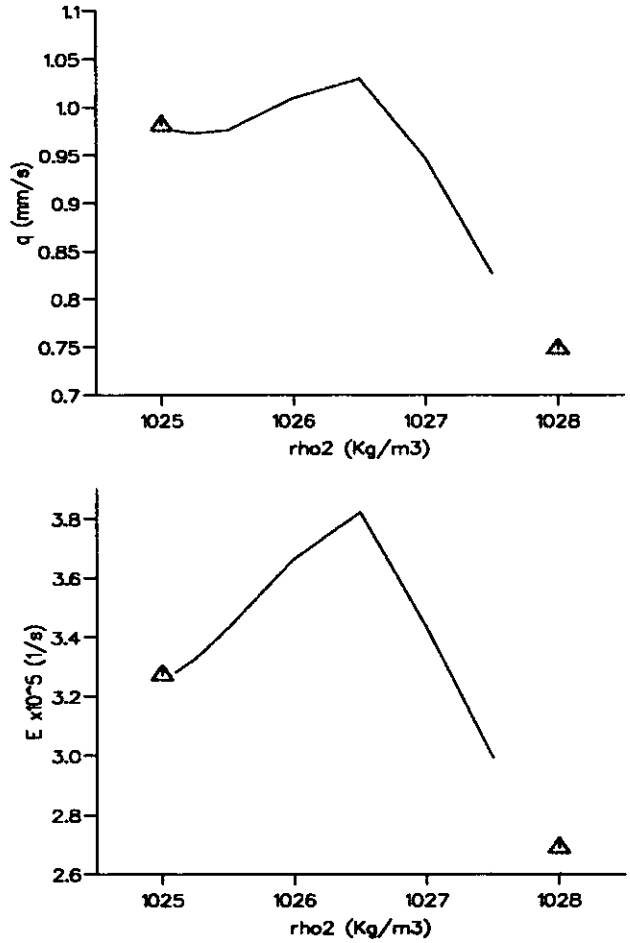

Figure 19: Maximum values of the free surface velocity (q) and shear (E) for a variation of ρ_2 when the body is in the lower layer. $U_0 = 2.0\ m/s$ ($F_n = 0.064$) $L = 100.0\ m$ $d = 10.000\ m$ $\rho_1 = 1025.0\ Kg/m^3$ $\rho_3 = 1028.0\ Kg/m^3$ $t_1 = 30.0\ m$ $t_2 = 30.0\ m$ $f = 75\ m$